2010-06-08

Numerical Analysis of the Effectiveness of Limited Width Gravel Backfills in Increasing Lateral Passive Resistance

Mo'oud Nasr
Brigham Young University - Provo

Numerical Analysis of the Effectiveness of Limited Width Gravel Backfills in Increasing Lateral Passive Resistance

Mo'oud Nasr

A thesis submitted to the faculty of
Brigham Young University
in partial fulfillment of the requirements for the degree of

Master of Science

Kyle M. Rollins, Chair
Travis M. Gerber
Norman L. Jones

Department of Civil and Environmental Engineering

Brigham Young University

August 2010

ABSTRACT

Numerical Analysis of the Effectiveness of Limited Width Gravel

Backfills in Increasing Lateral Passive Resistance

Mo'oud Nasr

Department of Civil and Environmental Engineering

Master of Science

Two series of static full-scale lateral pile cap tests were conducted on pile caps with different aspect ratios, with full width (homogeneous) and limited width backfill conditions involving loose sand and dense gravel. The limited width backfills were constructed by placing a relatively narrow zone (3 to 6 ft (0.91 to 1.83 m)) of higher density gravel material adjacent to the cap with loose sand beyond the gravel zone. Test results indicated that large increases in lateral passive resistance could be expected for limited width backfills.

The main focus of this study is to assess the contribution of plane strain stress effects and 3D geometric end effects to the total passive resistance mobilized by limited width backfills, using soil and pile cap properties associated with the field tests. For this purpose, the finite element program, PLAXIS 2D was used to investigate the static plane strain passive behavior of the full-scale tests. To validate the procedure, numerical results were calibrated against analytical results obtained from PYCAP and ABUTMENT. The analytical models were additionally validated by comparison with measured ultimate passive resistances. The calibrated model was then used to simulate the passive behavior of limited width gravel backfills. Parametric studies were also executed to evaluate the influence of a range of selected design parameters, related to the pile cap geometry and backfill soil type, on the passive resistance of limited width backfills.

Numerical results indicated that significant increases in passive resistance could be expected for long abutment walls where end effects are less pronounced and the geometry is closer to a plane strain condition. Comparisons between measured and numerical results indicated that using the Brinch-Hansen 3D correction factor, R_{3D}, as a multiplier to the plane strain resistances, will provide a conservative estimate of the actual 3D passive response of a pile cap with a limited width backfill. Based on results obtained from the parametric studies, a design method was developed for predicting the ultimate passive resistance of limited width backfills, for both plane strain and 3D geometries.

Keywords: abutment, gravel, compacted fill, passive force, lateral earth pressure

ACKNOWLEDGEMENTS

I owe my deepest gratitude to my advisor and committee chair, Dr. Kyle M. Rollins whose encouragement, support, and guidance has enabled the completion of this thesis. I would also like to thank the members of my thesis committee, Dr. Travis M. Gerber and Dr. Norman L. Jones for their participation and advice.

My sincere thanks are extended to Dr. Anoosh Shamsabadi for taking the time to answer my questions related to computer modeling with "PLAXIS". To David Trevino, I offer my thanks for solving computer related obstacles.

I offer my gratitude for the generous scholarships provided by the Fulton College of Engineering, Department Civil and Environmental Engineering, and the Ralph and Betty Rollins Family. Their financial assistance has greatly helped me achieve my educational goals at Brigham Young University.

I would also like to acknowledge my fellow colleagues in the department, with whom I've shared many helpful discussions and memorable experiences. My special thanks go to Kevin Franke for his constructive comments on this thesis and helpful advice. I am also indebted to my friends Sara, Ali, Marjan, and Maryam for their constant support and encouragement throughout my studies.

Lastly, I am indebted to my family, whose contribution to my life can never be expressed in words. Without their love, support, and blessing in all that I do, the completion of this thesis would not have been possible.

TABLE OF CONTENTS

LIST OF TABLES

LIST OF FIGURES

1 RESEARCH STATEMENT

1.1 Background

Abutment walls and pile foundations are a common type of load transferring system used in infrastructure systems. These components serve the purpose of transferring loads safely from the superstructure to the bearing soil or rock stratum. During lateral loadings induced by earthquake excitations, wind loads, impact loads, etc. abutment walls and pile caps are designed to resist applied loadings by mobilizing the passive earth pressure that develops in the backfill. The magnitude of this mobilized earth pressure depends on several factors, including the strength and stiffness of the backfill material, the degree of frictional resistance that exists between the wall and backfill, the magnitude and direction of wall movement, and the geometric shape of the wall supporting the backfill (Duncan and Mokwa, 2001). The type of backfill material and the geometry of the wall are also factors that are relevant to the subject area of this study.

The geometric shape of the abutment wall or pile cap is a critical factor controlling the shape of the failure surface, and influences the magnitude of the mobilized passive resistance by the backfill. For the purpose of analysis, plane strain assumptions are applicable in situations where the loading and geometry of the structure are constant in an extended length in one direction. Under this assumption, central and end points of the structure are subjected to equal stresses and zero strains. For relatively long abutment walls (≈ 30 m) or abutments bounded by

vertical wing walls, plane strain assumptions may generally be applicable. However, for pile caps and narrow abutment walls, the failure surface may be more three-dimensional, and shear zones may extend beyond the edges of the abutment wall or pile cap, as illustrated in Figure 1-1.

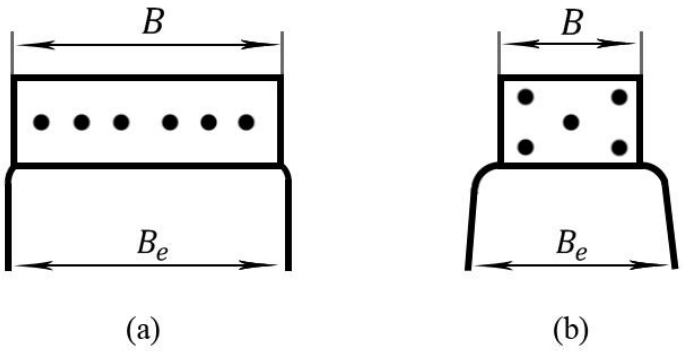

Figure 1-1: Plan view of a (a) relatively long abutment wall and (b) pile cap, showing the extent of 3D edge effects

Another critical factor influencing the magnitude of passive earth pressure is the strength and stiffness of the backfill material. In the last decade, a number of experimental studies have been conducted on backfilled retaining wall structures under lateral loading conditions. These tests have provided valuable information, indicating the significant effect of backfill soil type on the magnitude of the ultimate passive resistance mobilized by the backfill. Examples of related research include experimental studies performed by Rollins and Sparks (2002), and Rollins and Cole (2006), which involved full-scale pile caps with dense gravel backfill materials. These

studies have concluded that using a dense gravel backfill significantly increases the ultimate passive resistance compared to backfills consisting of dense sand, or more importantly, for looser sands. Unfortunately, gravel backfill material is not universally available at economical unit costs. Therefore, use of gravel backfill extending for the full length of the passive failure surface (roughly four times the height of the wall) is not practical in states such as California (Personal communication, Shamsabadi, 2009).

Since the lateral earth pressure problem can essentially be considered a bearing capacity problem, several observations made in studies related to the improvement of spread footing performance, may be useful to consider in solving lateral earth pressure problems. A typical procedure used to increase the bearing capacity of a given soil profile is to modify the profile by partial excavation and replacement of unsuitable soil layers, with a compacted higher quality granular fill. This procedure is often employed in circumstances where the complete removal and replacement of the poor material is infeasible due to economical constraints. According to Hanna and Meyerhof (1980), the procedure has proven to be effective in increasing the bearing capacity of the soil, when the fill thickness is equal to the width of the footing. The compacted fill would allow the dispersion of loads from the footing within the thickness of the fill, reducing stresses on the underlying weaker soil layers.

Rollins et al. (2010) made the observations presented in the paragraph above and applied a similar approach to lateral earth pressure problems. According to Rollins et al. (2010), this approach could especially be beneficial for lateral earth pressure cases where the full replacement of the backfill with select material would not be economically feasible. In addition, the depth of treatment could be relatively shallow because a significant portion of the passive resistance behind a bridge abutment has been shown to develop within a zone less than 6.6 to 8.2

ft (2.0 to 2.5 m) from the ground surface (Martin et al., 1996). To verify the potential benefit of limited width gravel backfills, Rollins et al. (2010) conducted full-scale lateral pile cap tests for a range of limited width backfill conditions, in which a higher density gravel material was placed adjacent to the cap with loose sand beyond the gravel zone. Full width (homogeneous) backfills consisting of loose sand and dense gravel were also tested, to quantify the effectiveness of limited width backfills. The full-scale tests indicated that large increases in lateral resistance (75 to 150%), relative to full width (homogeneous) loose sand backfills, could be expected for relatively narrow dense gravel zones (3 to 6 ft (0.91 to 1.83 m)).

Although the tests conducted by Rollins et al., (2010) confirm the practicality of the method, direct application of the test results is limited by several factors. First, the pile cap tests were performed for a limited number of pile cap and backfill geometries, and thus no standard methodology is available to design for other geometries. Second, the field tests were performed on pile caps where 3D end effects were significant. It is unclear if the same increases would be obtained for long abutment walls, where end effects are less pronounced and the geometry is closer to a 2D or plane strain condition. Third, it is unknown what effect variations in the unit weight, strength and stiffness of the limited dense zone would have on the overall efficiency of the procedure.

1.2 Objectives and Scope of Study

Considering the limited availability of large-scale experimental data to investigate the development of passive earth pressure in backfills, the existing test data from full-scale lateral pile cap tests conducted by Rollins et al. (2010) provided an excellent opportunity to assess the contribution of 2D and 3D effects on the total passive resistance mobilized by limited width

backfills. Using the test soil properties and pile cap geometries, plane strain finite element analyses were performed using the commercial computer software, PLAXIS 2D-Version 8, to simulate the development of passive earth pressures observed during the field tests, in two dimensions, for the various backfill conditions that were tested. Specifically, the objectives outlined for this numerical research study can be summarized as follows:

1) Quantify the contribution of 2D stress effects and 3D geometric end effects on the total passive resistance mobilized by limited width gravel backfills. This was accomplished by comparing 2D numerical analysis results obtained from PLAXIS, with investigations involving 2D analytical model solutions, and 3D field measurements.
2) Assess the effectiveness of using dense gravel backfills of limited width on the passive resistance of the backfill for long abutment walls where end effects are less pronounced and the geometry is closer to a 2D or plane strain condition.
3) Investigate the effect of varying typical pile cap and backfill parameters, including the pile cap height, the unit weight, strength, and stiffness of the limited dense zone, on the passive resistance of limited width dense gravel backfills.
4) Develop a simple design approach in the form of design curves and predictive equations that can be used by practicing engineers in designing limited width dense gravel backfills for both plane strain (2D) conditions and 3D geometries.

The numerical simulations were employed as a primary tool in the investigations, to capture the basic characteristics of the general failure mechanism, and deformed shape of the backfills, and to generate passive load versus pile cap displacement relationships. To verify the accuracy of the numerical models in simulating the passive behavior of the different backfill

conditions, numerical results were calibrated against those computed by analytical models, using similar soil property assumptions. Specifically, the verification was performed for the full width (homogeneous) backfill conditions tested experimentally, by matching numerical and analytical plane strain load-displacement curves. Once satisfactory agreement was achieved between numerical and analytical results, the calibrated models were then used to approximate the plane strain passive response of limited width dense gravel backfills, with the objective of evaluating the effectiveness of limited width dense gravel backfills in increasing the plane strain passive resistance of the backfill.

In addition, comparisons were made between measured and analytical results to allow an evaluation of the contribution of 3D edge effects on the total passive resistance mobilized in limited width gravel backfills. A series of parametric studies were also performed to assess the impact of various soil and pile cap geometry design parameters on the passive resistance of limited width backfills. Based on results obtained from numerical simulations and parametric studies performed, a simple design approach was developed that can be used as an aid in the design of limited width backfills for both plane strain and 3D geometries.

1.3 Organization of Thesis

This thesis contains 6 chapters. Chapter 2 provides a review of existing literature pertaining to the subject area of this study. Chapter 3 covers a general description of experimental tests conducted by Rollins et al. (2010), which are relevant to this study. In chapter 4, the numerical modeling and calibration procedure employed in simulating the passive response of a typical pile cap-backfill system is presented. Using the calibrated models developed in chapter 4, a range of numerical simulations are conducted to cover a wide variety

of full and limited width backfills, and pile cap heights with varying backfill soil parameters. Chapters 5 and 6 present the results and conclusions of the performed simulations.

2 LITERATURE REVIEW

2.1 Introduction

This chapter provides a summary and synthesis of published information relevant to the subject area of this study in the following three categories: analytical, experimental, and numerical methods. In the analytical methods section an overview of limit equilibrium passive earth pressure theories is presented. In addition, the development of analytical programs used in calibrating the numerical models employed in this study is summarized. These programs include PYCAP and ABUTMENT, developed by Duncan and Mokwa (2001) and Shamsabadi et al. (2007) respectively. The experimental full-scale test summarized in this chapter is the lateral pile cap testing of a range of dense gravel backfills of limited width as performed by Rollins et al. (2010) at a site located at I-15/South Temple in Salt Lake City, Utah. Rollins et al. (2010) employs limited width dense gravel backfills, with the objective of potentially increasing the mobilized passive resistance of the backfill. The numerical methods section covers a summary of recent numerical studies performed by Wilson (2009) and Shiau and Smith (2006).

2.2 Analytical Methods

2.2.1 Passive Earth Pressure

As an adjacent vertical retaining structure deflects horizontally into a backfill, passive earth pressures develop in the backfill, exerting horizontal stresses on the soil mass within the backfill. As the retaining structure proceeds to deflect into the soil mass, the soil fails in shear along a critical failure surface behind the structure. Depending on the situation in which passive conditions are mobilized in a backfill, the passive earth pressure can have favorable and detrimental effects on the performance of retaining structures. As stated in Wilson (2009), the passive resistance can help prevent sliding and overturning failures of externally stabilized retaining structures, which rely primarily on the weight of the backfill and frictional resistance between the base of the structure and backfill to resist applied loads (Lambe and Whitman, 1969). In the case of bulkhead or sheet piles which may be anchored to a wall, passive earth pressures, which develop below the dredge line, can prevent toe kick out failures from occurring in these structures (Lambe and Whitman, 1969). Passive pressure is also favorable in situations where the passive resistance of the backfill can be used to oppose earthquake-induced loads by increasing the lateral stiffness and capacity of abutment walls and pile caps (e.g. Cole and Rollins, 2006, and Rollins and Cole, 2006).

In contrast, passive earth pressures may also transmit unfavorable loads to the retaining structure which may jeopardize the overall performance of the structure. These loads include loads induced by thermal expansion, lateral spreading, and landslides (Duncan and Mokwa, 2001). The drastically different effects of passive earth pressure on the performance of retaining

structures, emphasizes the importance of quantifying the amount of mobilized passive resistance accurately.

2.2.2 Limit Equilibrium Theories

The solution of lateral passive earth pressure problems was initiated by the efforts undertaken by Coulomb (1776) and Rankine (1857). Since the pioneering works of Coulomb and Rankine, many researchers have approached the passive earth pressure problem with different assumptions. This has resulted in the development of a large number of methods for solving passive earth pressure problems over the last three centuries, including but not limited to the following: slip line method, limit analysis method, empirical methods, and various finite element and finite difference computer methods (Cole, 2003). Among the large number of theories available, the traditional limit equilibrium passive earth pressure theories, namely the Coulomb (1776), Rankine (1857), and log spiral Terzaghi et al. (1996) theories, are considered to be the most popular theories in engineering practice. Among these limit equilibrium methods, the log spiral theory has been known to provide a more accurate estimation of passive earth pressure. However, engineers have typically refrained from using the log spiral theory due to the complexity and time-consuming nature of the procedure involved. On the contrary, the Rankine and Coulomb theories have been two of the most commonly used limit equilibrium theories. Their extensive use can likely be attributed to their simplicity in predicting the passive resistance of backfills. A summary of the aforementioned limit equilibrium theories is provided in this section.

Rankine Theory

Several fundamental assumptions are made in the Rankine passive earth pressure theory. Some of the more significant assumptions include the following: (1) the soil is homogeneous and isotropic, (2) the soil shears along a planar failure surface, (3) the ground surface is planar, and (4) there is no friction on the interface between the wall and backfill. Based on the abovementioned assumptions, the Rankine coefficient of passive earth pressure, K_P, is given by the following expression:

$$K_P = \frac{cos\beta + \sqrt{cos^2\beta - cos^2\varphi}}{cos\beta - \sqrt{cos^2\beta - cos^2\varphi}} \quad (2\text{-}1)$$

where β is the embankment slope angle, and φ is the soil friction angle. The resultant passive force per unit width of the wall, E_p, can be found using equations 2-2 and 2-3 for cohesionless and cohesive soils, respectively. This force acts at a distance of H/3 from the base of the wall, as the passive earth pressure distribution with depth is assumed to be linear.

$$E_p = 0.5\gamma H^2 K_p \quad (2\text{-}2)$$

$$E_p = 0.5\gamma H^2 K_p + 2cH\sqrt{K_p} \quad (2\text{-}3)$$

where γ is the total unit weight of the backfill soil, H is the wall height, c is the soil cohesion intercept, and K_p is Rankine's coefficient of passive earth pressure. Because the Rankine earth

pressure theory neglects wall friction between the retaining wall and backfill, the resulting passive earth pressure is typically much lower than the actual pressure mobilized by the backfill.

Coulomb Theory

Assumptions used in the Coulomb theory are generally similar to those of the Rankine Theory. However, the two methods differ in that the Coulomb theory takes into account the frictional resistance between the wall and the backfill. This resistance is expressed as the resultant of the normal and shear forces acting on the wall, at angle of δ, from a perpendicular to the wall. Figure 2-1 shows the schematic of the failure surface assumed in the Coulomb theory.

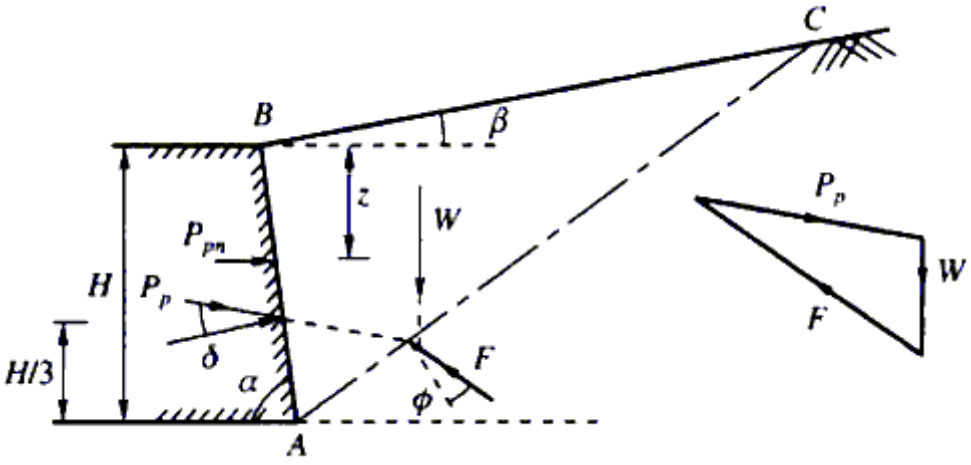

Figure 2-1: Coulomb failure surface in passive state

The Coulomb coefficient of passive earth pressure, K_P, is given by the following equation:

$$K_p = \frac{(cos\varphi)^2}{cos\delta\left[1 - \sqrt{\frac{\sin(\varphi + \delta)\sin(\varphi + \beta_s)}{cos\delta cos\beta_s}}\right]^2} \quad (2\text{-}4)$$

where β is the embankment slope angle, φ is the soil friction angle, and δ is the wall friction angle. Similar to the Rankine theory, the resultant passive force per unit width of the wall, E_p, can be found using equations 2-5 and 2-6 for cohesionless and cohesive soils, respectively. The point of application of this force is also at a distance of H/3 from the base of the wall, as the passive earth pressure distribution with depth is assumed to be linear.

$$E_p = 0.5\gamma H^2 K_p \quad (2\text{-}5)$$

$$E_p = 0.5\gamma H^2 K_p + 2cH\sqrt{K_p} \quad (2\text{-}6)$$

where γ is the total unit weight of the backfill soil, H is the wall height, c is the soil cohesion intercept, and K_p is Coulomb's coefficient of passive earth pressure. The inclusion of the wall friction angle in the theory, and the assumption of a planar failure surface under passive conditions can result in an overestimation of the calculated passive earth pressure. This overestimation of resistance becomes significant as the wall friction angle, δ, exceeds 50% of the soil friction angle. On the contrary, the Coulomb theory generally produces reasonable estimates

in active conditions, and thus can be used with confidence, keeping in mind the assumptions used in developing the theory.

Log Spiral Theory

The log spiral theory assumes a non-linear failure surface which is considered to be a more realistic representation of the failure mechanism involved in lateral earth pressure problems. The shape of this failure surface consists of a curved portion, defined by a logarithmic spiral, and a linear portion which intersects the ground surface. The theoretical shape associated with the log spiral failure surface is shown in Figure 2-2. The line passing through the center of the logarithmic spiral, "o", and point "b", referred to as the transition shear line, defines the boundary between two different shear zones within the failure surface. The triangular section abc, referred to as the Rankine zone, is bounded between the linear portion of the failure surface and the ground surface. The soil within this zone is assumed to be in the passive Rankine state. The Prandtl zone constitutes the radial portion of the failure surface.

The log spiral passive earth pressure coefficient, K_p, can be calculated using several approaches, including tables and charts, graphical methods, and computer programs. Caquot and Kerisel (1948) provided tables for estimating the passive earth pressure coefficient for granular cohesionless soils. These tables were generated based on the assumption that the wall friction angle and soil friction angles have equal values ($\varphi=\delta$). The U.S. Navy (1982) published the Caquot and Kerisel (1948) tables in graphical format, and provided corrections to adjust for lower wall friction values.

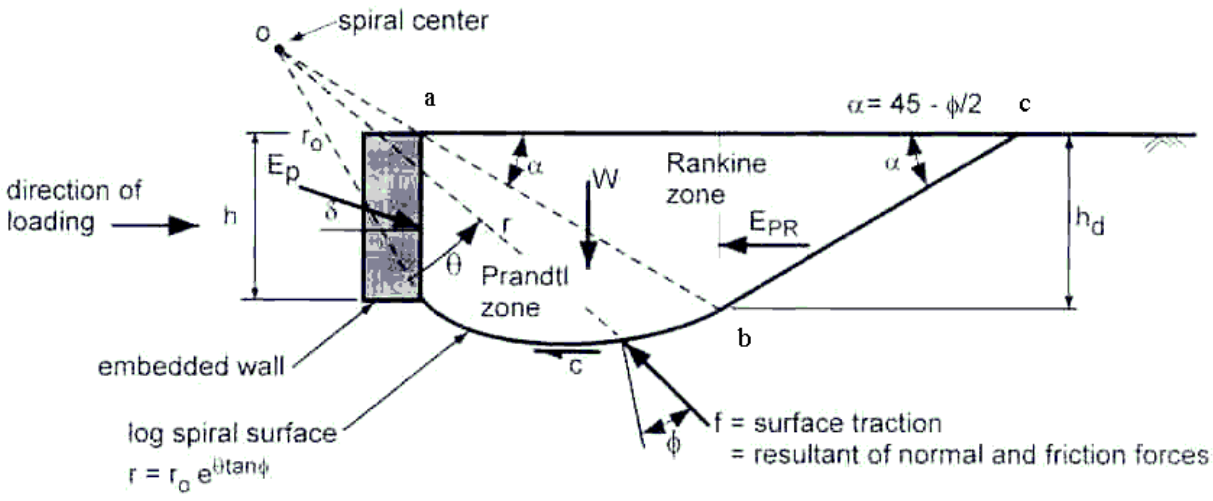

Figure 2-2: Log spiral failure surface, adapted from (Duncan and Mokwa, 2001)

The graphical procedure of estimating the log spiral passive earth pressure coefficient was developed by Terzaghi (1943) and Terzaghi et al. (1996). This method involves an iterative process of varying the log spiral center, with the objective of calculating the lowest passive resistance of the wall-backfill system. Unlike tables and charts developed by Caquot and Kerisel (1948) and U.S. Navy (1982), the graphical procedure accounts for cohesion in soils. However, due to the extensive time and effort associated with the graphical procedure, engineers have often refrained from using this method of calculation for estimating the log spiral passive earth pressure coefficient. Based on the log spiral graphical procedure, Duncan and Mokwa (2001) developed a spreadsheet program referred to as PYCAP, in which the log spiral theory is modeled numerically to estimate the passive earth pressure coefficient. A summary of this numerical analysis is provided later in this chapter.

Despite inherent limitations associated with the log spiral theory due to plane strain assumptions, it is generally considered to be the most theoretically sound and accurate method in estimating the passive earth pressure among limit equilibrium theories (Fang et al., 1994, Gadre, 1997, Duncan and Mokwa, 2001, Rollins and Sparks, 2002). As mentioned previously, in addition to the frictional resistance between the wall and backfill soil, the theory accounts for the curvilinear shape of the failure surface assumed to develop in passive conditions.

2.2.3 Three-Dimensional Effects

As stated in Cole (2003), the limit equilibrium theories discussed in the previous section make plane strain assumptions in calculating the passive earth resistance mobilized by a backfill. However, for pile caps and narrow abutment walls, this assumption does not account for the frictional resistance provided by shear surfaces at the edges of the structure in passive conditions (see Figure 1-1). Many approaches have been taken to account for the 3D edge effects by increasing the plane strain passive resistance to represent the development of a three dimensional failure surface. In this section, several approaches presented by Brinch Hansen (1966), Ovesen and Stromann (1972), and Soubra and Regenass (2000) are summarized.

Brinch Hansen (1966)

Ovesen (1964) identified the different boundary conditions that exist between the central and end sections of an anchor slab, by performing several small-scale lateral earth pressure tests on granular soils. In light of the experimental test results obtained from Ovesen (1964), Brinch Hansen (1966) proposed an empirical expression (Equation 2-7) for calculating the three dimensional passive resistance, P_{3D}, of rectangular anchor slabs:

$$P_{3D} = E_P . B . R_{3D} \quad (2\text{-}7)$$

where E_P is the passive resistance of the anchor slab per unit length, B is the width of the anchor slab, and R_{3D} is the Brinch Hansen three dimensional resistance factor defined by the following equation:

$$R_{3D} = \left[1 + +(K_p - K_a)^{0.67}\left(1.1A^4 + \frac{1.6B_b}{1 + 5(B/h)} + \frac{0.4R_0A^3B_b^2}{1 + 0.05(B/h)}\right)\right] \quad (2\text{-}8)$$

where A and B_b are dimensionless parameters related to the anchor slab height, h, embedment depth, H, and spacing between a row of anchor slabs, S′, as defined in Figure 2-3. A and B_b are determined by Equations 2-9 and 2-10.

$$A = 1 - \frac{h}{H} \quad (2\text{-}9)$$

$$B_b = 1 - \left(\frac{B}{S'}\right)^2 \quad (2\text{-}10)$$

Ovesen and Stromann (1972)

Based on model tests performed by Ovesen (1964) and Hueckel (1957), and field tests performed by the U.S. Naval Civil Engineering Laboratory (1966), Ovesen and Stromann (1972) proposed a new design method for estimating the passive resistance of a row of rectangular anchor slabs or an individual anchor slab in granular soils. In this method, an equivalent width,

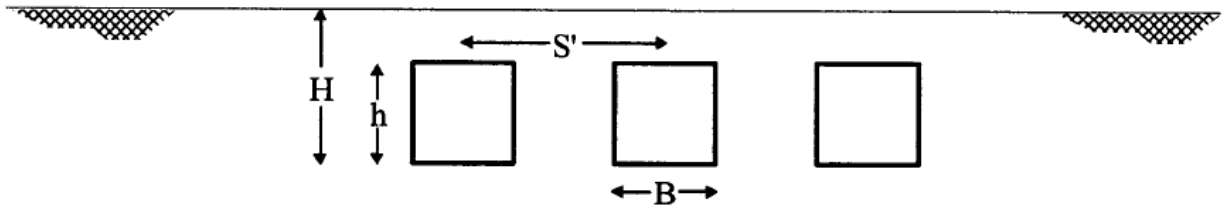

Figure 2-3: Geometrical parameters of a vertical rectangular anchor slab, adapted from (Ovesen and Stromann, 1972)

B_e, is calculated for the anchor slab which is dependent on several geometrical parameters, including the depth of anchor slab embedment, H, the height, h, and the spacing between a row of anchor slabs, S′. The three dimensional passive resistance, P_{3D}, of rectangular anchor slabs is calculated using the following expression:

$$P_{3D} = E_P . \left(\frac{A_S}{A_O}\right) . B_e \qquad (2\text{-}11)$$

where B_e is the effective or equivalent width of the anchor slab, E_p is the passive resistance of the anchor slab per unit length, and A_s/A_o is the ratio of the resistance of an anchor slab with limited height and limited length over the resistance of an anchor slab in the basic case. The basic case anchor slab is defined as an anchor slab with the top reaching the ground surface and with infinite length. The effective width, B_e, and the A_s/A_o ratio are determined from Figure 2-4.

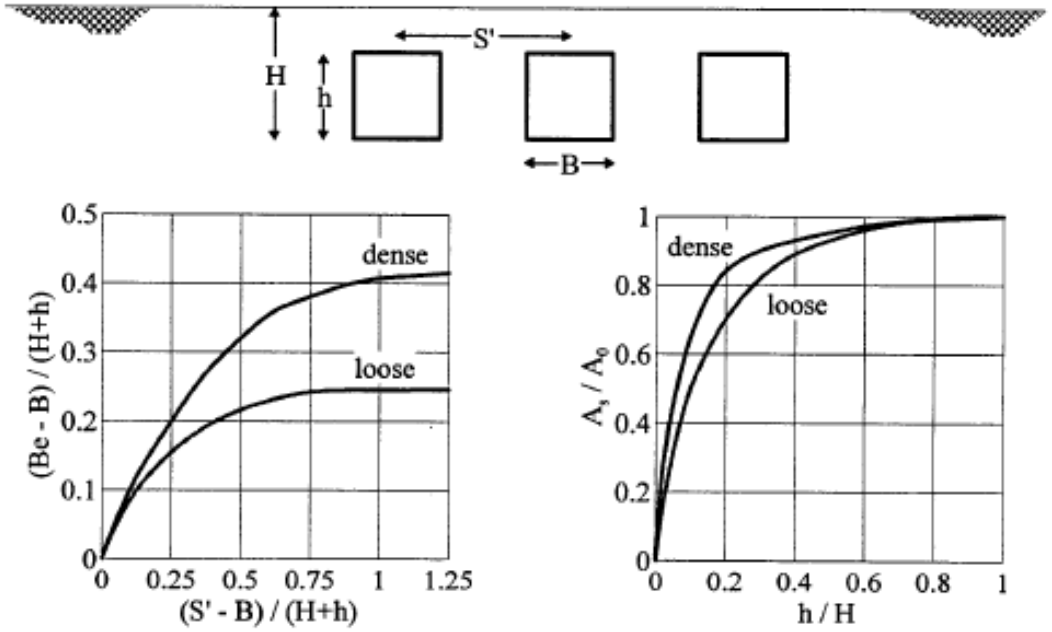

Figure 2-4: Diagrams for design of vertical rectangular anchor slabs in sand (Ovesen and Stromann, 1972)

Soubra and Regenass (2000)

Soubra and Regenass (2000) use the upper-bound method of the limit analysis theory to explore the three dimensional development of passive earth pressure in backfills. To represent the failure mechanism of various backfills, three general mechanisms, referred to as *M1*, *Mn*, and *Mnt*, are considered in the calculations. The first failure mechanism, *M1*, is referred to as the one-block mechanism, since a single rectangular rigid block is assumed to represent the horizontal movement of the backfill soil mass. This block is the extension of the 2D Coulomb failure mechanism into three dimensions, and is assumed to translate rigidly in the direction of loading. To provide a more accurate representation of the passive failure mechanism, the second failure mechanism, *Mn*, is defined by a radial shear zone composed of "n" rigid blocks. Similar

to the one-block mechanism, the "n" blocks are assumed to translate as rigid bodies with wall deflection. In the third failure mechanism, *Mnt*, the multi-block mechanism is further improved by truncating the lateral and lower bounds of the mechanism by two portions of right circular cones. Figure 2-5 illustrates 3D and profile views of the three failure mechanisms, *M1*, *Mn*, and *Mnt*.

Based on the assumption that energy within a truncated multi-block mechanism is dissipated along interfaces between the rigid blocks, the soil-wall interface, and the failure surface interface, the work equation can be constructed by equating the rate of external work with the rate of internal energy dissipation. Applying this approach results in the derivation of Equation 2-12, for calculating the three dimensional passive force in a given backfill. This expression takes into account the effect of soil weight, cohesion, and surcharge loading by employing dimensionless coefficients of $K_{p\gamma}$, K_{pc}, and K_{pq}, respectively.

$$P_{3D} = \left(\frac{1}{2} K_{p\gamma} \gamma H^2 + K_{pc} cH + K_{pq} qH\right).B \qquad (2\text{-}12)$$

where γ and c are the unit weight and cohesion of the backfill soil, respectively, q is the surcharge on the ground surface, H is the height of the wall, B is the wall width, and $K_{p\gamma}$, K_{pc}, and K_{pq} are the passive earth coefficients due to soil weight, cohesion, and surcharge load, respectively. The passive earth coefficient associated with cohesion, K_{pc}, can be found from the following equation:

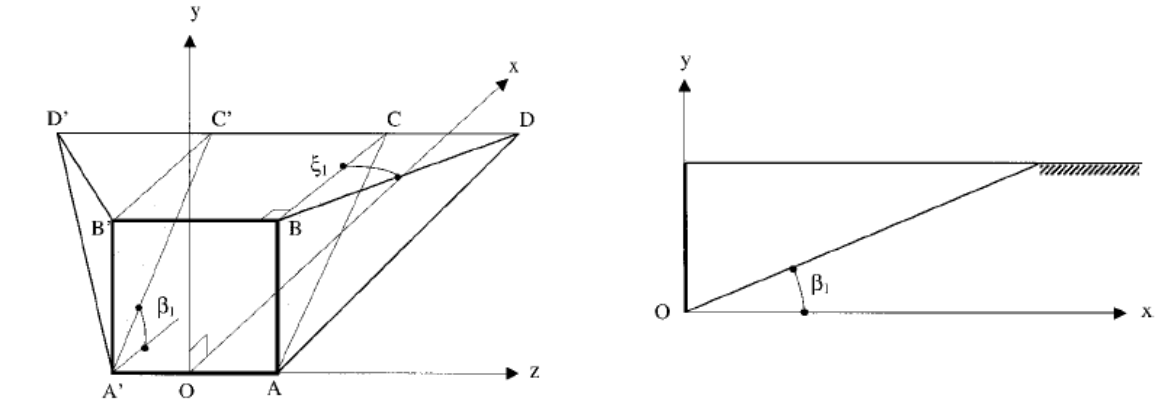

(a) One-block mechanism

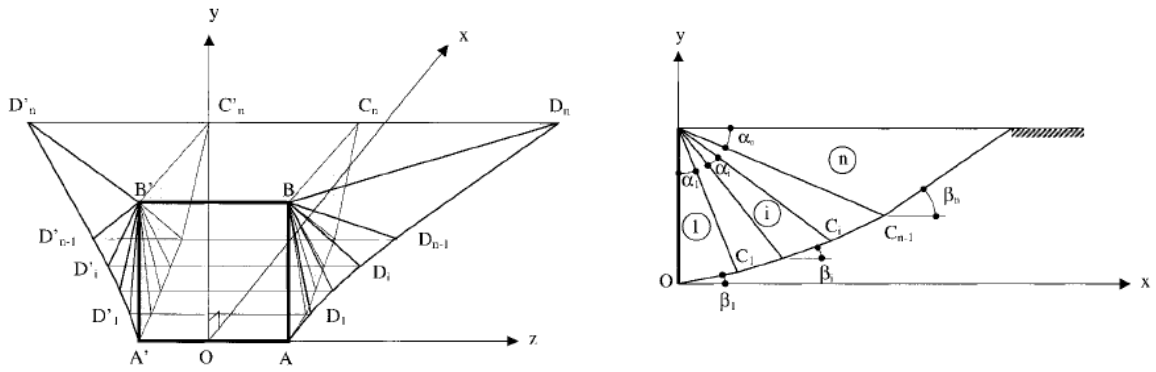

(b) Multi-block mechanism

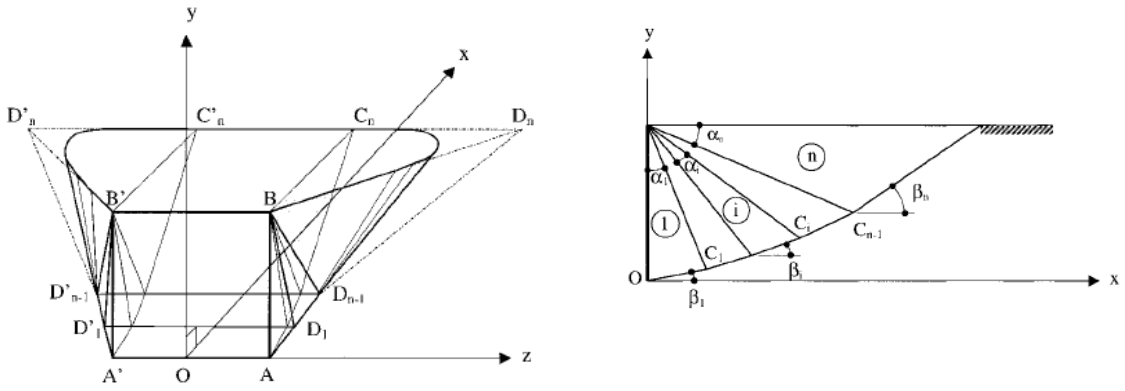

(c) Truncated multi-block mechanism

Figure 2-5: Three-dimensional and profile views of (a) one-block, (b) multi-block, and (c) truncated multi-block failure mechanisms (Soubra and Regenass, 2000)

$$K_{\mathrm{pc}} = \frac{K_{\mathrm{pq}} - \left({}^{1}/_{cos\delta}\right)}{tan\varphi} \tag{2-13}$$

where δ and φ are wall and soil friction angles, respectively.

2.2.4 Variation of Passive Force with Displacement

Duncan and Mokwa (2001)

Duncan and Mokwa (2001) provide a comparison of traditional passive earth pressure theories in accurately estimating the developed passive earth pressure in a given backfill. In this study, Duncan and Mokwa (2001) confirm the superior capability of the log spiral theory in accurately estimating the passive earth pressure, for conditions where the wall friction angle is greater than 40% of the soil friction angle ($\delta > 0.4\varphi$). In addition, factors that have the greatest effect on the magnitude of the ultimate passive resistance of the backfill are identified in the study. These factors include the strength and stiffness of the backfill material, the degree of frictional resistance that exists between the pile cap and the backfill, the magnitude and direction of pile cap movement, and the geometric shape of the pile cap supporting the backfill.

Using the aforementioned observations, Duncan and Mokwa (2001) developed an Excel spreadsheet computer program, referred to as PYCAP to facilitate the use of the log spiral theory for the engineering community. The soil and retaining structure properties required in PYCAP include the following: internal friction angle (φ), soil cohesion (c), wall friction angle (δ), adhesion factor (α), in-situ unit weight (γ), initial soil modulus (E_i), Poisson's ratio (ν), retaining structure height (H), width (b), and embedment depth (z), surcharge on ground surface (q), and

the deflection-to-wall height ratio (Δ_{max}/H), which is defined as the displacement associated with failure (Δ_{max}), normalized by the wall height (H).

The development of PYCAP is based on the traditional log spiral theory with corrections for Brinch Hansen 3D geometry effects. A hyperbolic model is incorporated into the theory to define the load-displacement relationship of the wall-backfill system. The hyperbolic relationship used in approximating the load-displacement relationship is defined by Equation 2-14.

$$P = \frac{y}{\left[\frac{1}{K_{max}} + R_f \frac{y}{P_{ult}}\right]} \tag{2-14}$$

where P is the passive resistance at a given pile cap deflection of y, K_{max} is the estimated initial slope of the load-displacement curve, and R_f is defined as the ratio of the ultimate passive load to the hyperbolic asymptote passive load. The recommended range of R_f values to be used in the program is 0.75 to 0.95 (Duncan and Chang, 1970). P_{ult} is the ultimate passive resistance of the backfill and is computed from Equation 2-15.

$$P_{ult} = E_P . R_{3D} . B \tag{2-15}$$

where E_P is the passive resistance of the backfill per unit length of the wall, R_{3D} is the Ovesen-Brinch Hansen 3D correction factor with an upper limit of two, and B is the embedded wall height. Figure 2-6 illustrates a schematic representation of the hyperbolic relationship used in the log spiral model corrected for 3D effects.

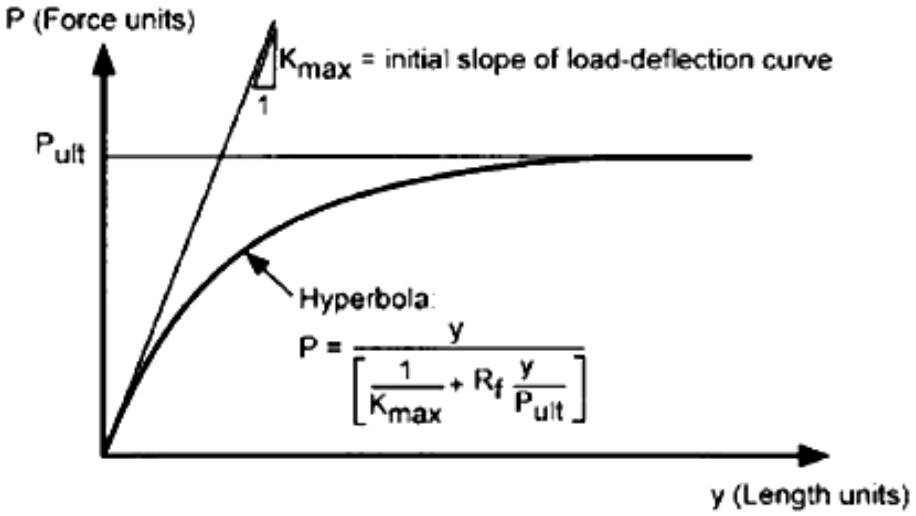

Figure 2-6: Hyperbolic load-displacement relationship used in PYCAP (Duncan and Mokwa, 2001)

The underlying mechanism of the numerical method employed in PYCAP relies on a procedure similar to the conventional log spiral theory graphical procedure described in Terzaghi (1943) and Terzaghi et al. (1996). The critical log spiral failure surface is determined through an iterative process of varying the log spiral center with the objective of calculating the lowest passive resistance of the wall-backfill system. The basic geometry of the log spiral failure surface consists of two sections: a curved logarithmic spiral section which bounds a radial shear zone referred to as the Prandtl zone, and a linear section that intersects the ground surface referred to as the Rankine zone. The failure mechanism assumed in the analysis procedure of PYCAP is shown in Figure 2-3.

In summary, Duncan and Mokwa (2001) conclude that the numerical application of the log spiral theory corrected for 3D effects in PYCAP supersedes the conventional log spiral theory in two ways: (1) it incorporates the shape effects of the wall into the analysis procedure,

and (2) it provides an estimate of the load-displacement relationship in the wall-backfill system. Duncan and Mokwa (2001) further conclude that the log spiral theory corrected for 3D effects provides the most accurate method in predicting the passive earth pressure, for conditions where the wall friction angle is greater than 40% of the soil friction angle. However, engineering judgment is an essential component affecting the performance of PYCAP in accurately estimating the passive earth pressure. Input values used must provide a close representation of the strength and stiffness of the soil under anticipated loading and drainage conditions. Users must also be aware of the limitations of the program concerning the type of surcharge loading, slope of ground surface, and wall alignment.

Shamsabadi et al. (2007)

The development of the mobilized logarithmic-spiral failure surfaces coupled with a modified hyperbolic soil stress-strain behavior (LSH) model presented in Shamsabadi et al. (2007), is based on the main assumption that as an abutment wall is pushed into the backfill, intermediate levels of strains and stresses are mobilized by the backfill, resulting in the development of intermediate failure surfaces. These intermediate failure surfaces progressively develop from the top to the bottom of wall as lateral movement increases. The ultimate failure surface is developed in the backfill, when the ultimate strain level is reached, and corresponds to the ultimate passive resistance of the backfill. The concept of incremental strains and failure surfaces was initially developed and used by Norris (1977) and Ashour et al. (1998) to estimate the lateral capacity of pile foundations by employing an exponential model to define the soil stress-strain relationship. Shamsabadi et al. (2007) builds upon this concept by coupling a mobilized log spiral failure surface model (LS) with a modified hyperbolic load-displacement

relationship (H) to predict the development of passive resistance with backfill displacement. To support the validity of the LSH model in predicting the passive response of abutment backfills, measurements obtained from a number of experimental, centrifuge, and small scale tests were compared with the performance of the model.

Shamsabadi et al. (2007) took an additional step and implemented the LSH model in the computer code ABUTMENT. Soil and retaining wall geometrical properties required in ABUTMENT include the following: internal friction angle (φ), soil cohesion (c), wall friction angle (δ), adhesion factor (α), in-situ unit weight (γ), Poisson's ratio (ν), strain at 50% strength (ε_{50}), and the failure ratio (R_f), which is defined as the ultimate passive load divided by the hyperbolic asymptotic value of passive resistance. Figure 2-7 shows a flowchart presented in Shamsabadi et al. (2007) which illustrates the steps involved in the procedure for determining the load-displacement curve of an abutment-backfill system using the LSH model. The equations referred to in the flowchart can be found in Shamsabadi et al. (2007).

2.3 Relevant Experimental Methods

Rollins et al. (2010)

In an attempt to evaluate the effectiveness of limited width dense gravel backfills in increasing the passive resistance of full width backfills consisting of loose sands, Rollins et al. (2010) carried out a series of lateral pile cap tests at a site located at the FHWA test bed site located at I-15/South Temple in Salt Lake City, Utah. The experimental tests were performed on a 3.67-ft (1.12-m) deep, 17-ft (5.18-m) wide, and 10-ft (3.05-m) long reinforced concrete pile cap with the following backfill conditions: (1) no backfill present; (2) full width (homogeneous) loose silty sand backfill; (3) limited width dense gravel backfill consisting of a 3-ft (0.91-m)

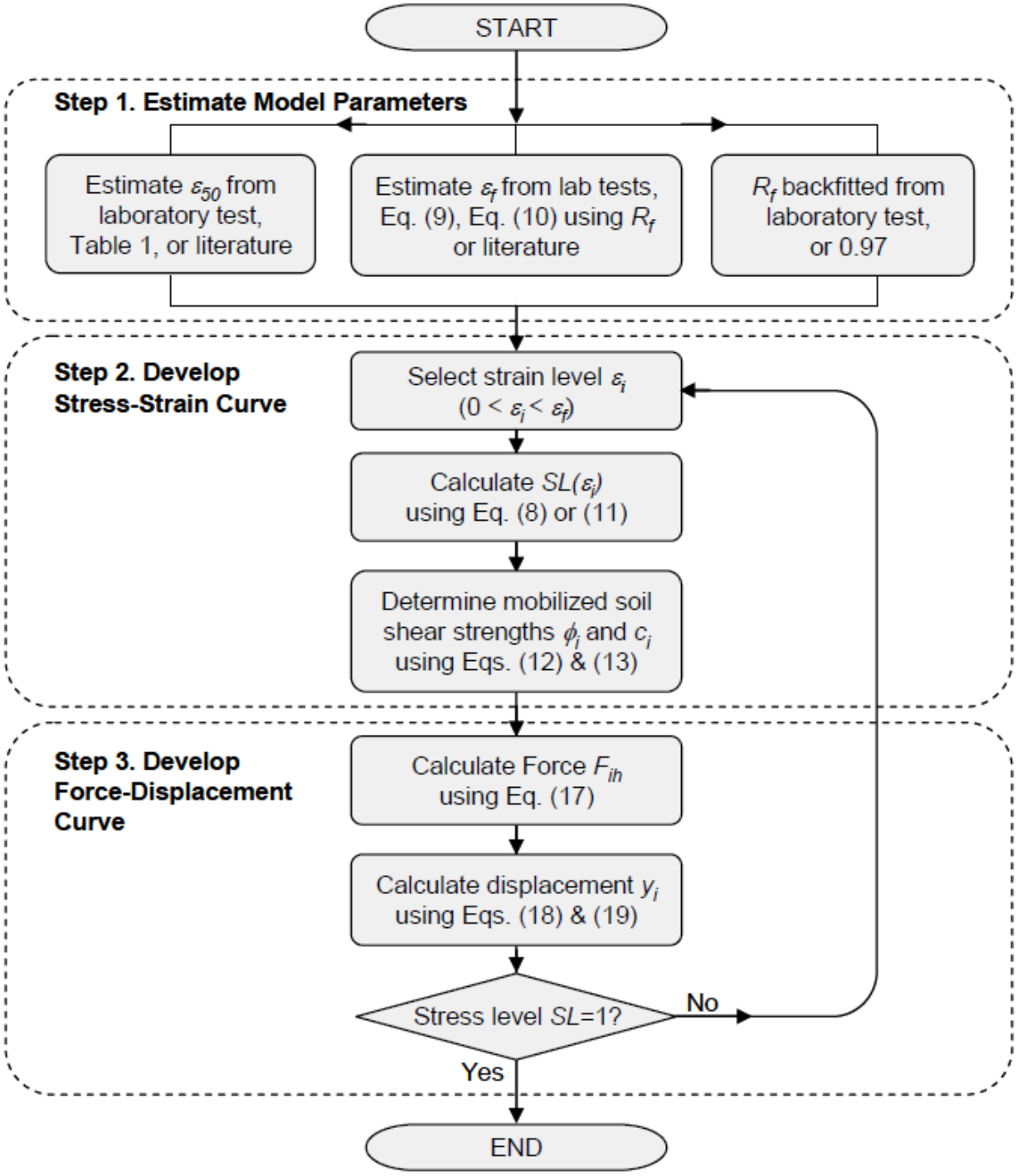

Figure 2-7: LSH methodology flow chart (Shamsabadi et al., 2007)

wide zone of dense gravel between the cap and loose silty sand; and (4) limited width dense gravel backfill consisting of 6-ft (1.83-m) wide zone of dense gravel between the cap and loose silty sand. The no backfill condition was used to obtain a "baseline" load-displacement relationship for the pile cap alone. The baseline curve was then used to plot the passive load-displacement curve for the backfill alone, by subtracting the baseline curve from the total load-displacement curve, for all other backfills. A schematic representation of the four backfill conditions tested is shown in Figure 2-8.

To simulate static loading conditions, equal horizontal forces were applied to both sides of the pile cap using two hydraulic actuators. The load application was conducted in a deflection-controlled procedure, achieving pre-determined pile cap target displacement levels with every static push. At each displacement level, the static load was held constant until the static response of the pile cap was monitored and recorded, followed by applying cyclic and dynamic loads to the pile cap. The hydraulic load actuators and eccentric mass shaker were used to simulate cyclic and dynamic loading conditions in the backfill, respectively. Once this was accomplished, the actuators were activated again to load the pile cap to the next target displacement and the process was repeated. Additional information regarding the test layout, instrumentation and testing procedure is presented in Chapter 3.

The experimental investigation presented in this study provides valuable insight into the static and dynamic passive behavior of gravel backfills of limited width. Based on the analysis of the static portion of test results, Rollins et al. (2010) concluded that placing a relatively thin layer of dense gravel between the pile cap and native loose silty sand material considerably increased the static passive resistance of the backfill. According to Rollins et al. (2010), using a

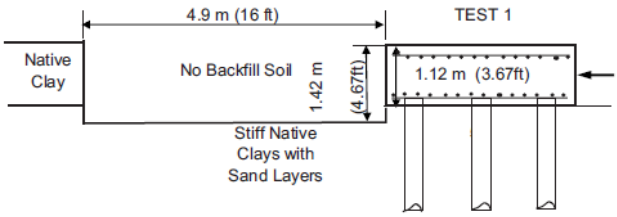

(a) no backfill present

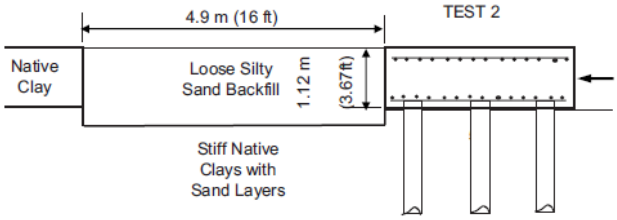

(b) Homogeneous loose silty sand

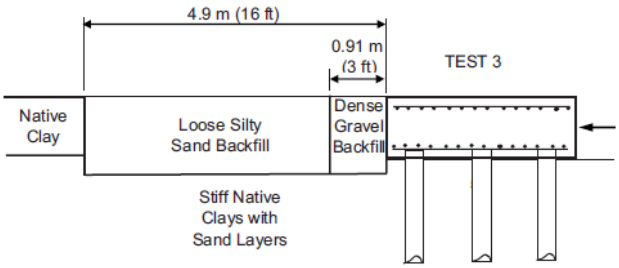

(c) 3-ft (0.91-m) wide dense gravel zone and loose silty sand

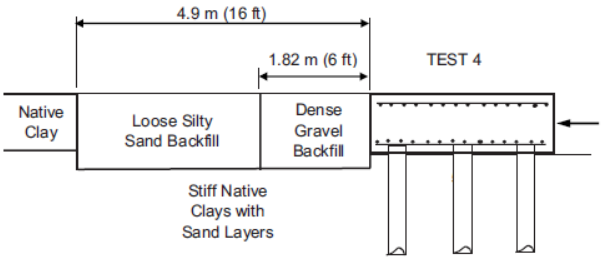

(d) 6-ft (1.83-m) wide dense gravel zone and loose silty sand

Figure 2-8: Schematic representation of full-scale lateral pile cap tests on 3.67-ft (1.12-m) deep pile cap with backfill conditions consisting of: (a) no backfill present; (b) homogeneous loose silty sand; (c) 3-ft (0.91-m) wide dense gravel zone and loose silty sand; and (d) 6-ft (1.83-m) wide dense gravel zone and loose silty sand (Rollins et al., 2010)

limited width dense gravel backfill would especially be appropriate for lateral earth pressure cases where the full replacement of the backfill with select material is financially restricted, despite the desire to enhance the passive performance of the backfill. Rollins et al. (2010) quantified the increase of passive resistance of dense gravel backfills of limited width relative to the full width (homogeneous) loose silty sand, and full width (homogeneous) dense gravel backfills. At any given pile cap deflection, the 3-ft (0.91-m) wide dense gravel zone and loose silty sand backfill increased the total static passive resistance by 75%-150% relative to the full width loose silty sand test. In the case of the 6-ft (1.83-m) wide dense gravel zone and loose silty sand backfill, the increase was quantified as 150%-225% relative to the full width loose silty sand backfill at any deflection. The limited width dense gravel backfills were also reported to have mobilized a significant portion of the total static passive resistance that would have been developed if full width (homogeneous) dense gravel backfills were used. The 3-ft (0.91-m) and 6-ft (1.83-m) wide dense gravel zone and loose silty sand backfills mobilized 54% and 78% of the passive resistance associated with the full width (homogeneous) dense gravel backfills, respectively.

2.4 Numerical Methods

Wilson (2009)

Clough and Duncan (1971) are considered to be pioneers in applying numerical techniques for solving geotechnical engineering problems involving soil-structure interaction. Since the work of Clough and Duncan (1971) a significant amount of additional research involving numerical methods has been conducted in investigating passive earth pressures. The research has typically been performed using commercially available geotechnical software

including PLAXIS, FLAC, etc. One of the most recent passive earth pressure numerical studies performed using PLAXIS was presented by Wilson (2009), in which he reported findings from an experimental study conducted at the University of California, San Diego, and supplemented the experimental testings with numerical simulations, in an effort to investigate the static passive resistance of various wall-backfill systems.

Two experimental tests with differing water contents (9.4% for Test 1 and 8.7% for Test 2) were performed on a relatively light large-scale sheet pile wall, which supported a dense sand backfill, in a large soil container. Lateral loads were applied to the abutment wall using four hydraulic jacks. Instrumentation included load cells, displacement and pressure transducers, and breakable foam cores to assist in recording the loads, displacements and pressure distributions, as well as identifying the failure wedge geometry developed in the backfill, respectively. Figure 2-9 presents a schematic diagram of the elevation view of the test configuration, showing the test wall, backfill, and soil container dimensions.

To investigate the static passive resistance of wall-backfill systems using numerical simulations, estimates of the backfill strength and stiffness parameters were made based on laboratory triaxial and in-situ direct shear test results, as well as the geometry of the observed failure surface. Based on the assumption that light structures have the ability to translate upwards under the application of lateral loading, Wilson (2009) developed a calibrated plane strain finite element model using PLAXIS 2D, with unrestrained vertical and horizontal wall movements to simulate low interface friction angle conditions of Test 1 and Test 2. The satisfactory agreement reached between the numerical simulations and experimental measurements up to 100% and 95% of the measured peak resistance of Test 1 and Test 2, respectively, is shown in Figure 2-10.

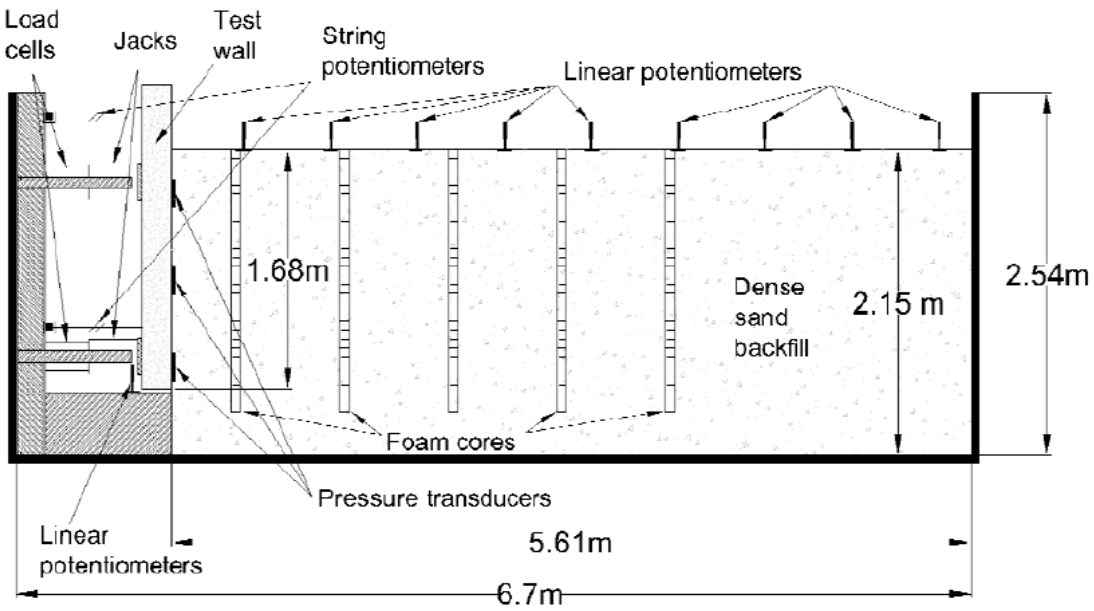

Figure 2-9: University of California, San Diego test configuration, (Wilson, 2009)

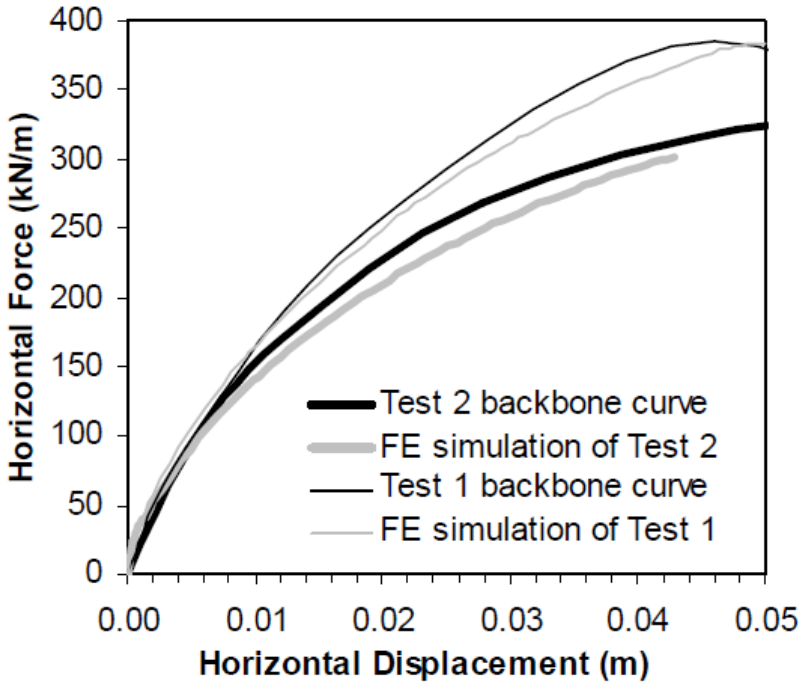

Figure 2-10: Numerical model calibration against Test 1 and Test 2 (Wilson, 2009)

Following these acceptable matches, Wilson (2009) performed additional numerical simulations for a range of cohesion and soil friction angles, under a "low" δ_{mob} condition in which the vertical uplift of the wall is unrestricted, and under a "high" δ_{mob} condition where the vertical uplift of the wall was restricted by setting $\delta_{mob}=0.35\varphi$. Based on these simulations, Wilson (2009) concluded that restraining the vertical movement of the wall increased the passive resistance significantly, compared to the case where unrestricted wall movements were modeled.

Wilson (2009) further utilized the calibrated finite element model to simulate the passive behavior of a wider range of commonly used backfill soil parameters, and wall heights, with the objective of evaluating the passive behavior of different combinations of retaining wall-backfill systems in practical applications. The numerical analyses performed were based on a "high" δ_{mob} condition where $\delta_{mob}=0.35\varphi$. Based on these results, Wilson (2009) confirmed that the soil strength and stiffness, as well as the wall height, have a significant effect on the passive response of the backfill. The observed differences in the passive response of various wall-backfill systems emphasized the importance of selecting design parameters that accurately represent the strength and stiffness characteristics of the backfill soil under field conditions.

Shiau and Smith (2006)

Traditional passive earth pressure theories assume an associative flow rule, which assumes that the dilation angle of the soil is equal to the friction angle. To investigate the effect of using associative ($\psi = \varphi$) and non-associative ($\psi \leq \varphi$) flow rules on the magnitude of the passive earth pressure coefficient, K_P, a parametric study was conducted by Shiau and Smith (2006). Shiau and Smith (2006) performed numerical simulations using the commercial finite difference computer code, FLAC, to calculate the passive earth pressures acting on a vertical

gravity wall supporting a backfill with a level surface. The constitutive model used to represent soil behavior included the elastic-perfectly plastic Mohr-Coulomb model with the application of both associative and non-associative flow rules. Shiau and Smith (2006) concluded that using a non-associated flow rule yields more consistent results with what may be observed in reality, as the dilation angle was shown to have a significant effect on the calculated ultimate passive resistance of the backfill.

3 FIELD TESTING

3.1 Introduction

Two series of full-scale lateral pile cap tests that involved dense gravel backfills of limited width were conducted in August of 2005, and in May and June of 2007, at test sites located near the intersection of Interstate-15 (I-15) and South Temple, and in the proximity of the Salt Lake City International Airport in Salt Lake City, Utah, respectively. Each series of tests consisted of laterally loading a range of full-scale pile caps using hydraulic actuators and an eccentric mass shaker, and recording the passive resistance mobilized by a range of full width and limited width backfill conditions. The main objective of the conducted tests was to better assess the passive resistance of various backfill conditions under static, cyclic, and dynamic loading conditions. However, the tests including limited width gravel zones were designed to determine whether the narrow gravel zone would cause any increase in passive resistance.

The aim of this chapter is to provide general background information for the experimental investigations mentioned above, and to lay the necessary groundwork for introducing the numerical analyses performed in this study. Information presented include a brief summary of the testing configuration, subsurface conditions, backfill soil properties, instrumentation and data acquisition, and experimental test results for both series of tests. Emphasis is placed on experimental results pertaining to the scope of this study. The

information presented in this chapter as related to the South Temple pile cap tests is based on the works of Cole (2003) and Rollins et al. (2010), and Kwon (2007). Gerber et al. (2010) can be referenced as the primary source of information for the SLC Airport tests.

3.2 Subsurface Conditions

3.2.1 South Temple Testing

The lateral pile cap testing performed in August of 2005 was carried out at the Interstate 15 (I-15) National Test Bed site, located in Salt Lake City, Utah, at South Temple Street near 700 West, underneath I-15. Subsurface characterization at the South Temple test site was based on information obtained from a combination of various in-situ and laboratory tests. In-situ testing included the following: Standard Penetration Testing (SPT), Cone Penetration Testing (CPT), Pressuremeter Testing (PMT), Vane Shear Testing (VST), Borehole Shear Testing (BST), Shear Wave Velocity Testing (SCPT), nuclear density testing, and direct shear testing. The laboratory testing was conducted on samples obtained from the site using thin-walled Shelby tubes, a split-spoon sampler, a hand auger, and bulk samples. Soil profile interpretation was largely based on CPT results and laboratory test results of soils sampled in the vicinity of the pile cap. In general, the near surface soil deposits were stiff clay, with some sand layers, while deeper soils in the first 31 ft (9.5 m) of the subsurface profile consisted of moderately to highly plastic clays interbedded with medium dense silty sand layers, underlain by highly plastic, sensitive clays. The soil profile extending to greater depths is composed of alternating layers of silty sand and moderately plastic clay. Figure 3-1 shows the idealized soil profile and CPT results adapted from Cole, (2003).

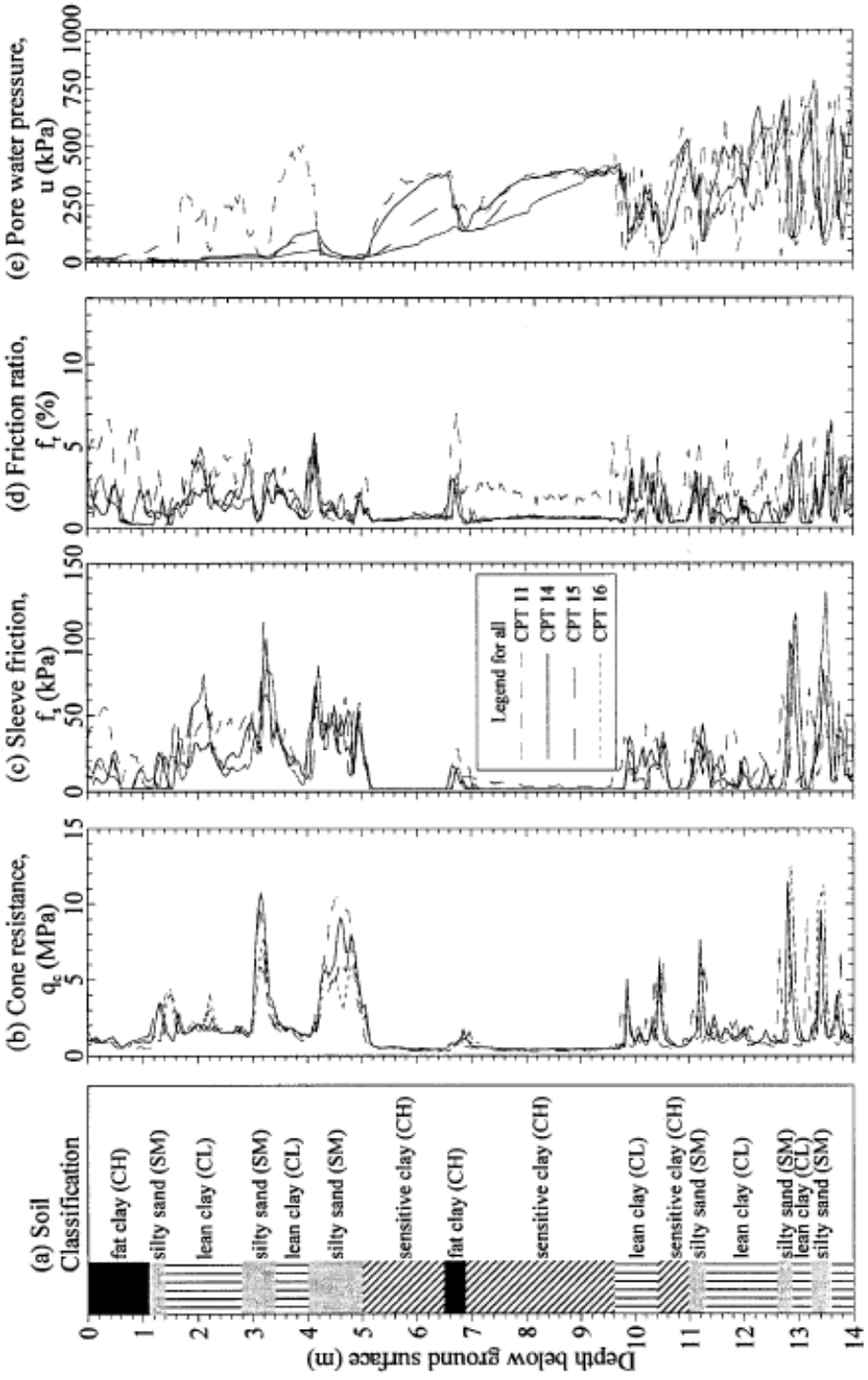

Figure 3-1: Idealized soil profile of South Temple test site based on CPT data adapted from (Cole, 2003)

3.2.2 SLC Airport Testing

The site devoted to the lateral pile cap testing performed in 2007, is located approximately 1000 ft (300 m) north of the control tower at the Salt Lake City (SLC) International Airport, in Salt Lake City, Utah. Information regarding the SLC Airport test site subsurface soil characteristics was obtained from a combination of in-situ field tests including Standard Penetration Testing (SPT) and Cone Penetration Testing (CPT), as well as laboratory shear strength and index property testing. A significant portion of this information was available from prior subsurface investigations conducted for full-scale experimental tests performed at the site in previous years, involving deep foundations. These studies include the investigations conducted by Peterson (1996), Rollins et al. (2005a, 2005b), Christensen (2006), and Taylor (2006). Figure 3-2 shows an idealized subsurface profile of the test site based on CPT results, adapted from Christensen (2006). According to the idealized soil profile, lean clay and sandy silt soils with two 5 to 6.5-ft (1.5 to 2-m) thick silty sand and poorly graded sand layers underlaid the pile cap to a depth of about 33-ft (10-m). Deeper soil layers consisted of interbedded sandy silts and silty sands. In addition, the water table fluctuated between 0 to 6-in (150-mm) above the base of the pile cap, during the testing of the pile cap.

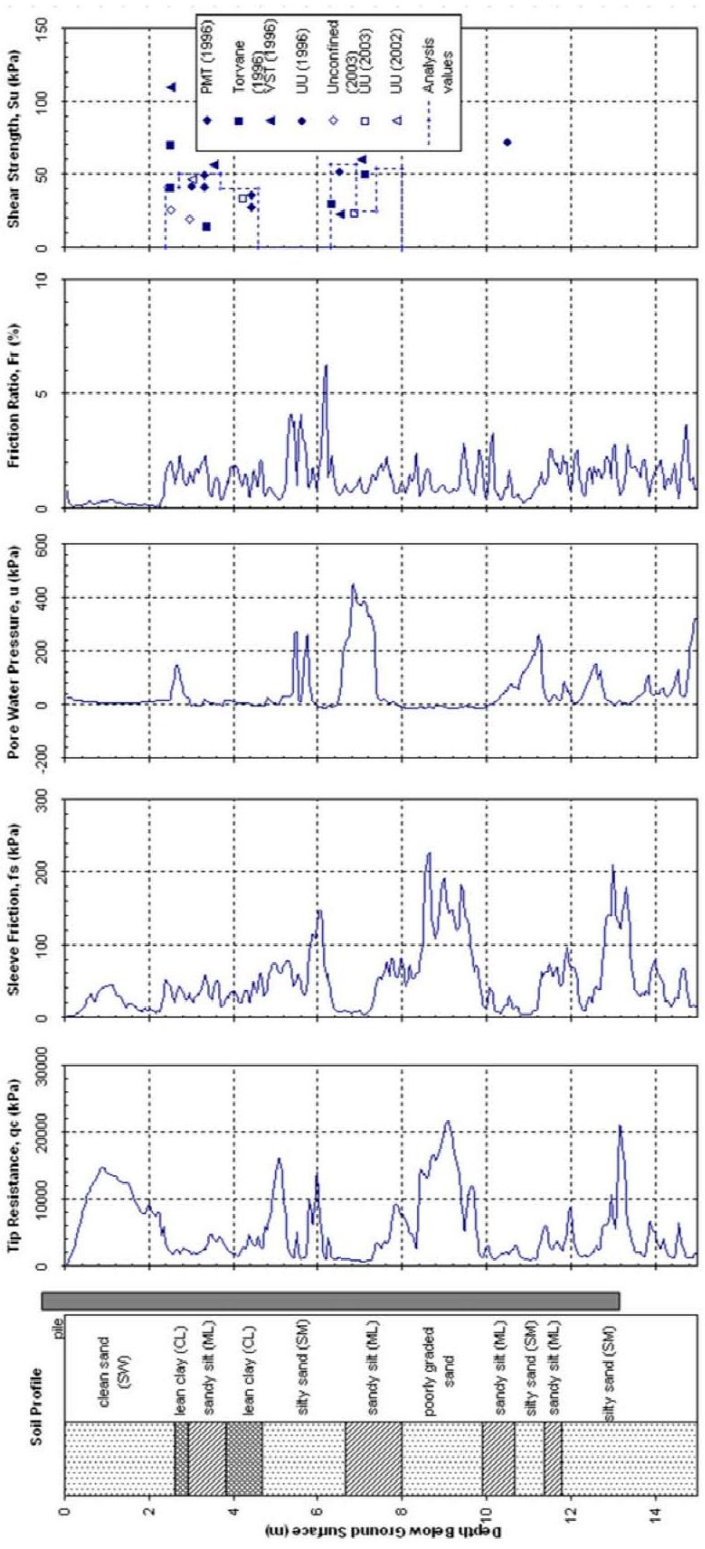

Figure 3-2: Idealized soil profile of SLC Airport test site based on CPT data (Christensen, 2006)

3.3 Testing Layout

3.3.1 South Temple Testing

The test configuration at the South Temple site was mainly comprised of a reaction foundation, a test pile cap, and the backfill. The plan and profile views of the test configuration are illustrated in Figure 3-3. The reaction foundation was supported by a pile group, consisting of 9 open-ended steel pipe piles, with an outside diameter and wall thickness of 24 and 0.5 in (610 and 12.7 mm), respectively. The piles were driven to a depth of approximately 40-ft (12.2-m) below the ground surface with a center to center spacing of 6 ft (1.83 m) in both directions.

The reinforced concrete pile cap was 10 ft (3.05 m) long, 17 ft (5.18 m) wide, and 3.67 ft (1.12 m) deep, and was constructed over a pile group, consisting of 12 closed-ended steel pipe piles, with an outside diameter and wall thickness of 12.75 and 0.375-in (324 and 9.5-mm), respectively. This pile cap was originally constructed by Rollins et al. (2003) specifically for use in experimental testing conducted by Rollins and Cole (2006). The piles were driven to a depth of approximately 40 ft (12.2 m) below the ground surface with center to center spacings of 4.7 and 3.5 ft (1.42 and 1.06 m) in the East-West and North-South directions, respectively. The concrete used in the cap had a compressive strength of 5000 psi (34.5 MPa). The steel reinforcement in the cap mainly consisted of a reinforcement mat with transverse and longitudinal reinforcing bars placed in both the top and the bottom of the cap.

The 17 ft (5.18 m) wide by 3.67 ft (1.12 m) deep side of the pile cap was backfilled from the base of the pile cap to a height of approximately 3.67 ft (1.12 m). The backfill was extended approximately 16 ft (4.9 m) behind the pile cap and 6 ft (1.8 m) laterally beyond the edges of the cap on each side. The final dimensions of the backfill zone after placement were approximately

29 ft (8.8 m) wide and 16 ft (4.9 m) long. In the case of limited width dense gravel backfills, 3-ft (0.91-m) and 6-ft (1.83-m) wide zones of dense gravel were compacted between the pile cap face and the loose silty sand.

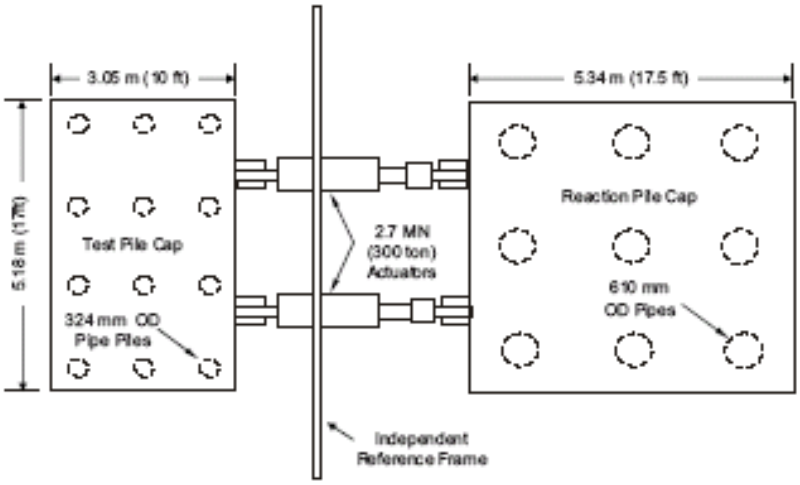

(a) Plan view

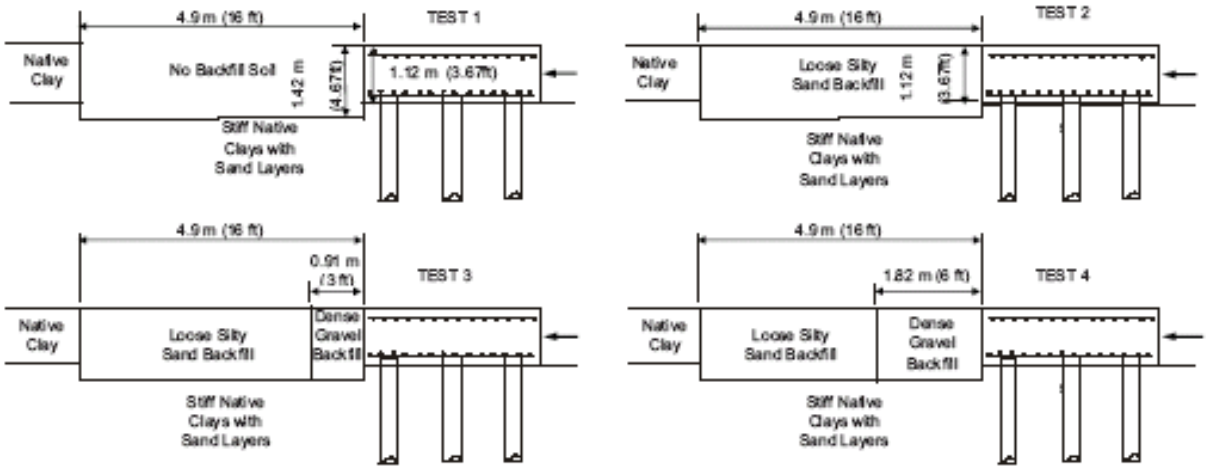

(b) Profile views

Figure 3-3: Plan and profile views of South Temple test configuration (Rollins et al., 2010)

3.3.2 SLC Airport Testing

The test configuration at the SLC Airport site mainly consisted of a reaction foundation, a test pile cap, and the backfill. The plan and profile views of the test configuration are shown in Figure 3-4. The reaction foundation was supported by two 4 ft (1.2 m) diameter drilled shafts, spaced 12 ft (3.66 m) center to center. The reinforced concrete pile cap was 5.5-ft (1.68-m) deep, 15-ft (4.57-m) long, 11-ft (3.35-m) wide and was constructed over a pile group, consisting of 6 ASTM A252 Grade 3 closed-ended steel pipe piles, with an outside diameter and wall thickness of 12.75 and 0.375-in (324 and 9.5-mm), respectively. The piles were driven for use in previously conducted full-scale deep foundation tests at the site, to a depth of approximately in 42.6 ft (13 m) below the ground surface, with a center to center spacing of 12 ft (3.66 m) in the direction of loading. The concrete used in the cap had a compressive strength of 6000 psi (41 MPa). The cap reinforcement mainly consisted of longitudinal and transverse reinforcing bars, placed in both the top and the bottom of the cap.

The 11-ft (3.35-m) wide by 5.5-ft (1.68-m) high side of the pile cap was backfilled from the base of the pile cap to a height of approximately 5.5-ft (1.68-m). The final dimensions of the backfill zone after placement were approximately 23 ft (7.0 m) wide and 28 ft (8.5 m) long. In the case of limited width dense gravel backfills, 3-ft (0.91-m) and 6-ft (1.83-m) wide zones of dense gravel were compacted between the pile cap face and the loose clean sand. The gravel zones were also placed beyond the edges of the pile cap in the lateral direction by the same dimensions as their respective widths.

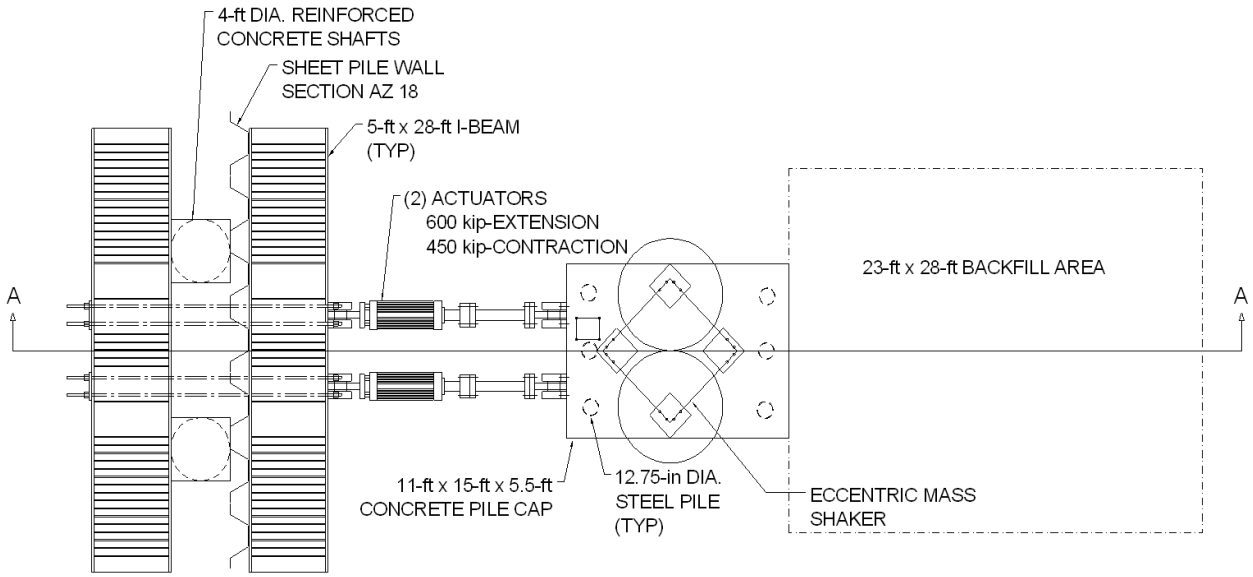

(a) Plan view

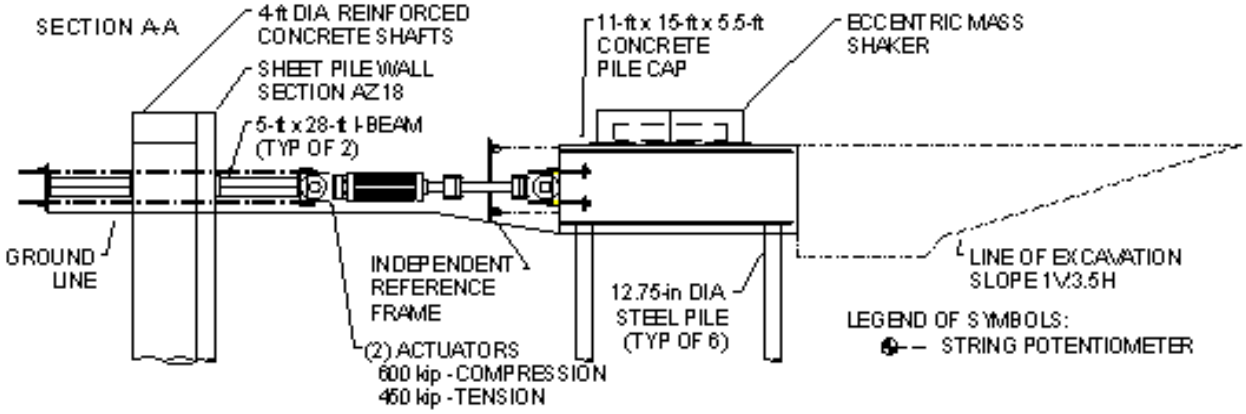

(b) Profile view

Figure 3-4: Plan and profile views of SLC Airport test configuration (Gerber et al., 2010)

3.4 Backfill Soil Properties

This section summarizes the soil properties associated with the backfill materials used in the South Temple and SLC Airport backfill conditions pertaining to the scope of this study. Information presented in this section was subsequently used to numerically model soil behavior, as well as the interaction between the soil and the pile cap. Although this information served as the basis for selecting input parameters used in the numerical models, various adjustments were made to the soil parameters defined in this section to obtain satisfactory agreement between analytical, numerical, and field results. Details regarding the selection and adjustment of input parameters used in the numerical models are provided in chapter 4.

3.4.1 South Temple Testing

Five different backfill conditions were tested at the South Temple site in 2005. The full range of backfill conditions tested include: (1) no backfill present; (2) full width (homogeneous) loose silty sand backfill; (3) full width (homogeneous) dense silty sand backfill; (4) limited width dense gravel backfill consisting of a 3-ft (0.91-m) wide zone of dense gravel between the cap and loose silty sand; and (5) limited width dense gravel backfill consisting of 6-ft (1.83-m) wide zone of dense gravel between the cap and loose silty sand. The backfill conditions tested at the South Temple site that are relevant to this study are presented in Table 3-1.

Two types of backfill materials used in the tests are relevant to this study: silty sand and fine gravel. According to the Unified Soil Classification (USC) System the silty sand classified as SM. The American Association of State Highway and Transportation Officials (AASHTO) classification of the material is A-4. The maximum particle size of the fill was (12.5 mm) with approximately 90% passing the No. 40 sieve and 45% non-plastic fines content. The coefficient

of uniformity, C_u, and curvature, C_c, were 14.8 and 2.8, respectively. The standard and modified Proctor maximum unit weights were 107.6 and 113.0 pcf (16.9 and 17.75 kN/m^3), respectively. The fine gravel used as the compacted fill was a typical roadbase material, which classified as silty, clayey gravel with sand (GC-GM) according to the USC System. The AASHTO Classification of the material is A-1-b. The gravel fill had a maximum particle size of (19 mm). C_u and C_c were 454 and 1.2, respectively. The standard and modified Proctor maximum unit weights were 127.7 and 138.0 pcf (20.06 and 21.68 kN/m^3), respectively. Index properties associated with the silty sand and fine gravel materials are summarized in Table 3-2.

Table 3-1: Summary of relevant backfill conditions tested at the South Temple site

Date	Backfill Type
August 16, 2005	No backfill (free response)
August 18, 2005	Full width (homogeneous) loose silty sand
August 24, 2005	3-ft(0.91-m) wide gravel zone and loose silty sand
August 26, 2005	6-ft(1.83-m) wide gravel zone and loose silty sand

Table 3-2: Index properties for silty sand and fine gravel backfill materials

Backfill Type	Gravel (%)	Sand (%)	Fines (%)	C_u	C_c	Mod. Proctor	Stand. Proctor
						γ_d pcf (kN/m^3)	γ_d pcf (kN/m^3)
Silty Sand	2.4	52.9	44.7	15	2.8	113.0 (17.75)	107.6 (16.9)
Fine gravel	49.7	30.5	19.9	454	1.2	138.0 (21.68)	127.7 (20.06)

Several in-situ and laboratory direct shear tests provided estimates of the loose silty sand strength parameters. Strength parameters associated with the dense fine gravel were estimated based on direct shear tests performed on a comparable material at a different site. Nuclear density tests were performed during compaction on each layer of compacted silty sand and fine gravel fill to determine the average dry unit weight, $\gamma_{d\ (avg)}$. The relative density (D_r). was estimated based on the average dry unit weight using correlations developed by Lee and Singh, (1971). The interface friction angle, δ, was determined by performing soil-concrete direct shear tests, as well as recommendations given by Potyondy, (1961). A summary of the engineering characteristics of the loose silty sand and dense fine gravel materials is summarized in Table 3-3.

Table 3-3: Summary of the direct shear test data for loose silty sand and dense fine gravel backfill materials

Backfill Type	$\gamma_{d\ (avg)}$ pcf (kN/m^3)	w_{avg} (%)	D_r (%)	φ (°)	c psf (kPa)	δ/φ
Loose Silty Sand	99.9 (15.7)	11.1	40	27.7	142.0 (6.8)	0.75
Dense Fine gravel	132.4 (20.8)	6.1	85	42.0*	409.3 (19.6)	0.75

*This value is based on back-analysis of measured versus analytical load-displacement curves.

3.4.2 SLC Airport Testing

Nine different backfill conditions were tested at the Salt Lake City International Airport site in 2007. The full range of backfill conditions tested include: (1) no backfill present; (2) full width (homogeneous) loose clean sand backfill; (3) full width (homogeneous) dense clean sand

backfill; (4) full width (homogeneous) loose fine gravel backfill; (5) full width (homogeneous) dense fine gravel backfill; (6) full width (homogeneous) loose coarse gravel backfill; (7) full width (homogeneous) dense coarse gravel backfill; (8) full width (homogeneous) dense clean sand backfill with MSE walls; (9) limited width dense gravel backfill consisting of a 3-ft (0.91-m) wide zone of dense coarse gravel between the cap and loose clean sand; and (10) limited width dense gravel backfill consisting of a 6-ft (1.83-m) wide zone of dense coarse gravel between the cap and loose clean sand. The backfill conditions tested at the SLC Airport site that are relevant to this study are presented in Table 3-4.

Table 3-4: Summary of relevant backfill conditions tested at the SLC Airport site

Date	Backfill Type
May 29, 2007	Full width (homogeneous) loose clean sand
June 1, 2007	3-ft(0.91-m) wide gravel zone with loose silty sand
June 4, 2007	6-ft(1.83-m) wide gravel zone with loose silty sand
June 11, 2007	Full width (homogeneous) dense fine gravel
June 21, 2007	No backfill (free response)

Two types of backfill materials used in the tests are relevant to this study: clean sand and fine gravel. According to the USC System, the clean sand classified as a well graded sand (SW). The AASHTO Classification of the material is A-2-6(0). The coefficient of uniformity and curvature of the clean sand fill were 8.7 and 1.2, respectively. The standard and modified Proctor maximum unit weights were 105 and 111 pcf (16.5 and 17.4 kN/m^3), respectively. The

fine gravel classifies as a well graded sand with gravel (SW) according to USC System. The AASHTO Classification of the material is A-1-a. The coefficient of uniformity and curvature of the gravel fill were 22.5 and 1.2, respectively. The standard and modified Proctor maximum unit weights were 122.0 and 131.8 pcf (19.2 and 20.7 kN/m^3), respectively. Index properties associated with the clean sand and fine gravel fills are summarized in Table 3-5.

Table 3-5: Index properties for clean sand and fine gravel backfill materials

Backfill Type	Gravel (%)	Sand (%)	Fines (%)	C_u	C_c	Mod. Proctor	Stand. Proctor
						γ_d pcf (kN/m^3)	γ_d pcf (kN/m^3)
Clean Sand	6	92	2	8.7	1.2	111.0 (17.4)	105.0 (16.5)
Fine gravel	39	57	4	22.5	1.2	131.8 (20.7)	122.0 (19.2)

To determine the shear characteristics of the clean sand and fine gravel a combination of laboratory-based and in-situ direct shear tests were performed. In-situ direct shear testing was not performed on the loose clean sand backfill. Laboratory direct shear tests for both backfill materials were conducted in accordance with ASTM D 3080 in the Brigham Young University soil mechanics laboratory. Nuclear density tests were also performed on each layer of compacted silty sand and fine gravel fill to determine the average dry unit weight, $\gamma_{d\ (avg)}$. The relative density, D_r, was estimated based on correlations developed by Lee and Singh, (1971). The interface friction angle, δ, was determined by performing a series of soil-concrete modified direct shear tests, using a sample of the concrete used in the pile cap and fine gravel. A summary

of the engineering characteristics of the loose clean sand and dense fine gravel fills are contained in Table 3-6.

Table 3-6: Summary of the direct shear test data for the loose clean sand and dense fine gravel backfill materials

Backfill Type	Laboratory Values				In-situ		δ/φ
	Peak		Ultimate				
	ϕ (°)	c psf (kPa)	ϕ (°)	c psf (kPa)	ϕ (°)	c psf (kPa)	
Loose Clean Sand	37.3	0	37.0	0	---	---	0.7
Dense Fine Gravel	52.0	270 (12.9)	50.0	275 (13.2)	44.3	410 (19.6)	0.61

Table 3-7: Summary of average unit weight and relative density properties for the loose clean sand and dense fine gravel backfill materials

Backfill Type	As Compacted		
	$\gamma_{d\ (avg)}$ pcf (kN/m^3)	w_{avg} (%)	D_r (%)
Loose Clean Sand	98.6 (15.5)	8.0	44
Dense Fine Gravel	125.4 (19.7)	9.7	74

3.5 Instrumentation and General Testing Procedure

Instrumentation for the South Temple and SLC Airport lateral pile cap tests included an independent reference frame, string potentiometers, triaxial accelerometers, and pressure cells. The independent reference frame was placed between the pile cap and reaction foundation,

providing a separate datum of reference for measuring pile cap movements. String potentiometers were installed in various locations on the pile cap, and the surface of the backfills, to provide measurements of the pile cap movement relative to the reference frame and backfill. Triaxial accelerometers were installed on the four corners of the pile cap and at a position near the center of the backfilled face of the cap. Data obtained from the accelerometers were used to obtain the pile cap displacements during dynamic tests. The pressure cells were installed along the central portion of the backfilled face of the pile cap. These pressure cells were used to determine the passive resistance of the backfill by measuring the earth pressure exerted along the face of the cap. Pressure distributions along the pile cap face were also monitored with the aid of the pressure cells.

Lateral load testing was performed on the pile cap using a load-deflection control procedure, with a combination of hydraulic load actuators and an eccentric mass shaker. Static loads were applied to the pile cap using a pair of 600-kip (2.7-MN) capacity hydraulic actuators to displace the pile cap into the backfill to an initial target displacement level. The load was then held at that displacement level for a few seconds, until the static response of the pile cap was monitored and recorded. Holding the static load constant at the target displacement level, cyclic loading was applied to the pile cap using the hydraulic load actuators, followed by the application of dynamic loads using the eccentric mass shaker to record the cyclic and dynamic responses of the pile cap. Once this was accomplished, the actuators were activated again to push the pile cap into the backfill to the next target displacement, and the outlined procedure was repeated.

3.6 Test Results

The main outcome of the South Temple and SLC Airport lateral pile cap tests include horizontal passive load versus displacement relationships, for various full width (homogenous) and limited width backfill conditions associated with static, cyclic, and dynamic loadings. Pressure distributions, cracking patterns, vertical and horizontal movements of the tested backfills were also part of the tests results obtained. In this section, the results presented are limited to static load-displacement responses, and vertical movements of the backfill surface associated with backfill conditions pertaining to the scope of the study. In addition a comparison of the limited width dense gravel backfills tested at the South Temple and SLC Airport sites is contained at the end of this section.

3.6.1 Static Load-Displacement Response

Two basic methods were used in developing load-displacement relationships for the South Temple and SLC Airport tests. In the first method, the development of load-displacement curves was based on actuator loading data. Total load-displacement curves for each pile cap-backfill system were developed by plotting the peak load at the end of each static actuator push, against the corresponding pile cap movement. The no backfill condition test was then used to obtain a "baseline" load-displacement relationship for the pile cap. Since the pile cap was statically loaded without the presence of any backfill, the resistance measured from this test was due to the resistance of the piles, the pile-soil interaction, and any friction existing between the base of the pile cap and the underlying soil. Once this was accomplished, the load-displacement curve associated with the backfill alone was determined, by subtracting the baseline curve from the total load-displacement curve of the system.

The second method calculates load-displacement curves using data obtained from the pressure cells installed along the face of the pile cap. By adjusting the measured data according to the tributary area associated with each pressure cell, the passive resistance of the pile cap was determined as a function of pile cap displacement. Load-displacement results presented in this section were obtained using the first method, and are associated with static loading conditions. In addition, these results are limited to the backfill conditions pertaining to the scope of study.

3.6.1.1 South Temple Testing

Figure 3-5 plots the backfill passive load-displacement curves associated with the South Temple lateral pile cap tests. The backfill conditions presented in the figure include: (1) full width (homogeneous) loose silty sand; (2) limited width dense gravel backfill consisting of a 3-ft (0.91-m) wide zone of dense gravel between the pile cap and loose silty sand and; (3) limited width dense gravel backfill consisting of a 6-ft (1.83-m) wide zone of dense gravel between the pile cap and loose silty sand. In each test, the total measured passive force has been normalized by the actual pile cap width of 17 ft (5.18 m) to obtain the force per width of pile cap.

The loose silty sand backfill appears to experience a gradual increase in resistance starting at a displacement level of 0.5 in (12.7 mm) to a maximum displacement of 2 in (51 mm). All the curves appear to show a slight upturn at a displacement of about 1.5 in. This load increase may have been due to reduced stiffness in the baseline curve at large displacements with multiple load cycles.

The measured ultimate passive resistance of each test is tabulated in Table 3-8 for comparison among different backfill conditions. The table also contains the displacements at which the ultimate resistances appear to mobilize. Note that these values may not represent the

actual maximum passive resistance of the backfill. As explained previously, the backfills experiences an abrupt increase in resistance starting at a displacement level of 1.5 in (12.7 mm) to a maximum displacement of 2 in (51 mm). This load increase may have been due to small variations in the slope of the measured baseline curve.

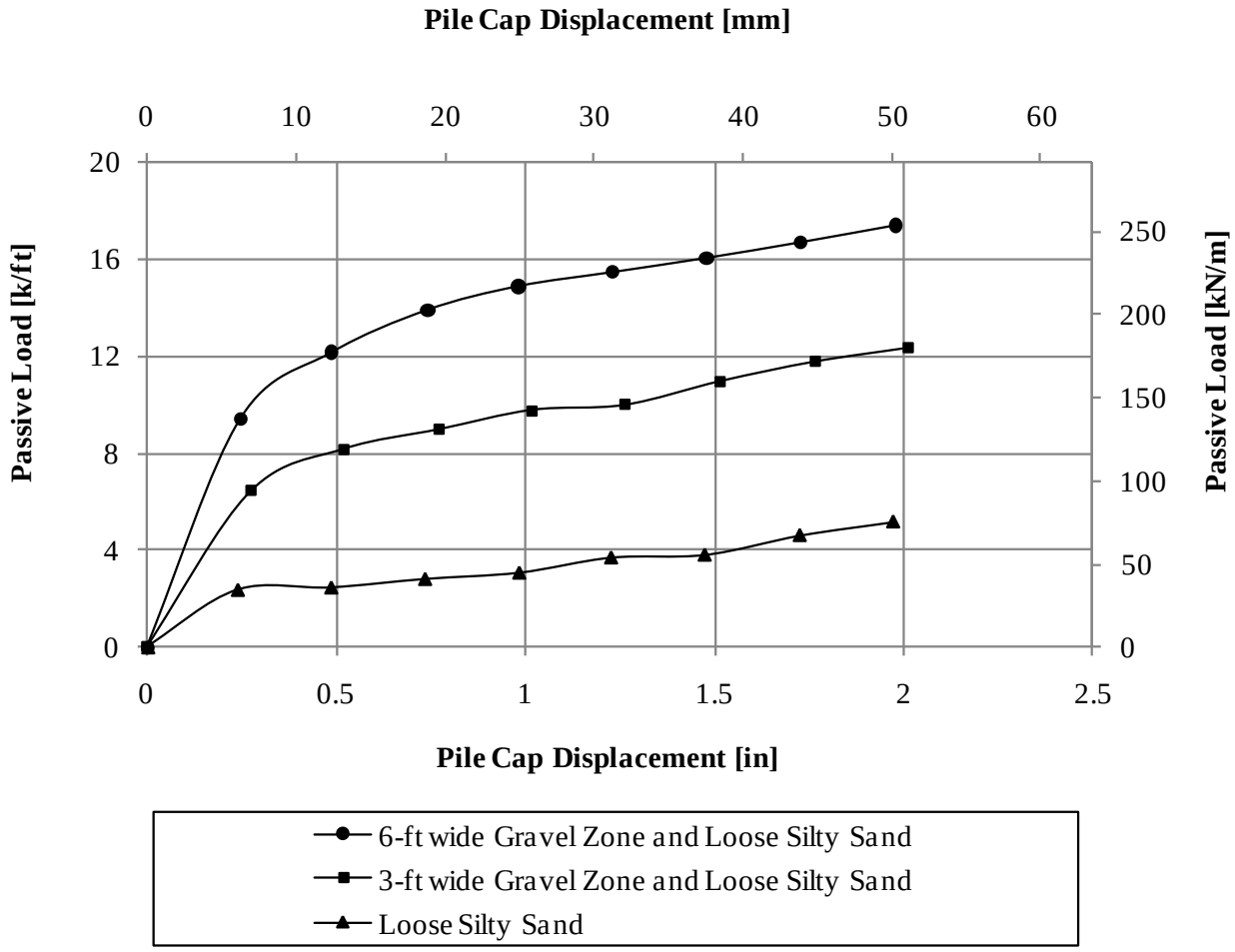

Figure 3-5: Comparison of measured load-displacement curves, normalized by the pile cap width of 17 ft (5.18 m), for South Temple backfill conditions consisting of: (1) full width (homogeneous) loose clean sand; (2) 3-ft (0.91-m) wide gravel zone and loose silty sand; and (3) 6-ft (1.83-m) wide gravel zone and loose silty sand

Table 3-8: Summary of measured South Temple ultimate passive earth resistance and associated displacement for different backfill conditions

Backfill Type	Peak Resistance, k/ft (kN/m)	Δ_{max}, in (mm)	Δ_{max}/H
Full width (homogeneous) loose silty sand	≅ 5.2 (75.8)	≅ 2 (51)	0.045
3-ft (0.91-m) wide gravel zone and loose silty sand	≅ 12.3 (179.8)	≅ 2 (51)	0.045
6-ft (1.83-m) wide gravel zone and loose silty sand	≅ 17.4 (253.7)	≅ 2 (51)	0.045

Based on the load-displacement curves presented in Figure 3-5, and the data contained in Table 3-8, the effectiveness of the limited width dense gravel backfills in increasing the passive resistance of the backfill can be quantified, relative to the full width (homogeneous) loose silty sand, and full width (homogeneous) dense gravel backfills. At any given pile cap deflection, the 3-ft (0.91-m) wide dense gravel zone and loose silty sand backfill increased the total static passive resistance by 75%-150% relative to the full width loose silty sand test. In the case of the 6-ft wide (1.83-m) dense gravel zone and loose silty sand backfill, the increase is 150%-225% relative to the full width loose silty sand backfill at any deflection. In addition, the limited width dense gravel backfills tested mobilized a significant portion of the resistance that would have been developed if full width (homogeneous) dense gravel backfills were used instead. The 3-ft (0.91-m) and 6-ft (1.83-m) wide dense gravel zone and loose silty sand backfills mobilized 54% and 78% of the passive resistance associated with full width dense gravel backfills, respectively.

3.6.1.2 SLC Airport Testing

Figure 3-6 plots the backfill passive load-displacement curves associated with the SLC Airport lateral pile cap tests. The backfill conditions presented in the figure include: (1) full width (homogeneous) loose clean sand; (2) full width (homogeneous) dense fine gravel; (3) limited width dense gravel backfill consisting of a 3-ft (0.91-m) wide zone of dense gravel between the pile cap and loose silty sand and; (4) limited width dense gravel backfill consisting of a 6-ft (1.83-m) wide zone of dense gravel between the pile cap and loose silty sand. In each test, the total measured passive force has been divided by the pile cap width of 11-ft (3.35-m) to obtain the force per width of pile cap.

In general, the curves shown in Figure 3-6 appear to have flatter slopes, as a result of lower initial loading stiffnesses, compared to slopes that are typical of static load-displacement curves. This behavior may be attributed to the following factors: (1) cyclic and dynamic loading effects, and (2) Creep displacement of the cap during the time between backfill placement and starting of the backfill tests (Gerber et al., 2010). Equipment malfunctioning during the full width (homogeneous) loose clean sand test led to the premature ending of the test. As a result, passive force measurements were not obtained for further than about 2 in (50 mm) of pile cap displacement. In addition, to prevent premature damages to the pile cap connections and alteration of the baseline response associated with the 3-ft (0.91-m) limited width dense gravel backfill, the pile cap was not pushed further than 2.5 in (64 mm) for this test. The load-displacement curve associated with the 6-ft (1.83-m) limited width backfill, showed a similar passive response to the 3-ft (0.91-m) limited width backfill. To help determine whether the 6-ft (1.83-m) limited width backfill had reached its maximum resistance at a displacement level of 2.5 in (64 mm), the pile cap was pushed further to a maximum displacement of 3 in (76.2 mm).

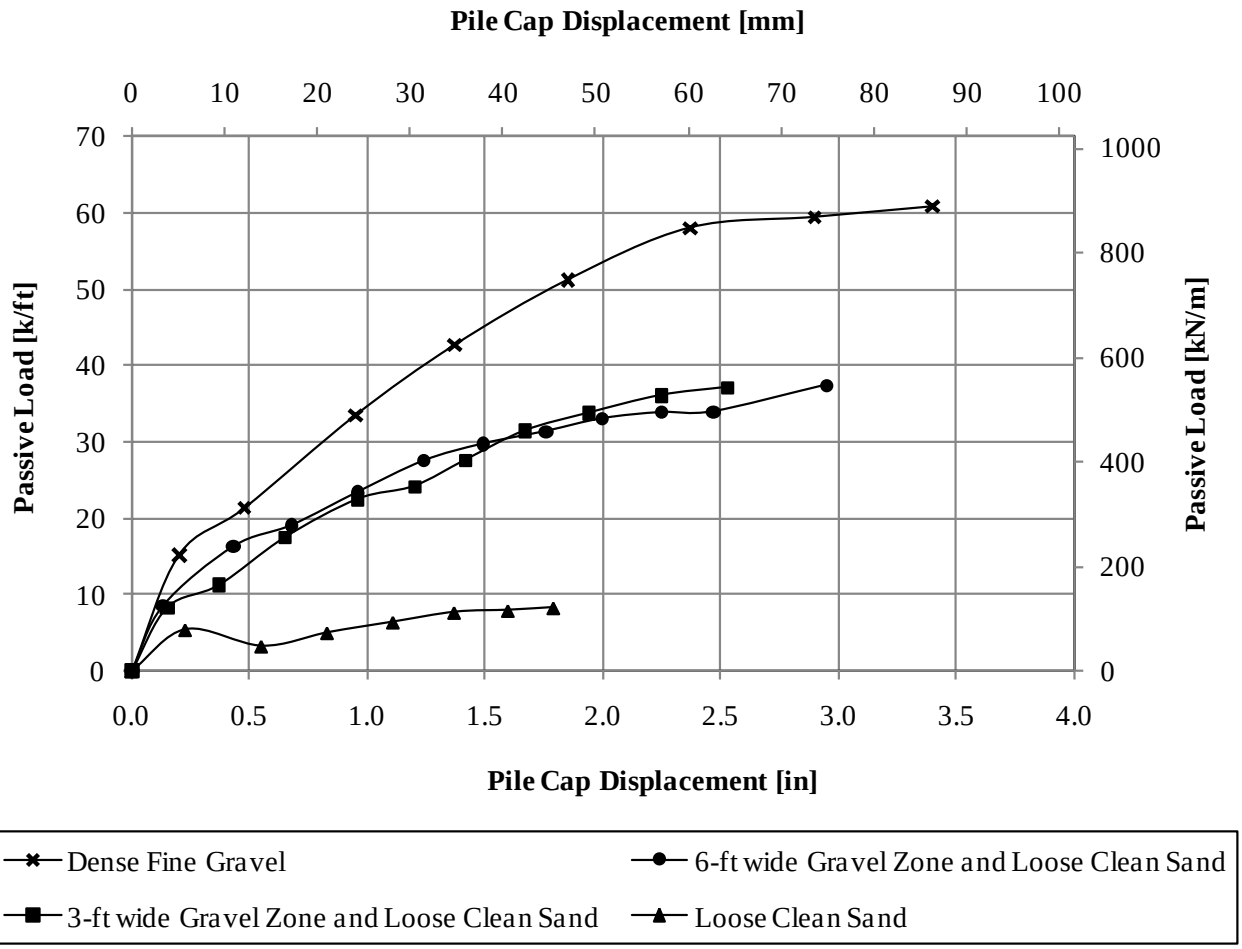

Figure 3-6: Comparison of measured load-displacement curves, normalized by the pile cap width of 11-ft (3.35-m), for SLC Airport backfill conditions consisting of: (1) full width (homogeneous) loose clean sand, (2) full width (homogeneous) dense fine gravel, (3) 3-ft (0.91-m) wide gravel zone and loose clean sand, and (4) 6-ft (1.83-m) wide gravel zone and loose clean sand

The measured ultimate passive resistance of each test is tabulated in Table 3-9 for comparison among the different backfill conditions. The table also contains the displacements at which the ultimate resistances were mobilized. Note that the ultimate resistance associated with the loose clean sand and the 6-ft (1.83-m) wide limited width backfills, is the maximum resistance mobilized in the backfill at the end of the test and may not be the actual peak passive

resistance associated with the backfills. It is likely that the maximum measured backfill resistances would have been higher if the pile cap was able to displace further into the backfill.

Table 3-9: Summary of measured SLC Airport ultimate passive earth resistance and associated displacement for different backfill conditions

Backfill Type	Peak Resistance, k/ft (kN/m)	Δ_{max}, in (mm)	Δ_{max}/H
Full width (homogeneous) loose clean sand	≅ 8 (116.7)	≅ 1.5 (38.1)	0.023
Full width (homogeneous) dense fine gravel	≅ 58.4 (852.2)	≅ 2.4 (61)	0.037
3-ft (0.91-m) wide gravel zone and loose silty sand	≅ 36.8 (537)	≅ 2.5 (63.5)	0.037
6-ft (1.83-m) wide gravel zone and loose silty sand	≅ 37.4 (545.8)	≅ 3.0 (76.2)	---

Based on the load-displacement curves presented in Figure 3-6, as well as the data contained in Table 3-9, the effectiveness of the limited width dense gravel backfills in increasing the passive resistance of the backfill can be quantified, relative to the full width (homogeneous) loose silty sand and full width (homogeneous) dense gravel backfills. At a displacement level of 1.8 in (45 mm), the 3-ft (0.91-m) and 6-ft (1.83-m) limited width backfills exhibit similar behaviors. At this displacement level, placement of either a 3-ft (0.91-m) or 6-ft (1.83-m) wide zone of dense gravel between the pile cap and loose clean sand backfill increased the total static passive resistance of the limited width backfills by approximately 300%, relative to the full width (homogeneous) loose clean sand backfill. This amount of passive resistance in the limited

width backfills can be quantified as about 60% of the resistance that would have developed if a full width (homogeneous) dense gravel backfill was used instead. However, at a higher displacement level (2.4 in (62 mm)), the 3-ft (0.91-m) limited width backfill provides approximately 3.1 k/ft (44.7 kN/m) more passive resistance than the 6-ft (1.83-m) limited width backfill.

3.6.2 Vertical Displacements

During the South Temple and SLC Airport tests vertical movements of the surface area of the backfills were monitored by utilizing traditional surveying equipment, and a painted grid on the surface of the backfills. For the South Temple and SLC Airport tests, 2-ft (0.61-m) square grids were painted on the surface of the backfill to provide a systematic method for recording elevation changes during the testing. Vertical surveys were performed at the beginning and end of each test, at the node points of the grids. Therefore, the results presented in this section include cyclic and dynamic loading effects.

3.6.2.1 South Temple Testing

Figure 3-7 plots the vertical displacement of the backfill surface as a function of distance from the pile cap face, illustrating the change in elevation of the surface of South Temple full width (homogeneous) and limited width backfills during testing. Vertical displacements represent the average elevation change at the node points in a given row (parallel to the face of the cap). Vertical displacement measurements were limited to the central portion of the pile cap to eliminate 3D effects from the pile cap edges.

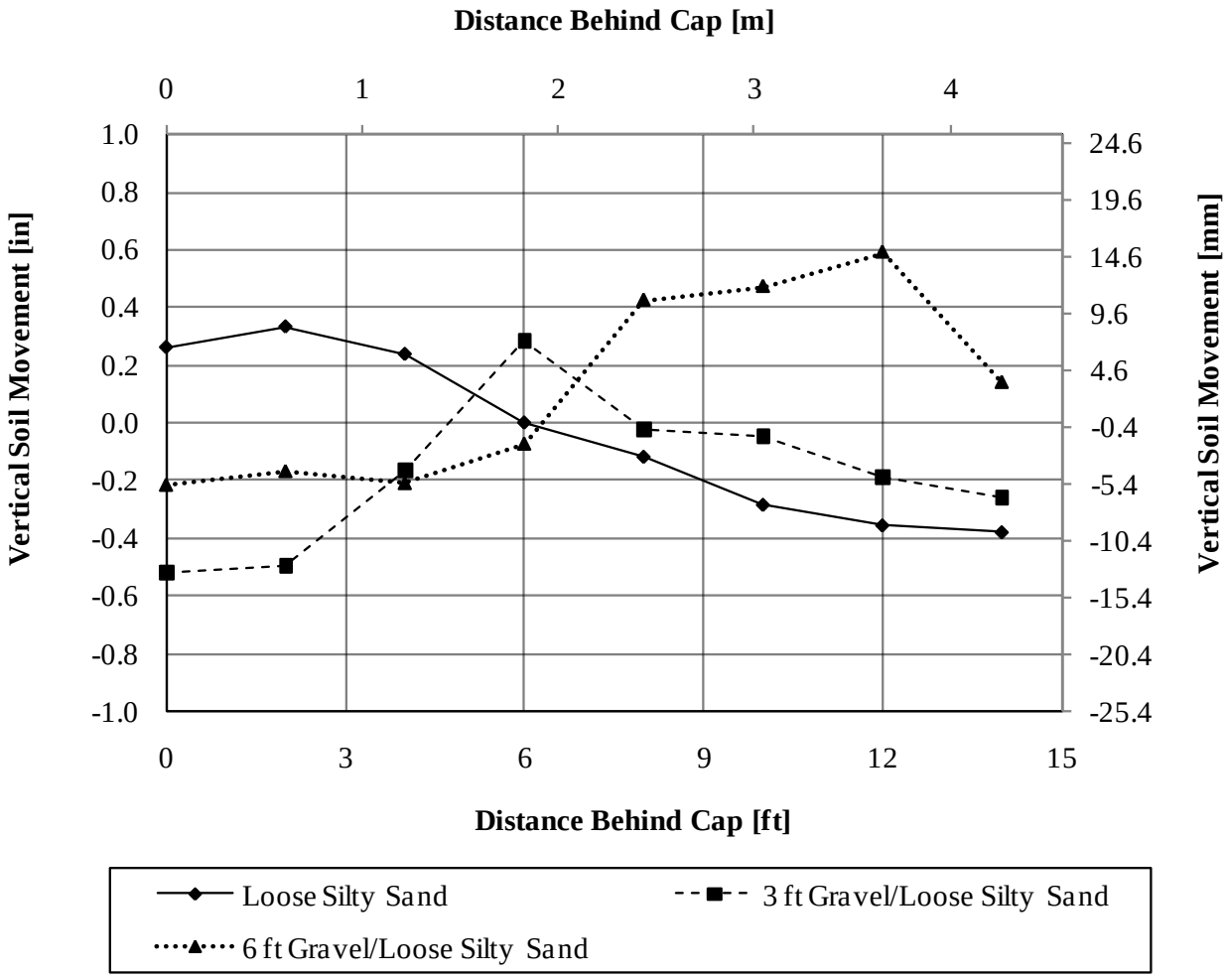

Figure 3-7: Heave/settlement profiles of South Temple backfills conditions consisting of: (1) full width (homogeneous) loose silty sand; (2) 3-ft (0.91-m) wide gravel zone and loose silty sand; and (3) 6-ft (1.83-m) wide gravel zone and loose silty sand

As is apparent in Figure 3-7, the loose silty sand backfill heaves to a maximum displacement of 0.33 in (8.38 mm) at a distance of 2 ft (0.61 m) from the pile cap face. The amount of heaving decreases gradually with increasing distance from the face of the pile cap. Beyond a distance of about 6 ft (1.83 m) from the pile cap, the backfill starts to settle and approaches a maximum downward displacement of 0.38 in (9.65 mm) at a distance of 14 ft (4.3

m) from the pile cap. Instead of heaving, the 3-ft (0.91-m) limited width backfill appears to settle during the test, excepting some heaving at a distance of about 6-ft (1.83-m) from the pile cap. This settlement may have been due to relaxation of soil near the pile cap face at the end of the test. A maximum settlement of 0.52 in (13.21 mm) is measured in close proximity to the pile cap face in this test. For the 6-ft (1.83-m) limited width backfill, relatively little settlement (maximum of about 0.2 in (5.1 mm)) is present in the dense gravel zone. Beyond this zone, increased heaving begins to occur with a maximum displacement of 0.59 in (14.99 mm) at a distance of 12 ft (3.66 m) from the pile cap.

3.6.2.2 SLC Airport Testing

Figure 3-8 plots the vertical displacement of the backfill surface as a function of distance from the pile cap face, illustrating the change in elevation of the surface of full width (homogeneous) and limited width dense gravel backfills during testing. The vertical displacements in Figure 3-8 represent the average elevation change at the node points in a given row (parallel to the face of the cap). Vertical displacement measurements were limited to the central portion of the pile cap to eliminate 3D edge effects from the pile cap.

The loose clean sand backfill settled to a maximum displacement of about 2.1 in (53.3 mm) near the pile cap face and gradually decreases in settlement with increasing distance from the cap face. This significant amount of settlement near the pile cap face may be due to the formation of cracks as a result of cyclic loading and therefore not a true representation of the static passive behavior of the backfill. The full width (homogeneous) dense gravel backfill appears to heave during the test, with a maximum measured displacement of 1.8 in (45.7 mm) at a distance of about 10 ft (3 m) from the pile cap. In addition, the zone of significant heaving

occurs in the first 16 ft (4.9 m) of the backfill. For the 3-ft (0.91-m) limited width backfill, a maximum increase in elevation (1.0 ft (0.3 m)) occurs in the clean sand portion of the backfill, at a distance of 8 ft (2.4 m) from the pile cap. Also, compared to the loose clean sand portion of the backfill, relatively little heaving occurs in the dense gravel zone. A similar observation can be

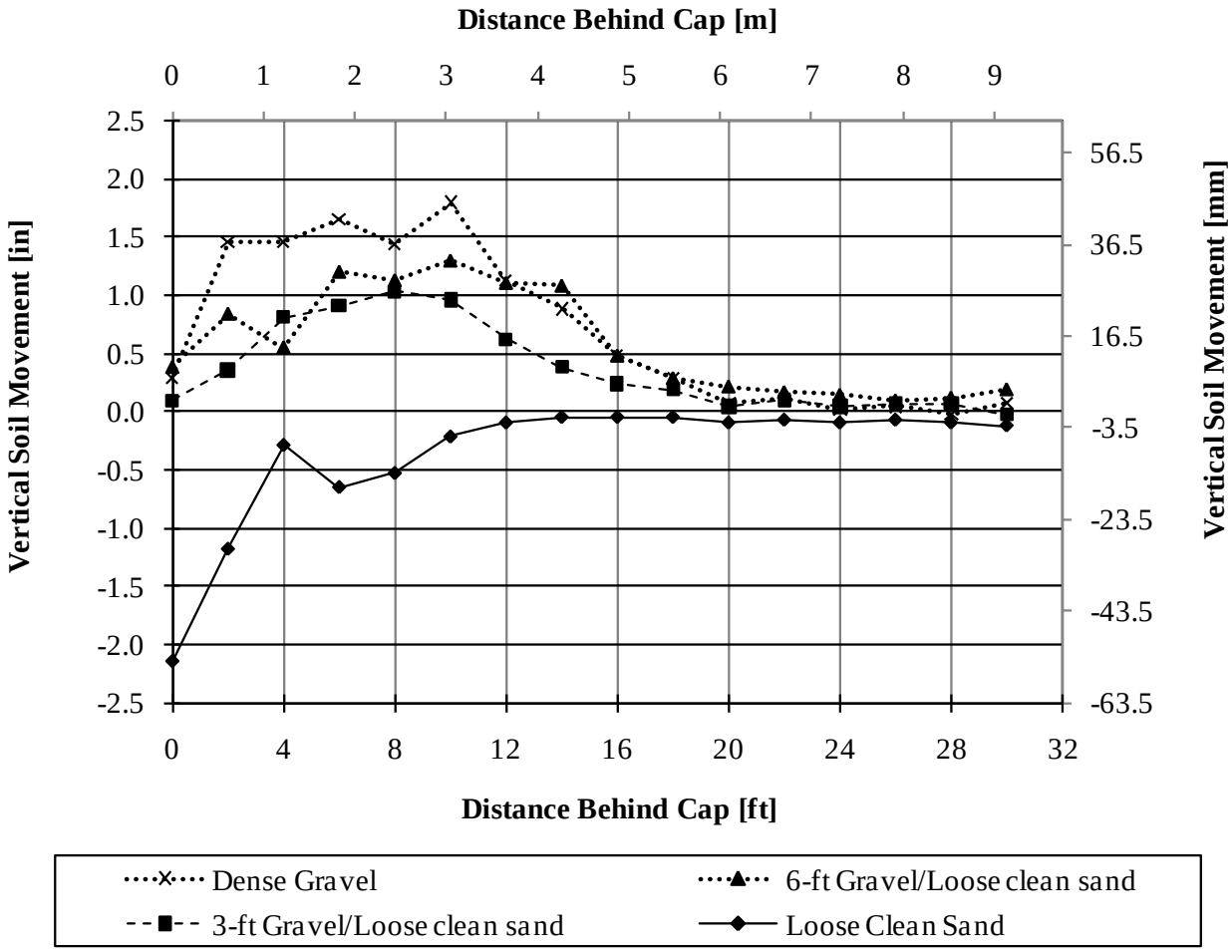

Figure 3-8: Heave/settlement profiles of SLC Airport backfills conditions consisting of: (1) full width (homogeneous) loose clean sand; (2) full width (homogeneous) dense fine gravel; (3) 3-ft (0.91-m) wide gravel zone and loose clean sand; and (4) 6-ft (1.83-m) wide gravel zone and loose clean sand

made for the 6-ft (1.83-m) limited width backfill. The maximum increase in elevation (1.3 in (33.0 mm)) occurs in the clean sand portion of the backfill, at a distance of 10 ft (3.0 m) from the pile cap. In addition, greater heave occurs in the loose clean sand portion of the backfill, compared to the dense gravel zone. In general, for all backfill conditions, it appears that beyond a distance of about 16 ft (4.5 m) from the pile cap, the backfill starts to approach minimum elevation change. Also it is apparent that magnitude of heaving generally decreases with decreasing width of gravel zone.

3.6.3 Comparison of South Temple and SLC Airport Limited Width Backfills

As mentioned previously, at a displacement level of 1.8 in (45 mm), the 3-ft (0.91-m) and 6-ft (1.83-m) limited width backfills, tested at the SLC Airport site, exhibit similar behaviors. According to (Gerber et al., 2010), this similar response is unexpected, considering the fact that the 3-ft (0.91-m) and 6-ft (1.83-m) limited width backfills, tested at the South Temple site, showed a notable increase in resistance with increasing width of dense gravel zone. Two reasons are identified by (Gerber et al., 2010) that explain the differing passive behavior of the South Temple and SLC Airport limited width backfill tests: (1) different pile cap face aspect ratios, and (2) different dense gravel width to pile cap height ratios. The pile cap face aspect ratio (pile cap height divided by the width) is believed to control the angle at which the developed failure surface would fan out with respect to a perpendicular plane to the pile cap face. As a result, the aspect ratio would possibly influence the extent of 3D edge effects on the total passive resistance of the backfill. In addition, the dense gravel width to pile cap height ratios influence the amount of failure wedge contained within the compacted gravel zone.

In terms of the heaving/settlement response, limited width backfills tested at the South Temple and SLC Airport sites generally show similar behaviors. Relatively little heaving is present in the dense gravel zone. However, as the gravel zone progressively translates into the loose sand layer, increased heaving begins to occur beyond the loose sand boundary. This elevation change in the gravel zone may possibly be an effect of the pile cap stresses being transmitted through the gravel zone into the loose silty sand portion of the limited width backfill (Gerber et al., 2010).

4 NUMERICAL MODELING

4.1 Introduction

The experimental results of BYU full-scale lateral pile cap tests conducted at the South Temple and SLC Airport sites, provide valuable sets of data for evaluating the static passive behavior of various full width (homogeneous) and limited width pile cap-backfill systems. However, it is not economically or practically feasible to conduct parametric full-scale experimental studies for all potential wall and soil geometries. With the introduction of modeling procedures for simulating the interface between soil and an adjacent structural member, there has been increased popularity and acceptance in the engineering community for using numerical modeling methods, including the Finite Element and Finite Difference methods, as a solution to soil-structure interaction problems. In many situations where full-scale testing may be economically unfeasible, numerical modeling can provide a cost-effective means for approximating the response of a soil-structure interaction problem. In addition, the capability of numerical modeling in handling problems that involve complex boundary or loading conditions, and non-homogeneous materials, makes it an even more valuable tool in geotechnical analysis and design.

In this study, the finite element modeling program PLAXIS 2D-Version 8 is used to simulate the passive behavior of a selected range of full width (homogeneous) and limited width

backfill conditions tested at both South Temple and SLC Airport sites under static loading conditions. Although the full-scale tests involved 3D geometries, the analyses performed in this study are restricted to 2D geometries. A comparison between the 2D and 3D results will allow for an assessment of the importance of 3D effects.

Initially, the analyses are performed for 3.67-ft (1.12-m) and 5.5-ft (1.68-m) deep pile caps with four different backfill conditions consisting of: (1) full width (homogeneous) loose silty sand; (2) full width (homogeneous) dense fine gravel; (3) limited width dense gravel backfill consisting of a 3-ft (0.91-m) wide zone of dense fine gravel between the pile cap and loose silty sand and; (4) limited width dense gravel backfill consisting of a 6-ft (1.83-m) wide zone of dense fine gravel between the pile cap and loose silty sand. Subsequently, additional simulations are performed for each case, involving different wall heights and soil strengths/densities to evaluate the passive behavior of commonly used pile cap geometry and backfill soil design parameters.

In this chapter, the general numerical modeling and calibration process involved in simulating the passive behavior of a typical pile-cap backfill system analyzed is presented. The information provided covers details related to approximating individual and interactive behaviors of various structural and non-structural components of the system, boundary conditions, and the steps involved in performing the finite element analysis. The limitations and challenges encountered in the numerical simulation process are also discussed at the end of this chapter.

4.2 Overview of PLAXIS 2D-Version 8

The following outline of basic PLAXIS features is based on the PLAXIS 2D-Version 8 Reference Manual. Plasticity Axisymmetry (PLAXIS) is a two-dimensional finite element

computer code package designed for the plane strain or axisymmetric modeling of a wide variety of geotechnical problems involving soil and/or rock. PLAXIS is designed to be used primarily by practicing engineers, providing a user-friendly and interactive interface through four programs: Input, Calculation, Output, and Curves. In the Input program, the user is able to construct a conceptual model of the problem, by inputting the geometry of the model graphically to represent a simplified version of field conditions. An automatic finite element mesh is also generated in the Input program with the option of introducing local refinements within clusters, around lines, and geometry points, for which high levels of stresses, strains, and displacements are anticipated. Simulation of the response of various geotechnical systems and phenomena, including tunnels, excavations, groundwater flow, and consolidation, can be performed by conducting deformation and stability analyses through the Calculation program. The main finite element analysis results, including deformations, stresses, and strains can be accessed in graphical and tabulated format in this program for the entire geometry of the problem, at any fixed moment during the calculation phase. In cases where localized analysis results are desired, the Curves program can be used to generate relationships, such as load-displacement curves and stress paths, which show the development of a specific variable for a pre-selected Gaussian stress point within the geometry of the problem at the end of the calculation phase.

To simulate the mechanical behavior of soil and rock, a number of soil models are available in PLAXIS with varying degrees of complexity. Among the models available are the Mohr-Coulomb, Hardening Soil, Soft Soil Creep, and Jointed Rock models. The Mohr-Coulomb model is a simple soil model designed to capture the basic characteristics of soil stress-strain behavior. For cases where the use of a more advanced soil model is desired, the Hardening Soil model can be applied to simulate the non-linear and stress-dependant behavior of soils with a

higher degree of accuracy. The Soft Soil Creep model is available to analyze the time-dependant creeping behavior of soft normally consolidated soils. The Jointed Rock model is a specialized model that deals with jointed rock analyses. In addition, PLAXIS gives users the option of compiling and applying a wide variety of user-defined soil models that are based on stress-strain data entered by the user.

4.3 Development and Calibration of Finite Element Model

Figure 4-1 shows the conceptual model associated with a typical 2D pile cap-backfill system created in PLAXIS. This model is a 2D approximation of the full-scale 3D field test conducted at the South Temple site, involving a full width (homogenous) backfill consisting entirely of loose silty sand. Details concerning the general testing layout and backfill soil properties of this test were described previously in chapter 3. The 10 ft (3.05 m) long, 17 ft (5.18 m) wide, and 3.67 ft (1.12 m) deep concrete pile cap is modeled as an individual beam element, with restrained movements in the vertical direction to simulate the effect of the piles. To replicate the general testing layout in the field using a simplified approach, the pile cap is placed on a 10-ft (3.05 m) deep homogeneous layer of loose silty sand, and is backfilled to a depth 3.67 ft (1.12 m) from the ground surface. In addition, the backfill is extended for a relatively long distance horizontally (38 ft (11.6 m)) in front of the pile cap, to ensure that the model boundaries have no significant influence on the output results. In the case of limited width gravel backfills, the gravel zone is extended 2 ft (0.61 m) below the base of the cap. In all backfill conditions, a drained condition is assumed throughout the soil mass, as the ground water table is assumed to be located well below the boundaries defined in the finite element model.

To support the validity of the finite element model in simulating the passive behavior of full width (homogeneous) backfills consisting of entirely loose sand or dense gravel, passive earth pressure calculations were first performed using PYCAP and ABUTMENT. As mentioned previously, PYCAP and ABUTMENT are analytical programs developed by Duncan and Mokwa (2001), and Shamsabadi et al. (2007), respectively, to estimate the passive earth pressure development in a backfill as a function of pile cap displacement. The calibration process involved comparing load-displacement curves generated by PLAXIS with curves obtained from the analytical models, until a satisfactory agreement (within 10%) was obtained between the results. Once this was accomplished, the calibrated model was used to approximate the passive response of pile caps with limited widths of dense gravel, placed between the cap and the looser sand.

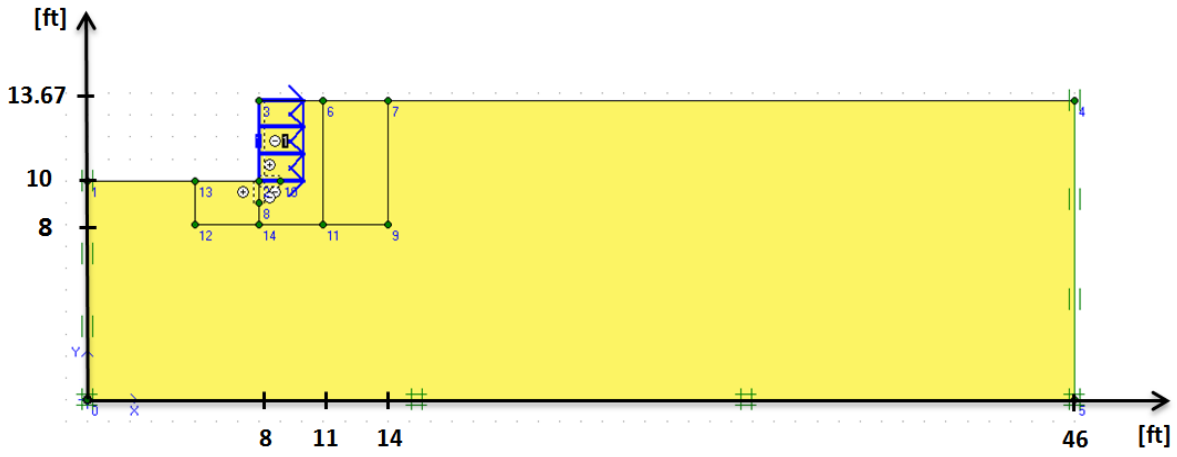

Figure 4-1: Conceptual PLAXIS model associated with a 3.67-ft (1.12-m) deep pile cap with a full width (homogeneous) loose silty sand backfill

This section covers a detailed discussion of the different constitutive models used in approximating the individual behavior of the pile cap and backfill, as well as the interactive behavior between the two components. Figure 4-2 shows a summary of constitutive models used for simulating the behavior of key components of the pile cap-backfill systems analyzed in this study. The Hardening Soil model is employed in approximating backfill soil behavior. A linear elastic model is used to represent the interactive behavior between the pile cap and backfill, and a beam element with elastic behavior is used to model the pile cap.

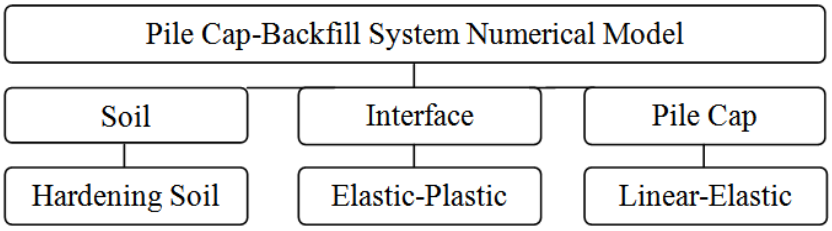

Figure 4-2: Diagram showing different constitutive models used for various components of the pile cap-backfill systems analyzed using PLAXIS

4.3.1 Stress-Strain Soil Modeling

It is generally accepted that the stress-strain behavior of soils is highly non-linear, and stress-dependant for small and large deformations, and inelastic for large deformations. Depending on the initial relative density, as well as the drainage condition of the soil, two general responses are observed under static loading conditions. Soils with low initial densities, such as loose sands, show a gradual non-linear strain-hardening response, as the shear strain increases. The increase in shear stress with increasing strain continues until a more or less

constant shear stress, referred to as the ultimate shear stress, τ_{ult} is reached. Loose sands show a tendency to contract to a denser arrangement as shear strain is applied until no more volume change is observed in the specimen with continuing shear strain. At this stage, the specimen has reached a state of critical void ratio and shear stress at the corresponding confining pressure.

The stress-strain behavior of dense sands and loose sands differs in that the behavior in dense sands shows rapid strain-hardening with increased shear strain until the peak shear stress, τ_{peak} is achieved. However, as larger shear strains are applied, localized failure zones called shear bands develop within the soil mass, causing the peak behavior of the soil to disappear and the specimen to strain soften to failure. Dense sands initially contract up to small strains, but then expand until the critical void ratio is attained. This expansive volume change during shearing is referred to as the dilatancy capacity, and has an important role in providing additional shear strength resistance for dense sands. Figure 4-3 compares the typical stress-strain and volumetric responses of low and high density sand specimens, subjected to static shearing forces in a direct shear testing device.

In addition to the initial relative density, the effective normal stress or confining pressure is another important variable that influences the shearing resistance of sands. The magnitude of the dilation capacity depends on the effective normal stresses acting on the specimen. A high confining pressure tends to suppress the amount of expansion the soil specimen can develop under loading, causing dense sands to exhibit behaviors similar to that of looser sands.

A wide variety of mathematical models have been developed, with the aim of simulating the stress-strain behavior of soils in different geotechnical applications. These soil models have different advantages and limitations depending on their application. The Hardening Soil model is one of the more advanced soil models supported by PLAXIS that attempts to take into account

key features of soil shearing response, including: (1) non-linearity of the stress-strain relationship, (2) confinement dependency of shear strength, and (3) dilative response. In general, the formulation of the Hardening Soil model is based on the framework of the Duncan & Chang, (1970) hyperbolic model, in achieving non-linearity of the stress strain relationship of soils. However, the Hardening Soil model is believed to provide a more accurate approximation of soil response than the Duncan and Chang hyperbolic model because it employs the theory of plasticity rather than the theory of elasticity, takes into account soil dilatancy, and introduces a yield cap (Schanz et al., 1999).

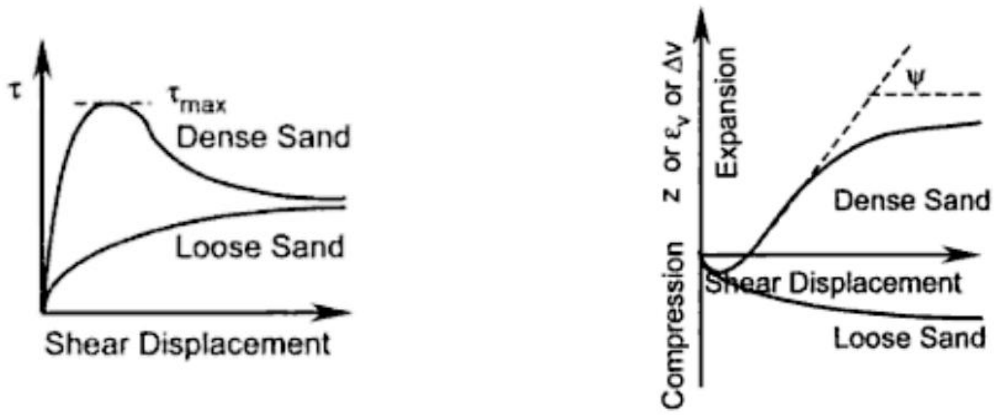

(a) **(b)**

Figure 4-3: Typical (a) stress-strain, and (b) volumetric responses of loose and dense sand specimens under static shearing load (Aysen, 2002)

In this numerical study, two different soil constitutive models were used in the analysis of the backfill soil materials: the elastic-perfectly plastic Mohr-Coulomb and the Hardening Soil

model. Due to its simplicity, the Mohr-Coulomb model was initially used to provide a first degree approximation of soil behavior. Once confidence was gained in the performance of the model, the Hardening Soil model was applied in the analysis for a more accurate representation of soil behavior.

Figure 4-4 illustrates the hyperbolic stress-strain relationship used in formulating the Hardening Soil model. In this relationship, the soil is assumed to gain strength with increasing shear strain, a behavior typically observed in the shearing response of loose sands and normally consolidated clays. The Hardening Soil model requires eight basic parameters. Three of these parameters are the soil strength parameters, cohesion c, soil friction angle φ, and the soil dilation angle ψ, which are used to define the Mohr-Coulomb failure criterion. The stress-dependant stiffness of the soil is approximated using three basic parameters: the secant stiffness in a standard drained triaxial test, E_{50}^{ref}, associated with a reference pressure of p^{ref}, the tangent stiffness for primary oedometer loading, E_{oed}^{ref}, associated with a reference pressure of p^{ref}, and the power m which quantifies the degree of stiffness stress dependency. E_{50}^{ref}, and E_{oed}^{ref} parameters account for plastic straining due to deviatoric loading and primary compression, respectively. The unloading/reloading stiffness parameters, E_{ur}^{ref} and ν_{ur} are used as advanced soil model parameters for elastic unloading and loading calculations.

The main limitation of the Hardening Soil model is its inability to model the post-peak behavior of dense sands and stiff clays, in which strain-softening occurs. Considering this significant limitation, the Hardening Soil model would be most applicable in modeling soils that primarily exhibit strain-hardening behavior, with little or no dilatancy capacity. If the Hardening Soil model is chosen to be used in approximating the response of strain-softening soils, the

dilation capacity of the soil should be ignored and ultimate strength parameters must be used to define the model.

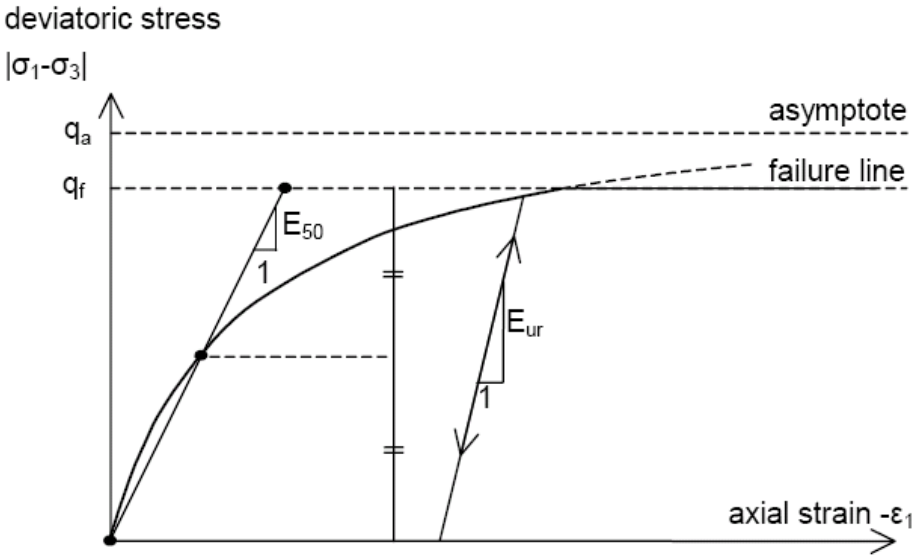

Figure 4-4: Schematic representation of the hyperbolic stress-strain relationship used in the Hardening Soil model (PLAXIS Reference Manual)

The errors due to the inability of the Hardening Soil model in accurately representing the dilative behavior of dense soils do not interfere with the objectives defined for this research study. Since the study is strictly concerned with the ultimate response of dilative and non-dilative soils at failure, the Hardening Soil model is appropriately used to represent the post-peak behavior of dense gravels used in the analysis. In addition, the assumption of using the Hardening Soil model in simulating the dense and loose sand behavior was proven to be reasonable, by performing calibrations between numerical and analytical results. This

conclusion is based on the fact that the calibrated models provided reasonable predictions (within 10%) of load-displacement relationships associated with analytical methods with similar soil property assumptions. Thus, the good agreement reached between the numerical and analytical results using the Hardening Soil model negated the need to use a more complex model to simulate the stress-strain behavior of the backfill soils. Finally, the field tests involving dense backfills described previously did not show any significant drop in lateral resistance within the displacement limits of the tests. A comprehensive comparison of numerical simulations and analytical results using the Hardening Soil model is presented in chapter 5.

4.3.2 Soil-Structure Interaction Modeling

One important capability of PLAXIS that makes it a powerful numerical analysis tool is its capability to represent problems involving interactions between soils and adjacent structural members. The interface between a retaining wall structure and soil mass is hardly ever perfectly smooth and frictionless. Depending on the type of soil and structural material used there is some degree of friction that influences the magnitude of passive earth pressure, and the shape of the failure surface that develops in the backfill. Similar to soils, soil-structure interfaces show non-linear and stress-dependant behaviors. Various interface models including quasi-linear and non-linear models have been developed to simulate the interface behavior.

In PLAXIS interface joint elements are used to approximate the interaction between the soil mass and the adjacent pile cap with elastic-plastic behavior. A strength reduction factor, R_{inter} is used as the basic interface element property to relate the wall friction and adhesion to the strength of the soil, defined by the soil cohesion and internal friction angle. This parameter is entered within soil property data sets, and is defined by the following equation:

$$R_{inter} = \frac{tan\delta}{tan\varphi} \quad (4\text{-}1)$$

where δ is the wall/interface friction angle, and φ is the soil friction angle. The elastic-plastic model used in representing the shearing behavior between the concrete and soil, simulates the interface behavior as elastic for small displacements, and uses a plastic model for permanent slipping (failure) between the pile cap and the soil. Equations 4-2 and 4-3 define the elastic and plastic interface behaviors, respectively:

$$|\tau| < \sigma_n tan\delta_i + c_i \quad (4\text{-}2)$$

$$|\tau| = \sigma_n tan\delta_i + c_i \quad (4\text{-}3)$$

where τ, and σ_n are the shear and effective normal stresses, and δ_i and c_i are the interface friction angle and adhesion.

In a soil-structure interaction problem involving a stiff structure with sharp edges, such as the problem investigated in this study, accurate modeling of the high stresses and strains that may develop around corner points is not easily feasible in PLAXIS. This may lead to oscillating stress distributions around structure corner points, as shown in Figure 4-5, which is unrealistic. To solve this problem, PLAXIS recommends extending the interface elements beyond the edges of the pile cap into the surrounding soil body. The interface elements which are extended around the base of the beam element for 1 ft (0.30 m) are shown in Figure 4-6. By introducing these extensions, the flexibility of the finite element mesh increases, resulting in a more uniform

distribution of stresses around the edges of the structure, as shown in Figure 4-5. It is important to note that interface element extensions are merely used as a tool to enhance the performance of the finite element mesh, and do not model the interaction between structure and soil. Therefore, the same material properties must be assigned to these extensions as the surrounding soil body (i.e. the R_{inter} is set equal to 1.0).

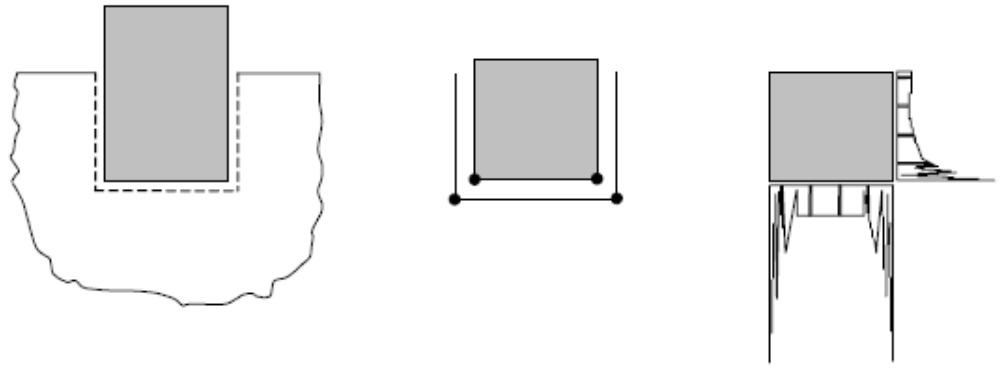

(a) inflexible corner points causing unrealistic stress results

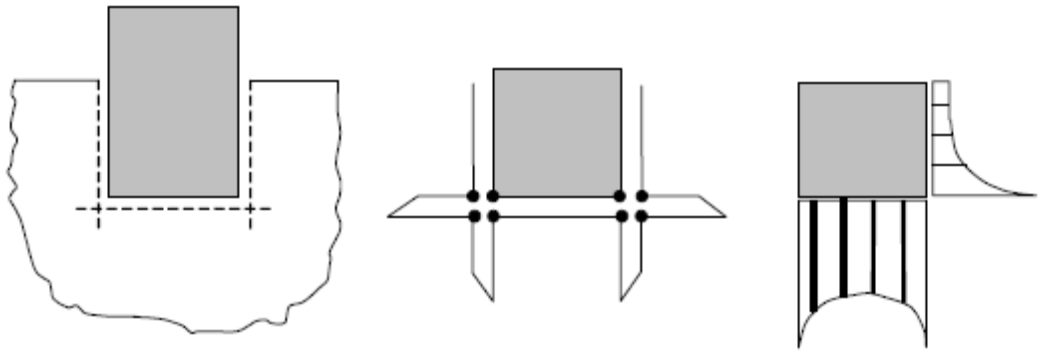

(a) flexible corner points with enhanced stress results using interface element extensions

Figure 4-5: Stress distributions around corners of a typical stiff structure with: (a) inflexible corner points, causing unrealistic stress results; and (b) flexible corner points with enhanced stress results using interface element extensions (PLAXIS Reference Manual)

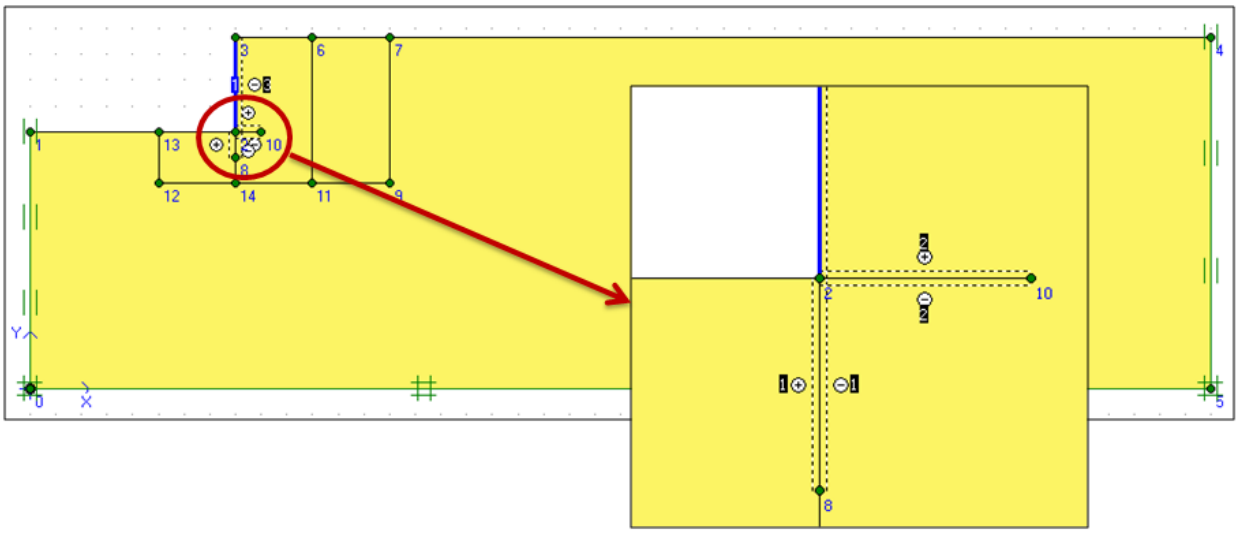

Figure 4-6: Modeling the interface between the beam element and loose silty sand in PLAXIS using interface element extensions

4.3.3 Hardening Soil Model Parameters

As discussed previously in chapter 3, two types of materials were used in the backfill conditions tested at the South Temple site, compacted against the 3.67-ft (1.12-m) deep pile cap: silty sand and fine gravel. For the 5.5-ft (1.68-m) deep pile cap tested at the SLC Airport site, clean sand and fine gravel were used as basic backfill materials. Using the modified spreadsheet program PYCAP, developed by Duncan and Mokwa (2001), the passive earth pressure coefficient, K_P, was calculated for both sets of gravel and sand materials, based on laboratory and in-situ measurements of soil parameters. The deflection-to-wall height ratio used in the analysis was determined from measured load-displacement curves associated with the full width (homogeneous) dense gravel and loose sand backfill conditions. Tables 4-1 and 4-2 provide a summary of PYCAP input and output parameters for the full width loose sand and dense gravel backfill conditions, respectively, tested at the South Temple and SLC Airport sites.

Table 4-1: Summary of test parameters for South Temple and SLC Airport loose sand materials

Parameter	Symbol	South Temple	SLC Airport	Unit
Pile cap height	H	3.67 (1.12)	5.5 (1.68)	ft (m)
Pile cap width	B	17 (5.18)	11 (3.35)	ft (m)
Soil friction angle	φ	27.7	37.0	degrees
Wall friction angle	δ	20.8	25.9	degrees
Cohesion	c_{ref}	142.0 (6.8)	0	psf (kPa)
Moist unit weight	γ_m	110.9 (17.4)	106.5 (16.7)	pcf (kN/m^3)
Maximum deflection	Δ_{max}	2.0 (51)	1.5 (38.1)	in (mm)
Displacement ratio	Δ_{max}/H	0.045	0.023	---
3D correction factor	R_{3D}	1.179	1.646	---
Passive coeff. (log spiral)	K_p	7.4	9.6	---

Despite the differences in measured engineering properties of the soils used in both series of tests, the passive earth pressure coefficients calculated for the tests were within 30% and 3% of each other for the loose sand (7.4 versus 9.6), and dense gravel materials (23.05 versus 23.6), respectively. Based on this observation, it would be reasonable to represent the plane strain passive behavior of the South Temple and SLC Airport backfill conditions involving dense fine gravel, using engineering parameters associated with the South Temple dense fine gravel. For the loose sand material, since the engineering properties associated with South Temple sand is expected to provide relatively conservative estimates of passive resistance, due to its looser state compared to the SLC Airport sand, the South Temple loose silty sand was used as the basic sandy material in the analysis. Although this approach is not a completely accurate representation of the different soils used in both series of tests, it will facilitate comparisons among numerical results, without introducing significant errors in the analysis.

Table 4-2: Summary of test parameters for South Temple and SLC Airport dense gravel materials

Parameter	Symbol	South Temple	SLC Airport	Unit
Pile cap height	H	3.67 (1.12)	5.5 (1.68)	ft (m)
Pile cap width	B	17 (5.18)	11 (3.35)	ft (m)
Soil friction angle	φ	42.0	44.3	degrees
Wall friction angle	δ	33.0	27.0	degrees
Cohesion	c_{ref}	409.3 (19.6)	410 (19.6)	psf (kPa)
Moist unit weight	γ_m	140.3 (22.0)	125.4 (19.7)	pcf (kN/m^3)
Maximum deflection	Δ_{max}	---*	2.4 (61)	in (mm)
Displacement ratio	Δ_{max}/H	0.04	0.037	---
3D correction factor	R_{3D}	1.440	1.982	---
Passive coeff. (log spiral)	K_p	23.05	23.6	---

*A full width backfill condition was not tested at the South Temple site, thus a measured maximum displacement is not available for this backfill condition.

The initial estimates of PLAXIS input parameters used to model the loose silty sand and dense fine gravel materials and the interaction between the pile cap and the adjacent backfill, were derived from laboratory-based measurements. These parameters were further adjusted iteratively by matching load-displacement curves measured experimentally and computed numerically, with curves computed from PYCAP and ABUTMENT. These comparisons are shown and discussed in detail in the subsequent chapter. Recommendations provided in the PLAXIS Tutorial, Reference, and Material manuals were also considered in the selection of input soil parameters. Table 4-3 contains the calibrated parameters used in the numerical analysis. In addition, the basis for the selection and adjustment of several key input parameters is listed as follows:

Table 4-3: Summary of Hardening Soil model input parameters

Parameter	Symbol	Loose Sand	Dense Gravel	Unit
Type of material behavior	Type	Drained	Drained	---
Soil un-saturated unit weight	γ_{unsat}	110 (17.3)	141 (22.1)	pcf (kN/m^3)
Secant CD triaxial stiffness	E_{50}^{ref}	330 (15.8)	1700 (81.4)	ksf (MPa)
Tangent oedometer stiffness	E_{oed}^{ref}	330 (15.8)	1700 (81.4)	ksf (MPa)
Unloading/reloading stiffness	E_{ur}^{ref}	990 (43.1)	5,100 (244.2)	ksf (MPa)
Power for stress dependant stiffness	m	0.5	0.5	---
Reference stress	P_{ref}	2 (100)	2 (100)	ksf (kPa)
Poisson's ratio	v_{ur}	0.2	0.2	---
Cohesion	c_{ref}	10 (0.5)	40 (1.9)	psf (kPa)
Friction angle	φ	27.7	42.0	Degrees
Dilation angle	ψ	0	12	Degrees
Strength reduction factor	R_{inter}	0.723	0.681	---

1) Values of soil friction angle, φ, and cohesion intercept, c, were primarily selected based on in-situ and laboratory direct shear test measurements for the loose silty sand and dense fine gravel materials. However, to provide a more general application of the numerical results obtained in this study, a cohesion value close to zero was used in PLAXIS, enough to produce sufficient numerical stability.
2) The value of the wall friction angle, δ, was estimated considering recommendations given by Potyondy (1961). Potyondy (1961) estimates δ/φ values of 0.5 and 0.84 for smooth concrete-cohesionless silt and smooth concrete-cohesive granular soil interfaces, respectively. Based on the sand and gravel contents of the silty sand and

fine gravel soils, a δ/φ value of 0.75 was selected for both materials. The basic interface element property in PLAXIS, R_{inter}, was calculated using Equation 4-1.

3) Unit weight characteristics of the loose silty sand and dense fine gravel were based on average unit weight parameters obtained from nuclear density testing during field compaction.

4) The secant stiffness parameter corresponding to a stress level of 50% of the ultimate stress, at a reference stress equal to 100 stress units, E_{50}^{ref}, is the main input stiffness parameter used in PLAXIS. E_{50}^{ref} values of 330 and 1700 ksf (15.8 and 81.4 MPa), were selected iteratively at a reference stress equal to atmospheric pressure (2000 psf (100 kPa)) for the loose sand and dense gravel materials, respectively. This selection was based on providing agreement (within 10%) between numerical and analytical results. The selected E_{50}^{ref} values also compare well with the range of initial stiffness modulus values E_i, recommended by Duncan and Mokwa, (2001) for shallow foundations on granular soils (E_{50}^{ref} values are approximately 70-80% of E_i values provided by Duncan and Mokwa, 2001, at a confining stress equal to atmospheric pressure).

5) E_{oed}^{ref}, and E_{ur}^{ref} values were computed based on default Hardening Soil relationships defined by Equations 4-4 and 4-5, respectively. Equation 4-6 represents the general form of the relationship used to calculate the stiffness moduli, E_{50}, .E_{oed}, and E_{ur}, at any given stress level. Recommendations provided in PLAXIS 2D suggested using a value of 0.5 for the power m, based upon reports made by Janbu (1963) for Norwegian sands and silts.

$$E_{oed}^{ref} = E_{50}^{ref} \tag{4-4}$$

$$E_{ur}^{ref} = 3E_{50}^{ref} \tag{4-5}$$

$$E = E^{ref}\left(\frac{c\ cos\varphi - \sigma_3' sin\varphi}{c\ cos\varphi + p^{ref} sin\varphi}\right)^m \tag{4-6}$$

where m is a power controlling the level of stress dependency of the stiffness parameters, and E represents E_{50}, E_{oed}, or E_{ur} at any given stress level.

6) The selection of the dilation angle, ψ was based on equation 4-7, an approximation presented in the PLAXIS Materials Manual for granular soils:

$$\psi \approx \begin{cases} \varphi - 30°, & for\ \varphi \geq 30° \\ 0°, & for\ \varphi \leq 30° \end{cases} \tag{4-7}$$

where φ is the soil friction angle.

4.3.4 Pile Cap Parameters

The concrete pile cap is modeled using an individual beam element with linear-elastic behavior. The elastic behavior of the beam element is defined by assigning an axial stiffness, EA, and a flexural rigidity, EI, as material properties. To restrain beam element movements in the vertical direction, a vertical fixity is applied to the base of the element. In addition, a high flexural rigidity value, EI, is assigned to the beam element to simulate the rigidity of the pile cap

and piles, and further restrain the translation of the beam element in the vertical direction. To simplify the model further, the piles were omitted from the finite element model, since their effect was considered by prescribing a zero vertical displacement boundary on the pile cap. This simplification in representing the pile foundation system is justified, based on the fact that the vertical movements of a rigid structure supported by pile foundations would be minimal in reality. Table 4-4 contains the calibrated finite element model properties used in the linear-elastic representation of the pile cap.

Table 4-4: Summary of pile cap input parameters used in PLAXIS

Parameter	Symbol	Value	Unit
Type of behavior	Material type	Elastic	---
Normal stiffness	EA	2.0×10^9	lb/ft
Flexural rigidity	EI	2.4×10^5	$lb.ft^2/ft$
Weight	w	550	lb/ft/ft
Poisson's ratio	ν	0	---

4.3.5 Boundary Conditions

The basic geometry of a typical 2D finite element model developed in PLAXIS is illustrated in Figure 4-1. As mentioned previously, the lowest soil layer boundary is 10 ft (3.05 m) from the base of the pile cap, and the silty sand layer extends horizontally to a distance of 38 ft (11.58 m) in front of the pile cap. The silty sand soil layer was extended for a large distance horizontally and vertically to ensure that the failure surface developed in the backfill, under

mobilization of passive forces, was embodied within the defined boundaries of the problem, and that the boundaries had no significant influence on the output results.

Boundary conditions were defined at each geometry point by prescribing a known force or displacement. The standard fixity boundary condition available in PLAXIS was applied to the nodes at the three sides of the soil mass. This option creates fixities in the horizontal and vertical directions at the horizontal boundary of the geometry, and rollers on the two vertical boundaries. An ultimate prescribed displacement boundary condition was applied to the pile cap with no vertical displacement. A prescribed displacement corresponding to a deflection-to-wall height ratio of 4% was applied to pile caps supporting full and limited width backfill conditions involving dense gravel. In the case of the full width loose silty sand backfill, a prescribed horizontal displacement corresponding to a deflection-to-wall height ratio of 6% was applied. For all other points in the soil mass, the prescribed force is assumed to be equal to zero, and the displacement is undefined and must to be determined through performing the finite element analysis.

4.4 Finite Element Analysis

To carry out the finite element analysis using PLAXIS, the following steps were followed:

1) A conceptual model was constructed in the Input program, to represent the problem graphically. Material properties and boundary conditions were assigned to the points, lines, and clusters of interest within the conceptual model.
2) A medium density finite element mesh was generated automatically in PLAXIS by dividing the defined geometric continuum into 6-noded triangular elements. Two

different element types are available in PLAXIS to define the finite element mesh: 6-noded and 15-noded triangular elements. In this study, results obtained from applying both element types were identical. Thus, 6-noded elements were used to save computational time. A medium mesh size was selected based on results obtained from performing a mesh dependency study. A detailed discussion on this study is presented in chapter 5. By generating the mesh, material properties and boundary conditions, defined previously in the conceptual model, were transferred from points and lines in the geometry, to nodes and elements in the generated mesh. In addition, local refinements were introduced in clusters around the pile cap where high levels of stress concentrations were anticipated. A typical finite element mesh developed for this study is shown in Figure 4-7.

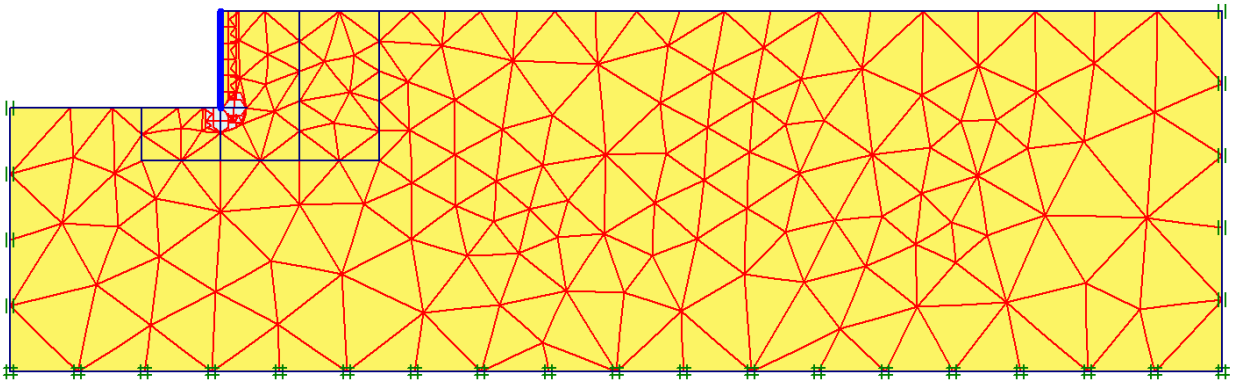

Figure 4-7: Typical 2D finite element mesh of medium coarseness generated in PLAXIS

3) Initial conditions were established to define the at-rest effective stress, pore pressure, and geometry configuration conditions.
4) Gaussian stress points were selected just behind the pile cap to monitor the development of passive earth pressure with the applied prescribed displacement.
5) The analysis was performed by defining a single calculation phase in which the interface elements and prescribed displacement boundary condition were activated. After the finite element analysis was completed, the load-displacement curves for the previously selected Gaussian points were accessed through the Curves program.

4.5 Summary of Numerical Modeling

The development of a typical 2D finite element model in PLAXIS was presented in this chapter along with the calibration procedure. The model consisted of a 3.67-ft (1.12-m) deep pile cap with a full width (homogenous) backfill consisting entirely of loose silty sand. The pile cap was modeled using an individual beam element with linear-elastic behavior. The PLAXIS Hardening Soil constitutive model was used to approximate the shearing behavior of the soil. Interface elements with an elastic-plastic model were used to simulate the behavior of the interface between the pile cap and surrounding soil. Backfill load-displacement curves were generated from the application of a prescribed displacement on the pile cap in the horizontal direction.

The calibration of the finite element model was primarily based on load-displacement relationships. At the end of the calculation phase, the load-displacement curves obtained from numerical simulations of full width (homogenous) backfills were compared with curves obtained from PYCAP and ABUTMENT, using similar soil property assumptions. The finite element

steps outlined in the previous section were then repeated until a stable numerical solution with satisfactory agreement (within 10 %) was achieved between curves generated from numerical and analytical models for each full width (homogeneous) backfill condition. Once a satisfactory calibrated model was developed, it was used to approximate the response of dense gravel backfills of limited width.

During this iterative process, various adjustments were made to soil parameters, as well as finite element mesh and interface element geometries. Soil parameters which appeared to have the greatest influence on the predicted ultimate resistance of analyzed backfills include: the soil friction angle φ, cohesion c, dilation angle ψ, and strength reduction factor R_{inter}. The pile cap height, depth of gravel zone placed below the base of the pile cap, length of interface element extensions, and degree of mesh refinement were also influential parameters on the passive resistance. Other parameters such as the soil stiffness value E_{50}^{ref}, controlled the sharpness or slope of the hyperbolic load-displacement curve. A detailed discussion pertaining to the effect of varying these parameters on the predicted ultimate passive response is presented in the next chapter as part of parametric studies performed on limited width dense gravel backfills.

Although PLAXIS proved to be a capable tool in meeting the objectives outlined in this study, the numerical simulations performed were not without limitations. Despite the inherent limitations associated with PLAXIS in representing soil and interface behaviors, a number of assumptions and simplifications were made in terms of soil properties and pile cap geometry, which may have contributed to limitations in accurately simulating the passive response of the backfills analyzed. These simplifications can be summarized as the following:

1) Limitations were involved in determining strength and stiffness Hardening Soil model input parameters to represent the behavior of the backfill soils with good accuracy. In addition, despite the differences in engineering properties of the soils used in South Temple and SLC Airport tests, soil parameters associated with the South Temple tests were used in the numerical and analytical analyses of both series of tests.
2) Deeper native soil layers, starting from a distance of approximately 1 ft (0.31 m) below the pile cap and extending to a depth of 10 ft (3.0 m), were modeled as homogeneous loose silty sands.
3) Several geometric assumptions were made in representing the pile cap. First, the contribution of the individual connections of the pile cap with loading equipment is lumped into one large rigid block that is pushed into the soil mass. Second, the piles supporting the pile cap were not included in the finite element model, based on the assumption that their affect could be modeled by restraining the pile cap movement in the vertical direction using fixities. As a result, the 2D finite element model may not contain the correct stiffness and structural strengths of the full-scale pile foundation components.

5 RESULTS AND DISCUSSION

5.1 Introduction

Chapter three contained a summary description of BYU full-scale lateral pile cap tests conducted at South Temple and SLC Airport test sites, in August 2005 and May 2007, respectively. The experimental tests involved the application of static lateral loadings to 3.67-ft (1.12-m) and 5.5-ft (1.68-m) deep pile caps, with a range of full width (homogeneous) and limited width dense gravel backfills. Using the basic soil and geometry field data, plane strain numerical simulations were performed using PLAXIS 2D, for backfill conditions relevant to the scope of this research study. These backfill conditions consisted of the following: (1) full width (homogeneous) loose silty sand; (2) full width (homogeneous) dense gravel; (3) limited width dense gravel backfill consisting of a 3-ft (0.91-m) wide zone of dense gravel between the pile cap and loose silty sand and; (4) limited width dense gravel backfill consisting of a 6-ft (1.83-m) wide zone of dense gravel between the pile cap and loose silty sand. Chapter four presented a detailed description of the steps involved in developing a calibrated finite element model that simulates the passive behavior of a typical pile cap-backfill system. That chapter helped to acquaint the reader with the general numerical modeling and calibration procedure employed in PLAXIS.

To support the validity of the numerical models, calibration procedures were first carried out for pile caps with full width (homogeneous) backfills. The calibration procedure was based on the comparison of passive load-displacement relationships generated numerically, with load-displacement curves computed by the analytical models, PYCAP and ABUTMENT. After obtaining an acceptable degree of agreement (within 10%) between analytical and numerical results, the calibrated models were then utilized in approximating the passive response of limited width dense gravel backfills. Obviously, the 2D numerical analysis ignored the 3D geometry of the full-scale tests. Thereby, comparisons between the results of the field tests and the plane strain numerical models allowed an evaluation of 3D end effects on the test results.

In this chapter, the calibration and numerical simulation results are presented for the four analyzed backfill conditions adjacent to the 3.67-ft (0.91-m) and 5.5-ft (1.83-m) deep pile caps. Comparisons are made among load-displacement curves generated from numerical simulations, experimental test data, and analytical solutions performed by PYCAP and ABUTMENT. Conclusions drawn from these comparisons are used to meet the objectives outlined for this study, in quantifying the extent of 3D end effects on the total passive resistance mobilized by limited width gravel backfills. Furthermore, a series of parametric studies are conducted by isolating a range of typical pile cap and backfill parameters with the objective of investigating the effect of the selected parameters on the ultimate passive resistance of limited width backfills. Based on the parametric study results, a simple design method is developed that can be used as an aid in designing limited width backfills for both plane strain and 3D geometries. Lastly, design examples are presented to demonstrate the application of the developed models in predicting the passive resistance of limited width backfills.

5.2 Calibration of Full Width (Homogeneous) Backfill Numerical Models

The calibration of full width (homogeneous) numerical models was primarily based on load-displacement curves generated analytically from the spread sheet program, PYCAP, and the computer program, ABUTMENT. As discussed previously in chapter 2, the development of PYCAP was based on the implementation of the modified log spiral theory, coupled with a hyperbolic stress-strain relationship for defining the shearing behavior of soils. Similarly, in ABUTMENT, Shamsabadi et al., (2007) incorporates a methodology which combines a modified hyperbolic stress-strain relationship with mobilized log spiral failure surfaces. Considering the fact that the development of both PYCAP and ABUTMENT is based on the log spiral theory, the selection of these models, as analytical tools employed in the calibration process involved in this study, is appropriate. As mentioned previously, the log spiral theory has been reported to give the most theoretically sound approximation of passive earth pressure among limit equilibrium theories (e.g. Duncan and Mokwa, 2001, Rollins and Sparks, 2002, and Cole and Rollins, 2006).

5.2.1 Analytical Model Input Parameters

Input parameters used in PYCAP and ABUTMENT to approximate the behavior of the silty sand and coarse gravel materials, as well as the interaction between the pile cap and the adjacent backfill, were based on: (1) a combination of field and laboratory test values, and (2) back-calculated parameters derived by matching load-displacement curves measured experimentally, with curves computed analytically from PYCAP and ABUTMENT. Analytical input parameters including the soil friction angle φ, soil in-situ unit weight γ_m, and interface friction angle δ, were primarily based on field and laboratory test values and were consistent with values used in the numerical models. Tables 5-1 and 5-2 contain a summary of key input

and output parameters used in the analyses performed by PYCAP for the South Temple and SLC Airport full width (homogeneous) backfills, respectively. A tabulation of key input and output parameters used in ABUTMENT for the South Temple and SLC Airport full width (homogeneous) backfills is presented in Tables 5-3 and 5-4, respectively. In addition, the basis for selecting and adjusting several key parameters used in the analytical models is described as follows:

Table 5-1: Summary of PYCAP parameters used in the analysis of 3.67-ft (0.91-m) deep pile cap with full width (homogeneous) loose silty sand and dense gravel backfills

Parameter	Symbol	Loose Sand	Dense Gravel	Unit
Soil friction angle	φ	27.7	42.0	degrees
Cohesion	c	10 (0.5)	0	psf (kPa)
Wall friction angle	δ	20.77	31.5	degrees
Soil moist unit weight	γ_m	110 (17.3)	141 (22.1)	pcf (kN/m^3)
Initial soil modulus	E_i	200.5 (9.6)	1040 (49.8)	ksf (MPa)
Poisson's ratio	ν	0.35	0.25	---
Elastic stiffness	k_{max}	371.6 (65.1)	1884.4 (330)	k/in (kN/mm)
Maximum deflection	Δ_{max}	2.64 (67.1)	1.76 (44.7)	in (mm)
Deflection-wall height ratio	Δ_{max}/H	0.06	0.04	---
Failure ratio	R_f	0.93	0.9	---
3D correction factor	R_{3D}	1.176	1.434	---
Passive coeff. (log spiral)	K_p	7.5	16.99	---
Resultant force	E_p	3.69 (53.8)	16.13 (235.3)	k/ft (kN/m)

1) As mentioned previously, relatively low (close to zero) cohesion values were used in PLAXIS, that were sufficient to achieve numerical stability as recommended in the PLAXIS Reference Manual. Specifically, values of 10 psf (0.5 kPa) and 40 psf (1.9 kPa) were used for the loose sand and dense gravel backfill materials, respectively. The cohesion values used in PYCAP and ABUTMENT associated with the full width loose silty sand backfills were consistent with the values used in the numerical models. However, for the full width dense gravel backfills, several iterative adjustments were required for the cohesion value in both analytical models to achieve a reasonable match between experimental, analytical and numerical results.

Table 5-2: Summary of PYCAP parameters used in the analysis of 5.5-ft (1.83-m) deep pile cap with full width (homogeneous) loose silty sand and dense gravel backfills

Parameter	Symbol	Loose Sand	Dense Gravel	Unit
Soil friction angle	φ	27.7	42.0	degrees
Cohesion	c	10 (0.5)	0	psf (kPa)
Wall friction angle	δ	20.77	31.5	degrees
Soil moist unit weight	γ_m	110 (17.3)	141 (22.1)	pcf (kN/m^3)
Initial soil modulus	E_i	200.5 (9.6)	1040 (49.8)	ksf (MPa)
Poisson's ratio	ν	0.35	0.25	---
Elastic stiffness	k_{max}	335.3 (58.7)	1711.8 (299.8)	k/in (kN/mm)
Maximum deflection	Δ_{max}	3.96 (100.6)	2.64 (67.1)	in (mm)
Deflection-wall height ratio	Δ_{max}/H	0.06	0.04	---
Failure ratio	R_f	0.91	0.85	---
3D correction factor	R_{3D}	1.387	1.954	---
Passive coeff. (log spiral)	K_p	7.5	16.99	---
Resultant force	E_p	8.14 (118.8)	36.2 (528.1)	k/ft (kN/m)

2) The dense gravel modeled in PYCAP was assumed to be cohesionless, to provide a more general application of results. This assumption provided reasonable agreement between analytical and experimental results for the full width (homogeneous) dense gravel backfill tested at the SLC Airport site.

3) In ABUTMENT, on the other hand, addition of relatively low cohesion values of 40 and 50 psf (1.9 and 2.4 kPa) was required for the 3.67-ft (0.91-m) and 5.5-ft (1.83-m) deep pile caps with full width (homogeneous) dense gravel backfills, respectively. The inclusion of cohesion in the analyses performed by ABUTMENT increased the ultimate passive resistance by 10 to 12%, compared to the cohesionless case, and produced a satisfactory match (within 9%) between numerical and analytical results.

Table 5-3: Summary of ABUTMENT parameters used in the analysis of South Temple full width (homogeneous) loose silty sand and dense gravel backfills

Parameter	Symbol	Loose Sand	Dense Gravel	Unit
Soil friction angle	φ	27.7	42.0	Degrees
Cohesion	c	10 (0.5)	40 (1.9)	psf (kPa)
Wall friction angle	δ	20.77	31.5	Degrees
Soil moist unit weight	γ_m	110 (17.3)	141 (22.1)	pcf (kN/m^3)
Strain at 50% of ultimate strength	ε_{50}	0.003	0.004	---
Poisson's ratio	ν	0.35	0.25	---
Failure ratio	R_f	0.97	0.95	---
Horizontal component of Passive coeff.	K_{ph}	4.5	14.1	---

4) The initial elastic soil modulus parameter used in PYCAP, E_i, was derived based on recommendations provided by Duncan and Mokwa, (2001) for "preloaded or compacted" dense sands and "normally loaded" loose sands.

5) The stiffness parameter used in ABUTMENT is the strain level at which 50% of the ultimate soil resistance is mobilized (ε_{50}). This parameter was selected based on values used by Shamsabadi et al. (2007) in analyzing similar backfill materials.

6) Values of Poisson's ratio for the dense gravel and loose sand were calculated using the following empirical equation provided in Duncan and Mokwa, (2001):

$$\nu = \frac{1 - sin\varphi}{2 - sin\varphi} \tag{5-1}$$

where φ is the soil friction angle.

7) The ultimate passive resistance of full width (homogeneous) backfills was assumed to develop at deflection-to-wall height ratios of 6% and 4% for loose silty sand, and dense gravel, respectively. This was based on the concept that the ultimate passive resistance typically develops with lateral movements within the range of 2 to 6% of the pile cap height (Rollins and Spark, 2002). Specifically, the displacement ratio used for the full width (homogeneous) dense gravel backfill is based on results from a number of full-scale pile cap load tests (e.g. Duncan and Mokwa, 2001, Rollins and Spark, 2002, Cole and Rollins, 2006, Rollins and Cole, 2006). The loose sand was assumed to mobilize its ultimate passive resistance at a higher displacement ratio of 6%. The selection of this value was based on the concept that sands with loose or

medium density will typically require more pile cap movement to mobilize the full passive resistance, relative to denser materials (Clough and Duncan, 1991).

Table 5-4: Summary of ABUTMENT parameters used in the analysis of SLC Airport full width (homogeneous) loose silty sand and dense gravel backfills

Parameter	Symbol	Loose Sand	Dense Gravel	Unit
Soil friction angle	φ	27.7	42.0	Degrees
Cohesion	c	10 (0.5)	50 (2.4)	psf (kPa)
Wall friction angle	δ	20.77	31.5	Degrees
Soil moist unit weight	γ_m	110 (17.3)	141 (22.1)	pcf (kN/m^3)
Strain at 50% of ultimate strength	ε_{50}	0.003	0.004	---
Poisson's ratio	ν	0.35	0.25	---
Failure ratio	R_f	0.97	0.95	---
Horizontal component of Passive coeff.	K_{ph}	4.5	13.8	---

5.2.2 Verification of Analytical Models Based on Field Tests

Since the calibration procedure employed in this study is primarily based on comparisons between analytical and numerical results, input parameters presented in Tables 5-1, 5-2, 5-3, and 5-4 were not optimized to provide an exact match between measured and analytical load-displacement curves. However, to validate the input parameters used in the analytical models for full width (homogeneous) backfills, measured load-displacement curves were compared with those predicted by PYCAP, taking into account 3D edge effects. The main objective of these comparisons was to ensure that the analytical models were predicting within a reasonable range

of measured ultimate resistances for both series of lateral load tests. The comparison presented for the South Temple tests is limited to the full width (homogeneous) loose silty sand backfill, since no measured data was available for the full width (homogeneous) dense gravel backfill condition. On the other hand, the comparisons presented for the SLC Airport tests include full width (homogeneous) backfill test results, for both loose clean sand and dense gravel backfills. In addition, emphasis was placed on obtaining agreement between the ultimate resistance of measured and analytical load-displacement relationships, rather than the initial loading stiffnesses. As explained previously in Chapter 3, the relatively flat slopes associated with the SLC Airport load-displacement curves may have been due to the cyclic and dynamic loading effects, and thereby not a true representation of the actual static passive resistance mobilized by the backfills.

5.2.2.1 South Temple Testing

Measured and computed load-displacement curves associated with the full width (homogeneous) loose silty sand backfill, tested at the South Temple site are shown in Figure 5-1. Also shown in Figure 5-1, is the analytical load-displacement curve computed using PYCAP for the full width (homogeneous) dense gravel backfill. In this comparison, the total measured and computed passive force has been normalized by the actual pile cap width of 17 ft (5.18 m) to obtain the force per width of pile cap. The measured ultimate passive resistance of the loose silty sand backfill appears to be about 5.2 k/ft (76 kN/m). This resistance level is developed at a pile cap displacement of approximately 2 in (50 mm), which corresponds to a deflection-to-wall height ratio of approximately 4.5%. The ultimate 3D resistance predicted by PYCAP for this backfill condition is about 4.1 k/ft (kN/m), and develops at a displacement of approximately 2.64

in (67 mm), which corresponds to a pre-defined wall height ratio of 6%. This value is within 22% of the measured ultimate resistance. As mentioned previously in chapter three, rather than flattening out, the loose silty sand backfill appears to experience a gradual increase in resistance starting at a displacement level of 0.5 in (12.7 mm) to a maximum displacement of 2 in (51 mm).

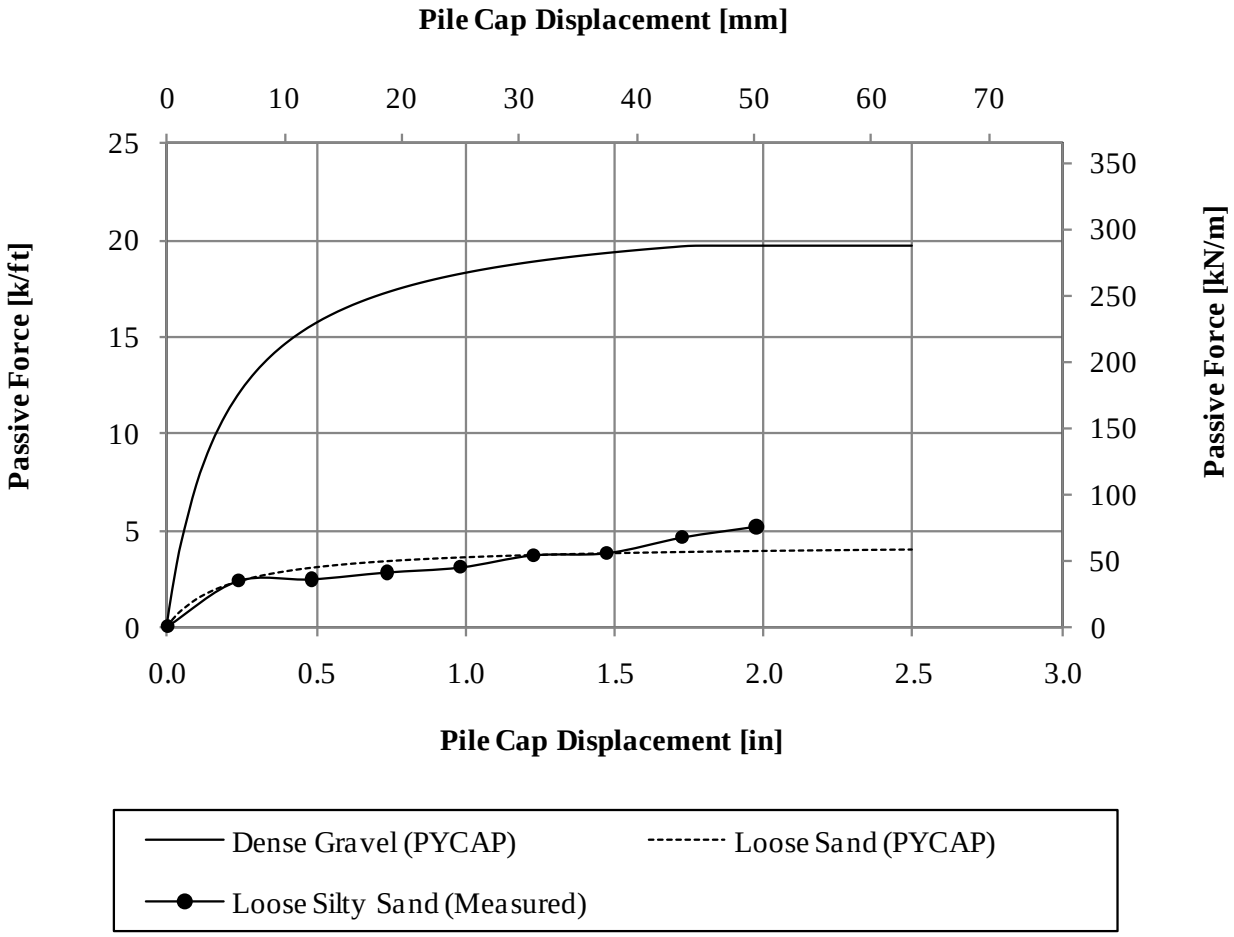

Figure 5-1: Comparison of measured and computed load-displacement curves, normalized by the pile cap width of 17 ft (5.18 m), for the South Temple full width (homogeneous) loose silty sand, and 3.67-ft (1.12-m) deep pile cap with full width (homogeneous) dense gravel backfills

This load increase may have been due to small variations in the slope of the measured baseline curve, and consequently not a true representation of the passive resistance of the backfill.

5.2.2.2 SLC Airport Testing

Measured and computed load-displacement curves associated with the 5.5-ft (1.83-m) deep pile cap with full width (homogeneous) loose clean sand and dense gravel backfills, tested at the SLC Airport site are shown in Figure 5-2. In this comparison, the total measured and computed passive force for each test has been normalized by the actual pile cap width of 11 ft (3.35 m) to obtain the force per width of pile cap.

The measured ultimate passive resistance of the full width (homogeneous) loose clean sand backfill appears to be about 7.9 k/ft (116.3 kN/m). This resistance level is achieved at a pile cap displacement of approximately 1.5 in (38 mm), which corresponds to a deflection-to-wall height ratio of approximately 2.3%. The ultimate 3D resistance predicted by PYCAP for this backfill condition is about 10.5 k/ft (153 kN/m), and develops at a displacement of approximately 3.96 in (100.6 mm), which corresponds to a pre-defined wall height ratio of 6%. This value is within 33% of the measured ultimate resistance.

As mentioned previously, equipment malfunctioning occurred during the full width (homogeneous) loose clean sand test, leading to the premature ending of the test. As a result, passive force measurements were not obtained further than 2 in (50 mm) of pile cap displacement. Therefore, the ultimate resistance associated with the loose clean, shown in Figure 5-2, is the maximum resistance mobilized in the backfill at the end of the test, and may not be the actual ultimate passive resistance associated with the loose clean sand backfill. It is likely that

the maximum measured backfill resistance would have been higher if the pile cap was able to displace further into the backfill.

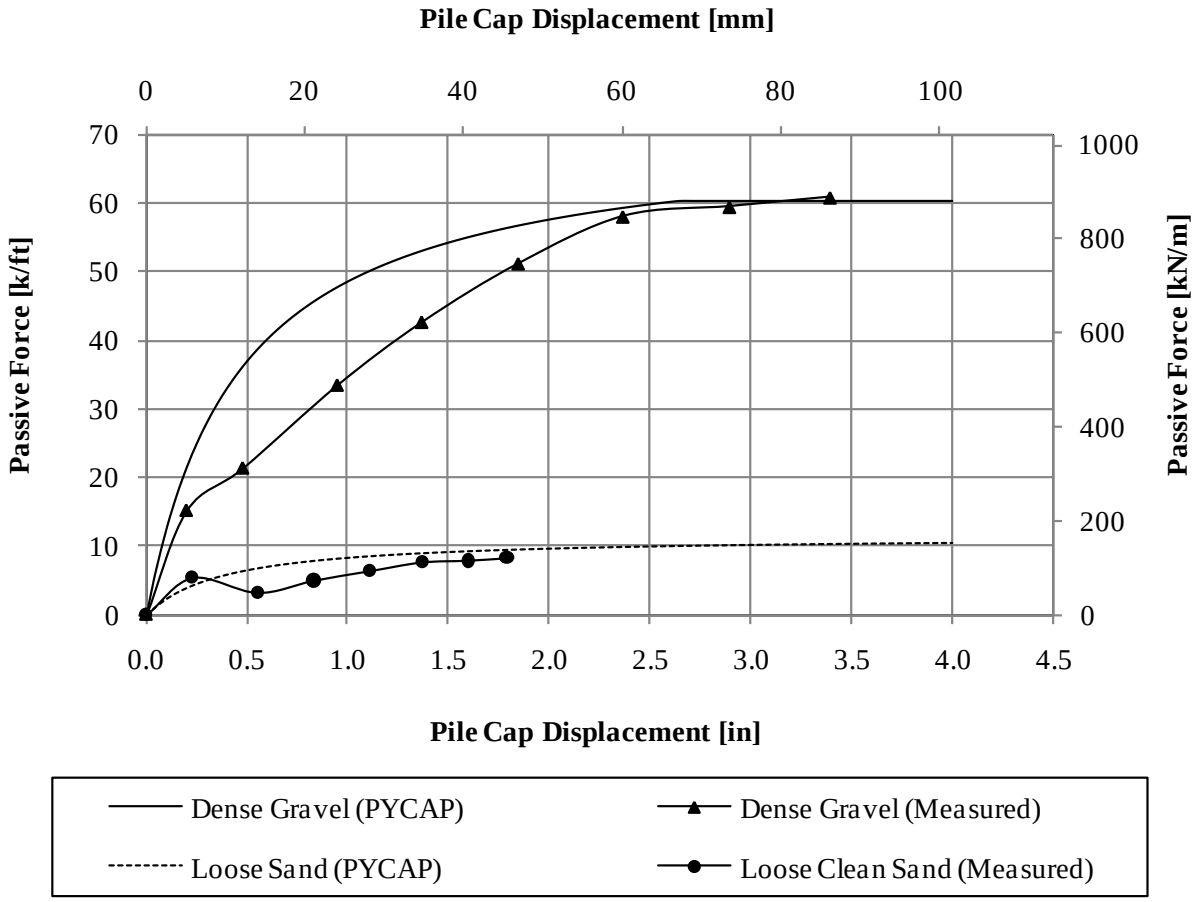

Figure 5-2: Comparison of measured and computed load-displacement curves, normalized by the pile cap width of 11 ft (3.35 m), for SLC Airport full width (homogeneous) loose silty sand and full width (homogeneous) dense gravel backfills

The measured ultimate passive resistance of the full width (homogeneous) dense gravel backfill appears to be about 58.2 k/ft (853 kN/m). This resistance level is developed at a pile cap

displacement of approximately 2.4 in (62 mm), which corresponds to a deflection-to-wall height ratio of approximately 3.7 %. The ultimate 3D resistance predicted by PYCAP for this backfill condition is about 60.4 k/ft (kN/m), and develops at a displacement of approximately 2.64 in (67 mm), which corresponds to a pre-defined deflection-to-wall height ratio of 4%. This value is within 4 % of the measured ultimate resistance.

5.2.3 Calibration of Numerical Models against Analytical Models

The calibration of full width (homogeneous) backfill numerical models is primarily based on comparing load-displacement relationships generated numerically and analytically. In this section, a comparison of ultimate resistances and corresponding displacement levels, computed from numerical and analytical models (PYCAP and ABUTMENT), for the South Temple and SLC Airport full width (homogeneous) loose silty sand and dense gravel backfills is presented. Results presented illustrate acceptable agreement (within 9%) achieved between the resistances computed from numerical and analytical models. Comparisons are made at a deflection-to-wall height ratio of 4% for full width (homogeneous) and limited width backfill conditions involving dense gravel. For full width (homogeneous) loose silty sand backfills, comparisons are made at a deflection-to-wall height ratio of 6%.

5.2.3.1 South Temple Testing

Computed load-displacement curves used in developing calibrated models for the full width (homogeneous) loose silty sand backfill, tested at the South Temple site are shown in Figure 5-3. In this comparison, the total computed passive force has been normalized by the effective pile cap width (actual pile cap width multiplied by the Brinch-Hansen 3D correction

factor) of 20.0 ft (6.1 m), which accounts for 3D loading effects, to obtain the plane strain force per width of pile cap. The ultimate passive resistance computed by PYCAP and ABUTMENT for this backfill condition, is 3.45 k/ft (50.3 kN/m) and 3.36 k/ft (49 kN/m), respectively.

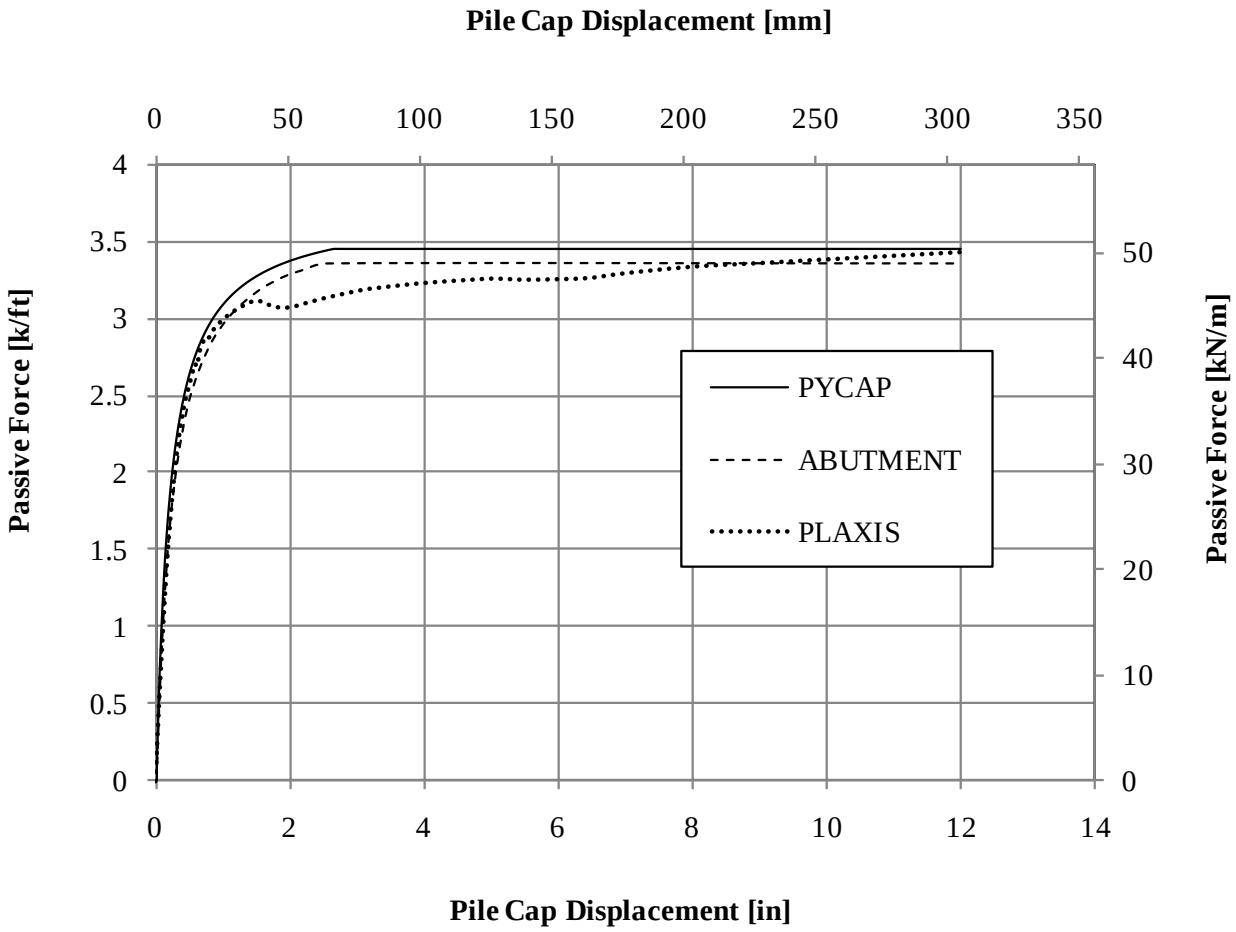

Figure 5-3: Comparison of load-displacement curves computed by ABUTMENT, PYCAP, and PLAXIS, normalized by the effective pile cap width of 20.0 ft (6.1 m), for the 3.67-ft (1.12-m) deep pile cap with a full width (homogeneous) loose silty sand backfill

These resistance levels develop at a pile cap displacement of approximately 2.6 in (66 mm), which corresponds to a pre-defined deflection-to-wall height ratio of approximately 6%. The ultimate resistance predicted by PLAXIS at this displacement level is about 3.15 k/ft (kN/m), which is within 6 to 9% of the ultimate resistance predicted by the analytical methods.

Computed load-displacement curves used in developing calibrated models for the 3.67-ft (1.12-m) deep pile cap with a full width (homogeneous) dense gravel backfill are shown in Figure 5-4. In this comparison, the total computed passive force has been normalized by the effective pile cap width of 24.4 ft (7.4 m) to obtain the plane strain force per width of pile cap. The ultimate passive resistance computed by PYCAP and ABUTMENT for this backfill condition, is 13.75 k/ft (kN/m) and 13.37 k/ft (kN/m), respectively. These resistance levels develop at a pile cap displacement of approximately 1.8 in (46 mm), which corresponds to a pre-defined deflection-to-wall height ratio of approximately 4%. The ultimate resistance predicted by PLAXIS at this displacement level is about 13.2 k/ft (192.6 kN/m), which is within 2 to 4% of the ultimate resistance predicted by the analytical models.

5.2.3.2 SLC Airport Testing

Computed load-displacement curves used in developing calibrated models for the full width (homogeneous) loose clean sand backfill, tested at the SLC Airport site are shown in Figure 5-5. In this comparison, the total computed passive force has been normalized by the effective pile cap width of 15.3 ft (4.7 m) to obtain the plane strain force per width of pile cap. The ultimate passive resistance computed by PYCAP and ABUTMENT for this backfill condition, is 7.6 k/ft (111 kN/m) and 7.4 k/ft (108 kN/m), respectively. These resistance levels develop at a pile cap displacement of approximately 4 in (102 mm), which corresponds to a pre-

defined deflection-to-wall height ratio of approximately 6%. The ultimate resistance predicted by PLAXIS at this displacement level is about 7.3 k/ft (106.5 kN/m), which is within 2 to 4% of the ultimate resistance predicted by the analytical models.

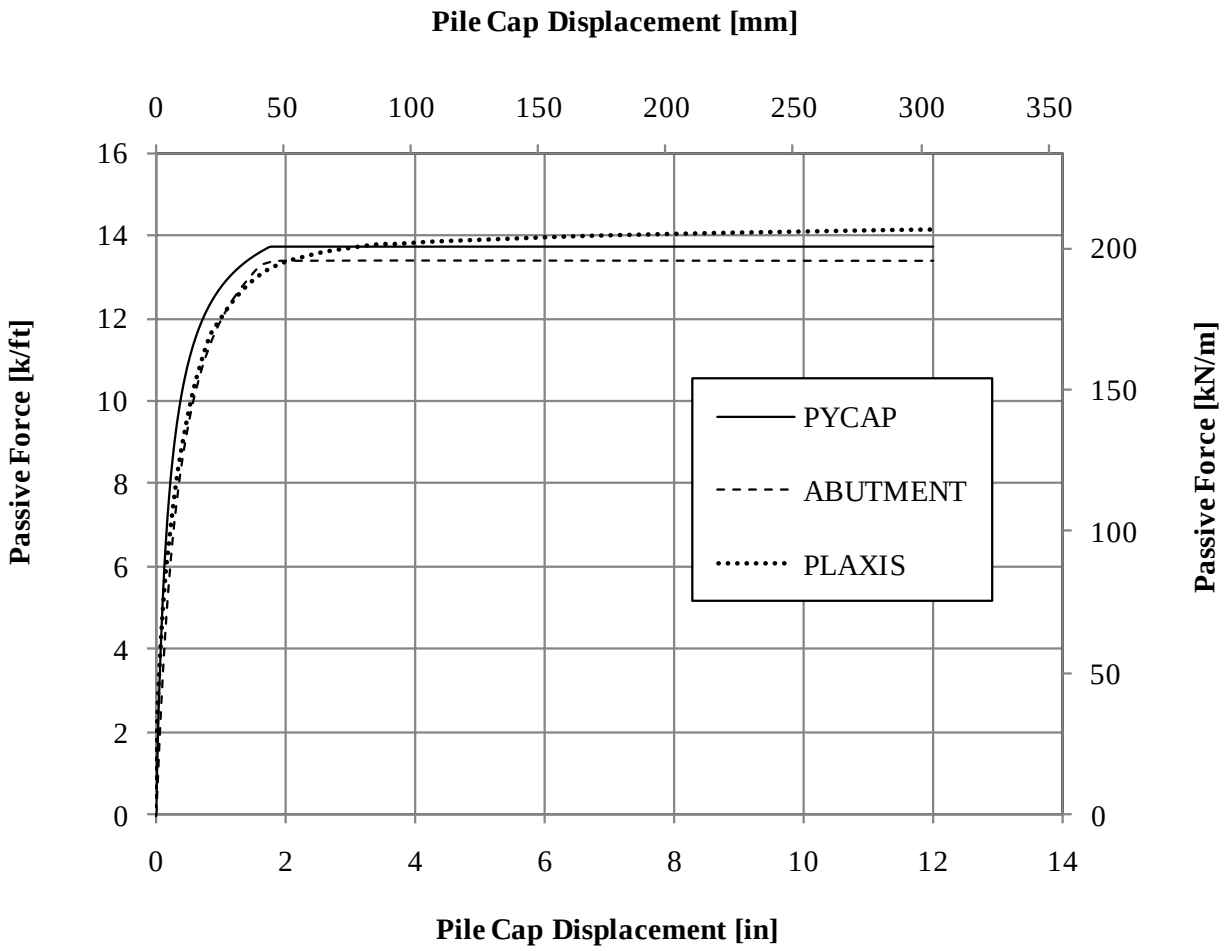

Figure 5-4: Comparison of load-displacement curves computed by ABUTMENT, PYCAP, and PLAXIS, normalized by the effective pile cap width of 24.4 ft (7.4 m), for the 3.67-ft (1.12-m) deep pile cap with a full width (homogeneous) dense gravel backfill

Computed load-displacement curves used in developing calibrated models for the full width (homogeneous) dense gravel backfill, tested at the SLC Airport site are shown in Figure 5-6. In this comparison, the total computed passive force has been normalized by the effective pile cap width of 21.5 ft (6.5 m) to obtain the plane strain force per width of pile cap.

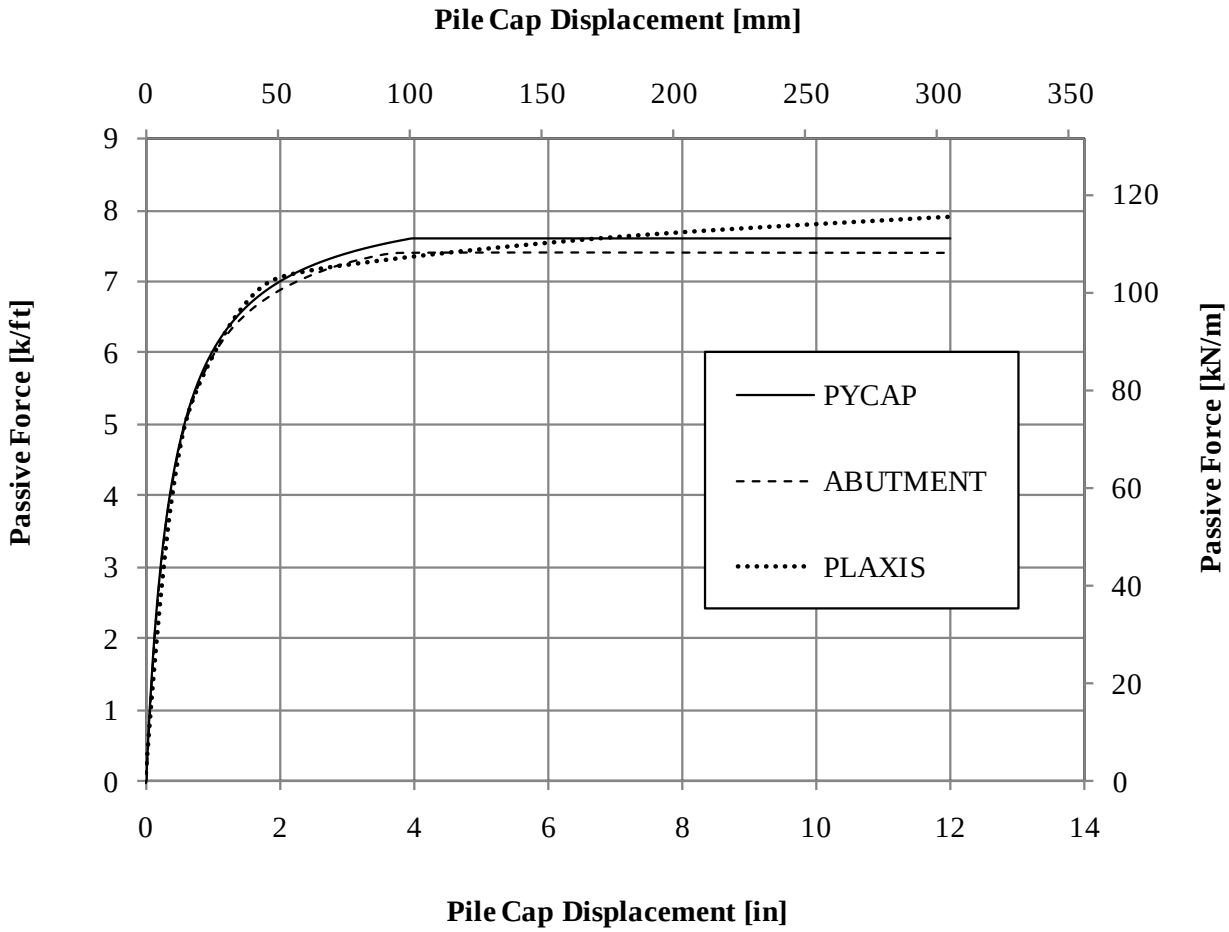

Figure 5-5: Comparison of load-displacement curves computed by ABUTMENT, PYCAP, and PLAXIS, normalized by the effective pile cap width of 15.3 ft (4.7 m), for the 5.5-ft (1.68-m) deep pile cap with a full width loose silty sand backfill

The ultimate passive resistance computed by PYCAP and ABUTMENT for this backfill condition, is 30.9 k/ft (450.9 kN/m) and 29.5 k/ft (430.6 kN/m), respectively. These resistance levels develop at a pile cap displacement of approximately 2.64 in (67 mm), which corresponds to a pre-defined deflection-to-wall height ratio of approximately 4%. The ultimate resistance predicted by PLAXIS at this displacement level is about 30.8 k/ft (449.5 kN/m), which is within 0.5 to 5% of the ultimate resistance predicted by the analytical models.

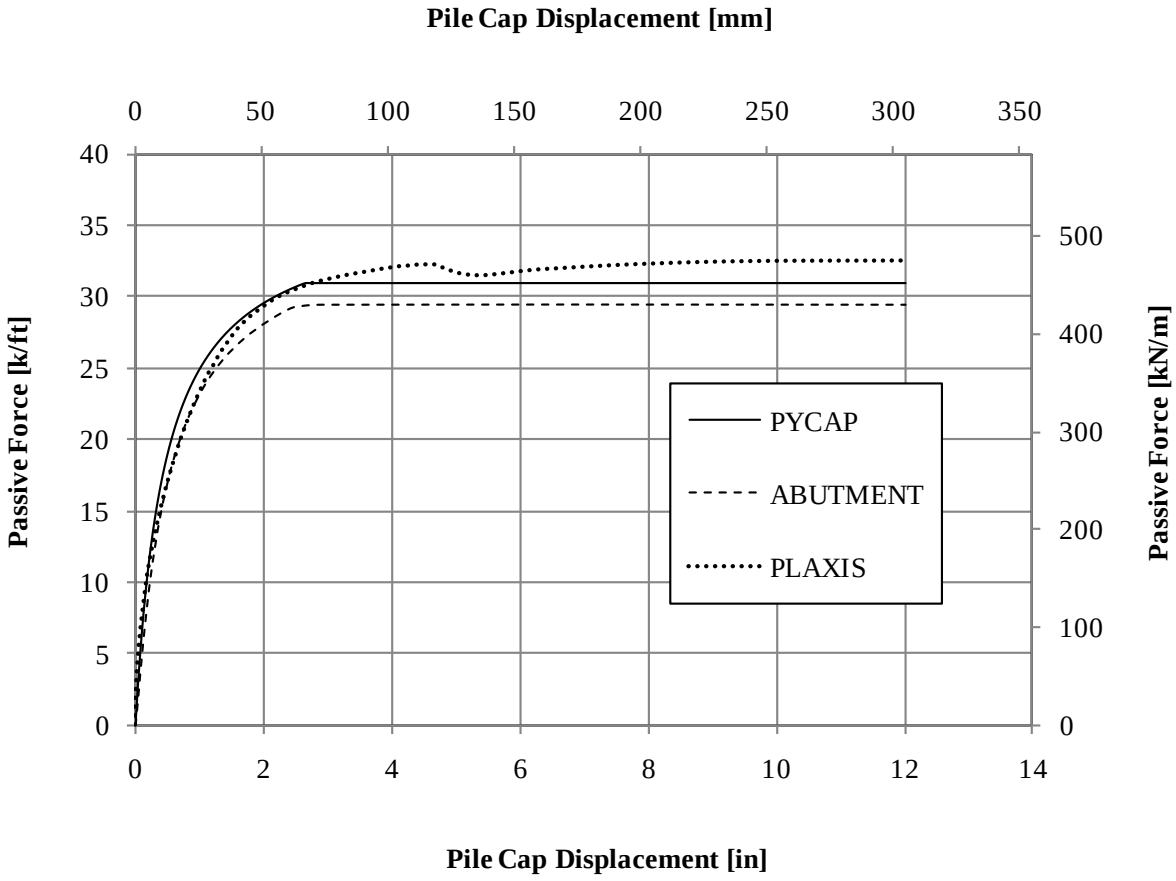

Figure 5-6: Comparison of load-displacement curves computed by ABUTMENT, PYCAP, and PLAXIS, normalized by the effective pile cap width of 21.5 ft (6.5 m), for the 5.5-ft (1.68-m) deep pile cap with a full width (homogeneous) dense gravel backfill

5.3 Numerical Simulation of Limited Width Dense Gravel Backfills

Following the calibration of numerical models, associated with full width (homogeneous) backfills, against load-displacement curves generated by PYCAP and ABUTMENT, the calibrated model was then employed to analyze the passive resistance of limited width dense gravel backfills, tested experimentally. In this section, numerical simulation results and discussions related to the plane strain analysis of limited width dense gravel backfills, consisting of 3-ft (0.91-m) and 6-ft (1.83-m) wide zones of dense gravel compacted between the pile cap and loose silty sand, is presented. These results include total displacements, incremental shear strains, and load-displacement curves.

5.3.1 Total Displacements

The numerical simulation is intended to replicate the vertical and horizontal movements of the soil mass within the defined boundaries of the backfill, as a result of the lateral deflection of the pile cap into the backfill. In PLAXIS, this is achieved by applying a uniformly distributed prescribed displacement to the pile cap face, in the horizontal direction. In order to induce passive conditions in full width (homogeneous) and limited width backfills involving dense gravel, a prescribed horizontal displacement corresponding to a deflection-to-wall height ratio of 4% was applied to the pile cap. As explained previously, this displacement ratio is based on results obtained from a number of full-scale pile cap load tests (e.g. Duncan and Mokwa, 2001, Rollins and Spark, 2002, Cole and Rollins, 2006, Rollins and Cole, 2006). In the case of the full width (homogeneous) loose silty sand backfill, a prescribed horizontal displacement corresponding to a deflection-to-wall height ratio of 6% was applied. This selection was based

on the concept that loose sands will typically require more pile cap movement to mobilize the full passive resistance of the backfill.

The combination of the total vertical and horizontal displacement components is computed at each node of the deformed finite element mesh, and is represented as an absolute quantity, referred to as total displacements, at the end of the defined calculation phase. The maximum total displacements predicted by PLAXIS for the analyzed backfill conditions are presented in Table 5-5.

Table 5-5: Maximum total backfill displacements predicted by PLAXIS for 3.67-ft (1.12-m) and 5-ft (1.68-m) deep pile caps with full width (homogeneous) and limited width backfill conditions at displacement ratios of 4 and 6%, for full and limited width backfill conditions involving dense gravel, and full width (homogeneous) loose silty sand backfills, respectively.

Backfill Type	Pile Cap Height ft (m)	Maximum Total Displacement in (mm)
Full width loose silty sand	3.67 (1.12) 5.5 (1.68)	2.7 (68.6) 4.2 (106.7)
Full width dense gravel	3.67 (1.12) 5.5 (1.68)	1.9 (48.3) 3.3 (83.8)
3-ft (0.91-m) wide gravel zone and loose silty sand	3.67 (1.12) 5.5 (1.68)	1.8 (45.7) 3.0 (76.2)
6-ft (1.83-m) wide gravel zone and loose silty sand	3.67 (1.12) 5.5 (1.68)	1.8 (45.7) 3.0 (76.2)

Figures 5-7 and 5-8 show deformed finite element mesh profiles of the simulated backfill conditions for the 3.67-ft (1.12-m) and 5.5-ft (1.68-m) deep pile caps, respectively. For the sake of visualization, these profiles have been magnified five times from their true scale. It should be observed that a significant amount of movement is predicted by the numerical models near the top of the pile cap for the homogenous backfills, where the soil has heaved upward owing to the lateral deflection of the pile cap. This observation is consistent with field measurements for the full width (homogeneous) dense gravel backfill tested at the SLC Airport site, where upward movement begins adjacent to the cap. Further comparison of deformed mesh profiles associated with full width (homogeneous) backfills, indicates that the zone of heaving is longer for the dense gravel backfill than for the loose sand backfill owing to the longer shear surface resulting from the higher friction angle. This observation is consistent with what is observed in the SLC Airport tests.

For the limited width gravel zones, the numerical model predicts that the dense gravel zone will deflect into the loose sand layer with relatively little heaving in the gravel, but that increased heaving would be expected just beyond the loose sand boundary. Vertical movements measured for limited width backfills tested experimentally show similar behaviors. As mentioned previously, the shift in elevation between the gravel zone and loose silty sand boundary may possibly be an effect of the pile cap stresses being transmitted through the gravel zone into the loose silty sand portion of the limited width backfill. Greater lengths of heaving are also predicted in the loose sand for the 3-ft (0.91-m) wide gravel zone than for the 6-ft (1.68-m) wide gravel zone. This is presumably due to the reduced pressures at the 6 ft (1.68-m) interface compared to the 3 ft (1.12-m) interface.

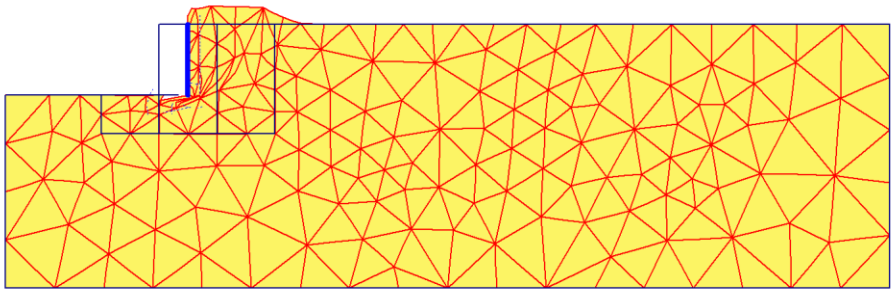

(a) Homogenous loose sand backfill

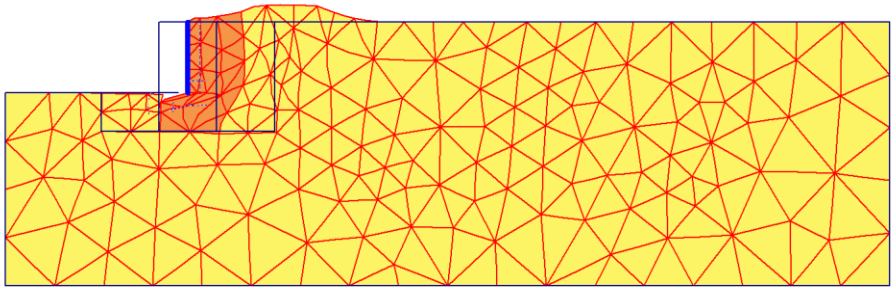

(b) 3 ft (0.91-m) gravel and loose sand backfill

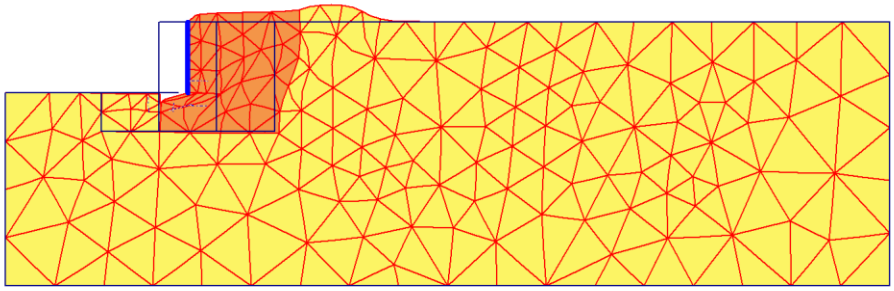

(c) 6 ft (1.83-m) gravel and loose sand backfill

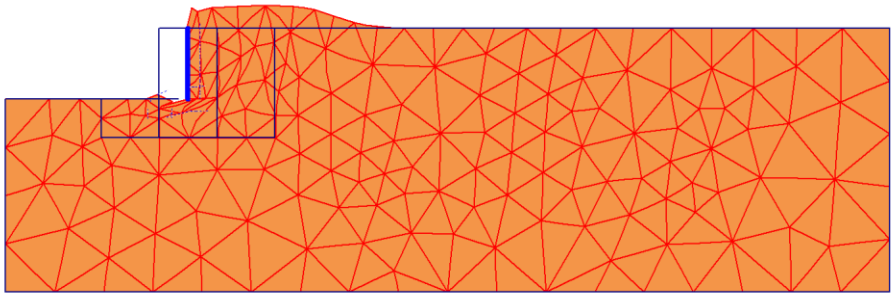

(d) Homogenous gravel backfill

Figure 5-7: Deformed mesh profiles of 3.67-ft (1.12-m) deep pile cap with backfills consisting of: (a) full width (homogeneous) loose silty sand; (b) 3-ft (0.91-m) wide dense gravel zone and loose silty sand; (c) 6-ft wide (1.83-m) dense gravel zone and loose silty sand; and (d) full width (homogeneous) dense gravel

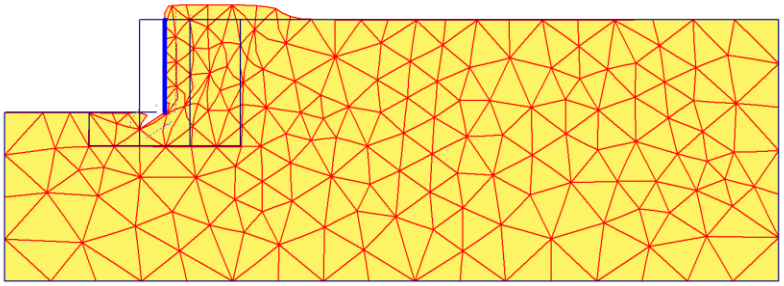

(a) Homogenous loose sand backfill

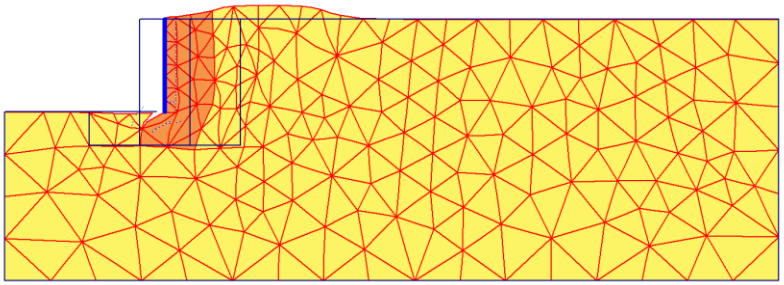

(b) 3 ft (0.91-m) gravel and loose sand backfill

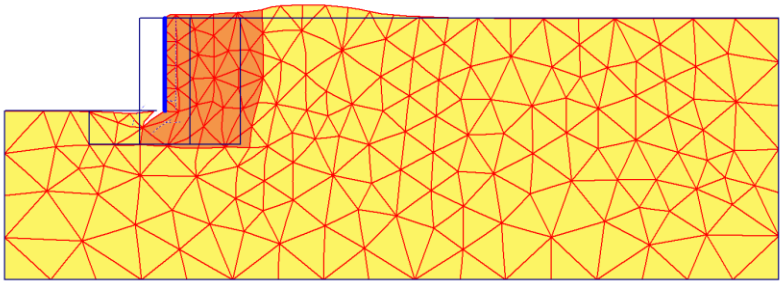

(c) 6 ft (1.83-m) gravel and loose sand backfill

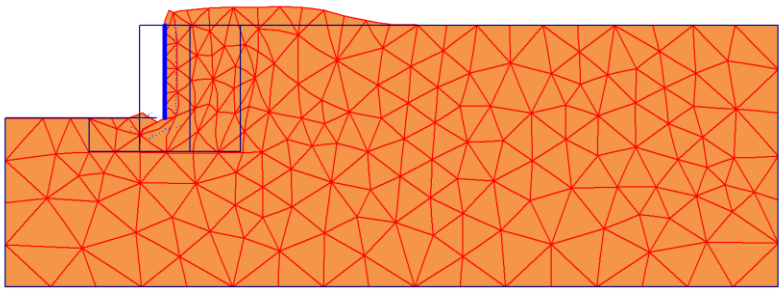

(d) Homogenous gravel backfill

Figure 5-8: Deformed mesh profiles of 5.5-ft (1.68-m) deep pile cap with backfills consisting of: (a) full width (homogeneous) loose silty sand; (b) 3-ft (0.91-m) wide dense gravel zone and loose silty sand; (c) 6-ft (1.83-m) wide dense gravel zone and loose silty sand; and (d) full width (homogeneous) dense gravel

In addition to displacements at the ground surface, major movements are concentrated at the base of the pile cap, in the deformed mesh profiles, where the shear zone displaces the soil. This observation emphasizes the importance of ensuring that the compacted dense gravel fill extends beneath the pile cap to intercept the shear zone, particularly for gravel zones of limited width.

5.3.2 Incremental Shear Strains

As the pile cap translates horizontally into the soil mass under the application of the prescribed displacements, the soil fails in shear along a critical failure surface behind the pile cap. This shear surface can be defined as a band of high shear strains and large incremental displacements from the computer output. To provide insight into the geometry of the potential shear surfaces developed in the analyzed backfills, incremental shear strain contours are illustrated in Figures 5-9, and 5-10, showing the shear patterns associated with the failure of the backfills.

For full width (homogeneous) loose silty sand backfills, the observed failure surface, resulting from possible punching shear behavior of the 3.67-ft (1.12-m) and 5.5-ft (1.68-m) deep pile caps, initiates from the base of the caps and extends outward in an approximately linear manner, until it intersects the ground surface. This is similar to a typical planar failure surface assumed in the Rankine theory of passive earth pressure. Shear strain contours of backfills involving dense gravel, show a more curvilinear failure surface, similar to a typical log spiral failure surface observed in dense gravels. The curved log spiral portion of the failure surface, initiates from the base of the pile cap, dipping approximately 2 ft (0.6 m) beneath the base of the pile cap, before it extends linearly to intersect the ground surface.

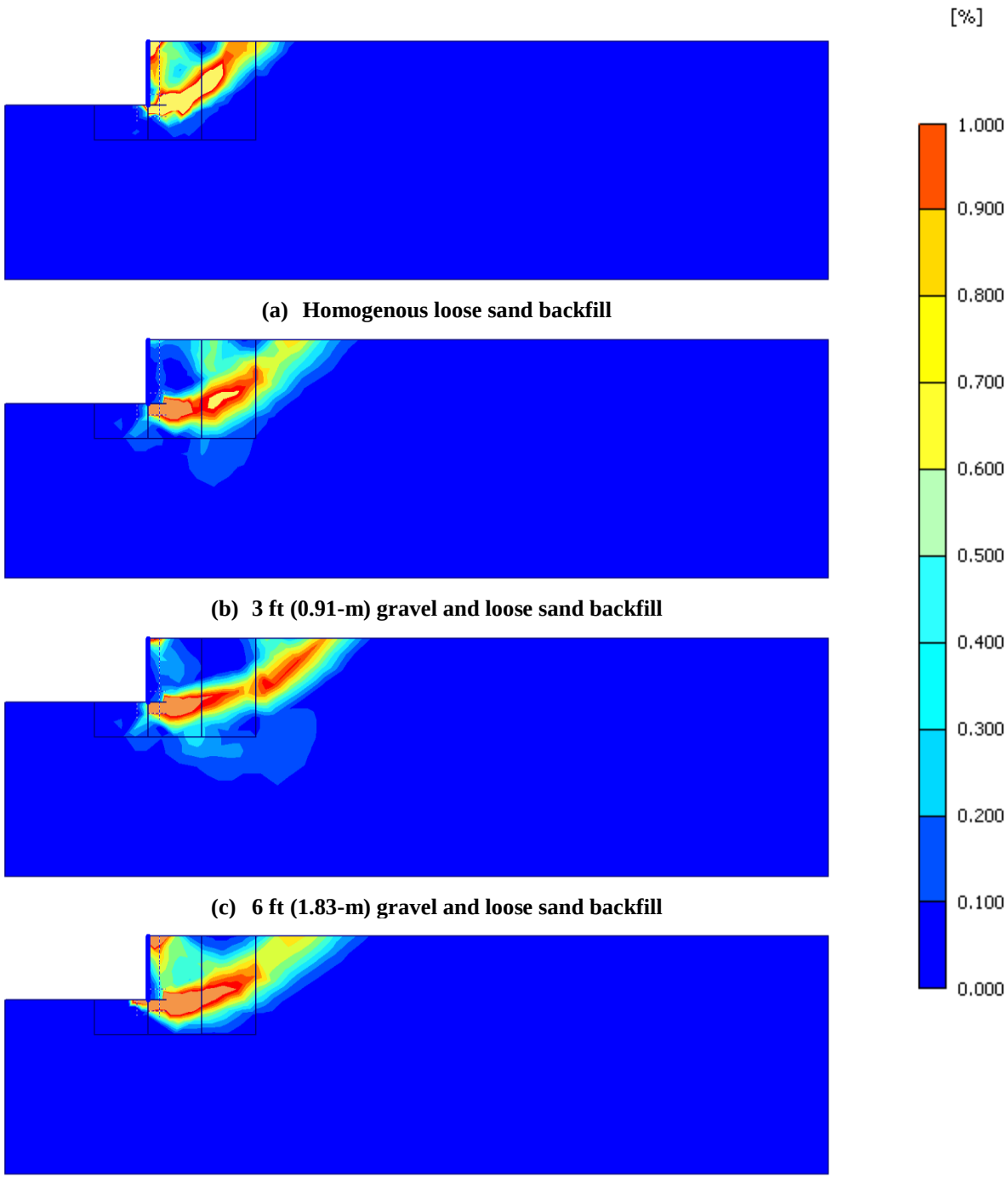

(a) Homogenous loose sand backfill

(b) 3 ft (0.91-m) gravel and loose sand backfill

(c) 6 ft (1.83-m) gravel and loose sand backfill

(d) Homogenous gravel backfill

Figure 5-9: Incremental shear strain profiles of 3.67-ft (1.12-m) deep pile cap with backfills consisting of: (a) full width (homogeneous) loose silty sand; (b) 3-ft (0.91-m) wide dense gravel zone and loose silty sand; (c) 6-ft (1.83-m) wide dense gravel zone and loose silty sand; and (d) full width (homogeneous) dense gravel

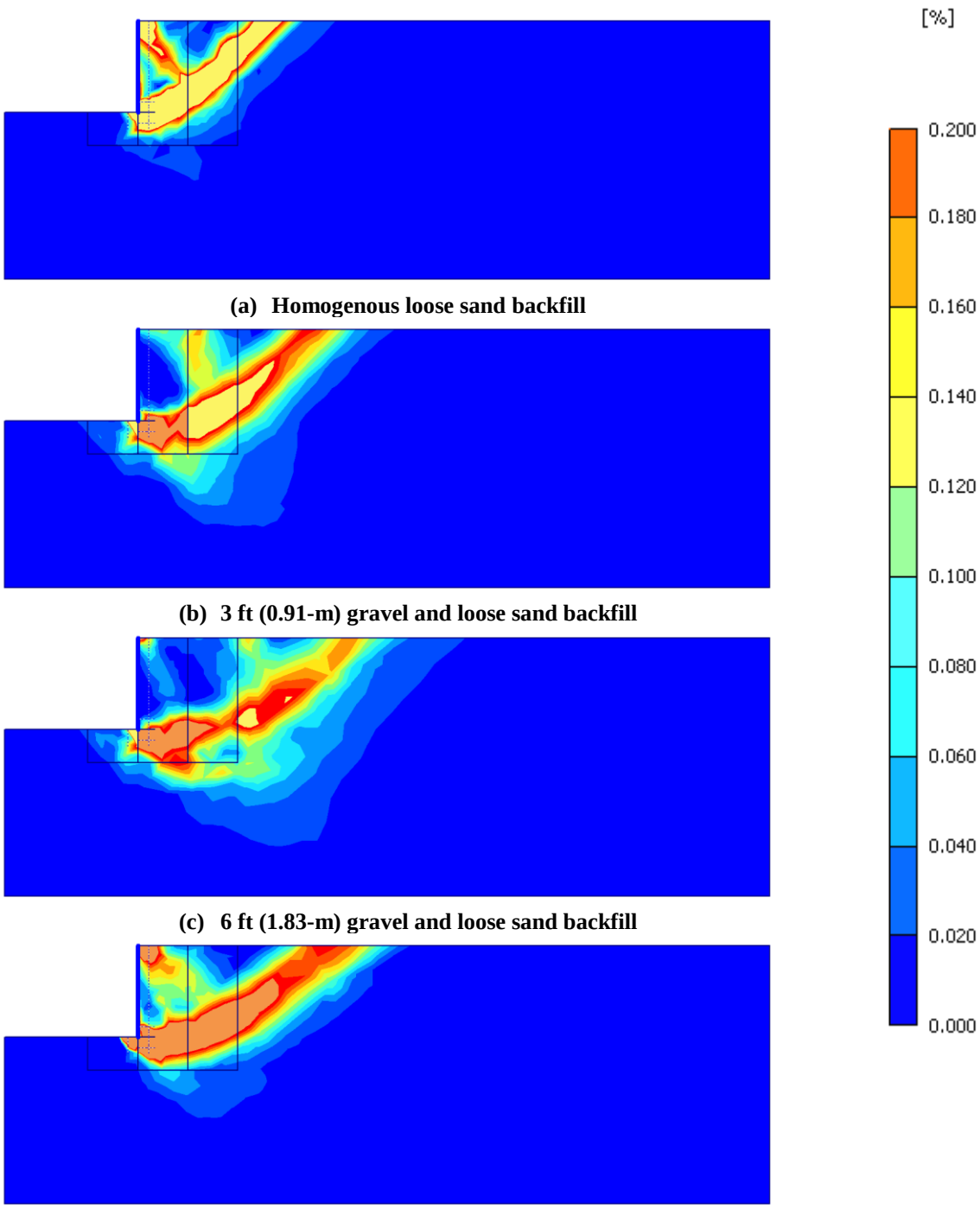

(a) Homogenous loose sand backfill

(b) 3 ft (0.91-m) gravel and loose sand backfill

(c) 6 ft (1.83-m) gravel and loose sand backfill

(d) Homogenous gravel backfill

Figure 5-10: Incremental shear strain profiles of 5.5-ft (1.68-m) deep pile cap with backfills consisting of: (a) full width (homogeneous) loose silty sand; (b) 3-ft (0.91-m) wide dense gravel zone and loose silty sand; (c) 6-ft (1.83-m) wide dense gravel zone and loose silty sand; and (d) full width (homogeneous) dense gravel

Comparing the shear shading plots of Figures 5-9 and 5-10, with deformed mesh profiles in the previous section, it appears that the failure surface intersects the ground surface beyond the zone of significant heaving, at a distance where the deformed mesh profile starts to approach the initial elevation of the backfill surface. In other words, the approximate exit point of the failure surface predicted by PLAXIS appears to coincide with the distance at which heaving becomes negligible. This observation is generally consistent with comparisons made between measured heave profiles presented in Chapter 3, and log spiral failure surfaces generated by PYCAP. To illustrate this point further, Table 5-6 compares the length of the developed shear failure surface predicted by PLAXIS and PYCAP with the length of significant heaving measured in field tests and predicted by PLAXIS, for the 3.67-ft (1.12-m) and 5.5-ft (1.68-m) deep pile caps. Note that the values presented in the Table 5-6 are approximate. In addition, the lengths associated with the failure surface and zone of significant heaving are measured from the pile cap face.

Another interesting aspect of shear strain patterns shown in Figures 5-9 and 5-10 is that for the 3.67-ft (1.12-m) deep pile cap, the failure surface appears to remain well within the gravel zone, as the gravel zone width increases, thereby providing greater passive resistance. In contrast, for the 5.5-ft (1.68-m) deep pile cap, even though the main portion of the shear zone passes through the gravel zone, shear strain concentrations appear to accumulate and extend around the gravel zone, with increasing gravel zone width. In this case, a smaller percentage of the failure surface would be contained in the gravel zone, relative to the 3.67-ft (1.12-m) deep pile cap, as the gravel zone width increases, resulting in relatively lower gains in passive resistance. This observation may be a possible explanation for the differences in resistance observed between the limited width backfills tested at the South Temple and SLC Airport sites. In addition, as mentioned in the previous section, this phenomenon emphasizes the importance of

ensuring that the compacted dense gravel fill extends sufficiently beneath the pile cap to intercept the shear zone developed in limited width dense gravel backfills.

Table 5-6: Comparison of predicted and measured significant heaving zone lengths with predicted failure surface lengths

Pile Cap Height ft (m)	Backfill Type	Length of Failure Surface, ft (m)		Length of Significant Heaving Zone, ft (m)	
		PLAXIS	Log Spiral	PLAXIS	Measured
3.67 (1.12)	Loose sand	8 (2.4)	8 (2.4)	8 (2.4)	6 (1.8)
	3-ft (0.91-m) gravel zone	12 (3.7)	---	12 (3.7)	4.5 (1.4)
	6-ft (1.83-m) gravel zone	12 (3.7)	---	12 (3.7)	6 (1.8)
	Dense gravel	12 (3.7)	13 (4.0)	12 (3.7)	---
5.5 (1.68)	Loose sand	12 (3.7)	12.5 (3.8)	12 (3.7)	12 (3.7)
	3-ft (0.91-m) gravel zone	15 (4.6)	---	15 (4.6)	21 (6.4)
	6-ft (1.83-m) gravel zone	20 (6.1)	---	20 (6.1)	24 (7.3)
	Dense gravel	17 (5.2)	20 (6.1)	17 (5.2)	27 (8.2)

Further examination of the shear strain contours associated with the 3-ft (0.91-m) and 6-ft (1.83-m) limited width dense gravel backfills, reveals information related to the development of transition shear lines, that define the boundary between the Prandtl and Rankine zones, within the developed log spiral failure surfaces. For the homogeneous soil backfills, these boundaries extend diagonally from the failure surface to a location near the top of the wall.

In the case of 3-ft (0.91-m) limited width dense gravel backfill, the transition line appears to develop outside the boundaries of the 3-ft (0.91-m) gravel zone. Relative to the full width

loose silty sand and full width dense gravel backfills, this occurrence allows the Prandtl zone to develop over a greater area embodied by the log spiral failure surface. A possible explanation for this observation could be that as the pile cap displaces laterally, the compacted 3-ft (0.91-m) wide dense gravel zone has the tendency to act integrally with the pile cap, causing the boundary between the Prandtl and Rankine zones to be pushed further back into the soil mass, beyond the compacted gravel zones. It is noteworthy to mention that this effect appears to be more dramatic for the 5.5-ft (1.68-m) deep pile cap analyzed, compared to what is observed for the 3.67-ft (1.12-m) deep pile cap.

In the case of the 6-ft (1.83-m) limited width dense gravel backfill, an additional boundary line develops within a distance of 3-ft (0.91-m) from the pile cap. This may be due to the fact that as a wider gravel zone is used, additional space becomes available between the pile cap and loose silty sand, allowing the development of a secondary boundary shear line within the gravel zone.

5.3.3 Load-Displacement Curves

In this section, a comparison of numerically generated load-displacement curves is presented among different backfill conditions, associated with the South Temple and SLC Airport lateral pile cap tests. Specifically, the backfill conditions included in the comparisons are as follows: (1) full width (homogeneous) dense gravel; (2) full width (homogeneous) loose silty sand; (3) 3-ft (0.91-m) wide gravel zone and loose silty sand; and (4) 6-ft (1.83-m) wide gravel zone and loose silty sand materials. Comparisons presented in this section are made at a deflection-to-wall height ratio of 4% for full width (homogeneous) and limited width backfill

conditions involving dense gravel. For full width (homogeneous) loose silty sand backfills, comparisons are made at a deflection-to-wall height ratio of 6%.

5.3.3.1 South Temple Testing

Figure 5-11 illustrates the effectiveness of limited width dense gravel backfills in increasing the plane strain passive resistance of the backfill, associated with the 3.67-ft (1.12-m) deep pile cap tested at the South Temple site. According to the numerical results, the limited width dense gravel backfills increase the passive resistance mobilized in the backfill considerably compared to the full width (homogeneous) loose silty sand and dense gravel backfills. Relative to the full width (homogeneous) loose silty sand backfill, placement of the 3-ft (0.91-m) and 6-ft (1.83-m) wide dense gravel zones between the pile cap and loose silty sand increased the passive resistance of the backfill 84% and 152%, respectively. In addition, the 3-ft (0.91-m) and 6-ft (1.83-m) wide dense gravel zones and loose silty sand backfills mobilized 43% and 59%, respectively, of the passive resistance associated with the full width (homogeneous) dense gravel backfills. Note that the increases in 2D resistances associated with the South Temple pile cap geometry are lower than the increases associated with the 3D case. This result is expected, as 3D end effects are anticipated to increase the passive resistance mobilized by the backfill by providing additional frictional resistance between the edges of the pile cap and the surrounding soil.

In addition to increasing the lateral passive resistance of the backfill, placement of the 3-ft (0.91-m) wide dense gravel zones between the pile cap and loose silty sand increased the initial loading stiffness by 53% relative to the full width (homogeneous) loose silty sand backfill. For the 6-ft (1.83-m) wide dense gravel zone this increase is 77%.

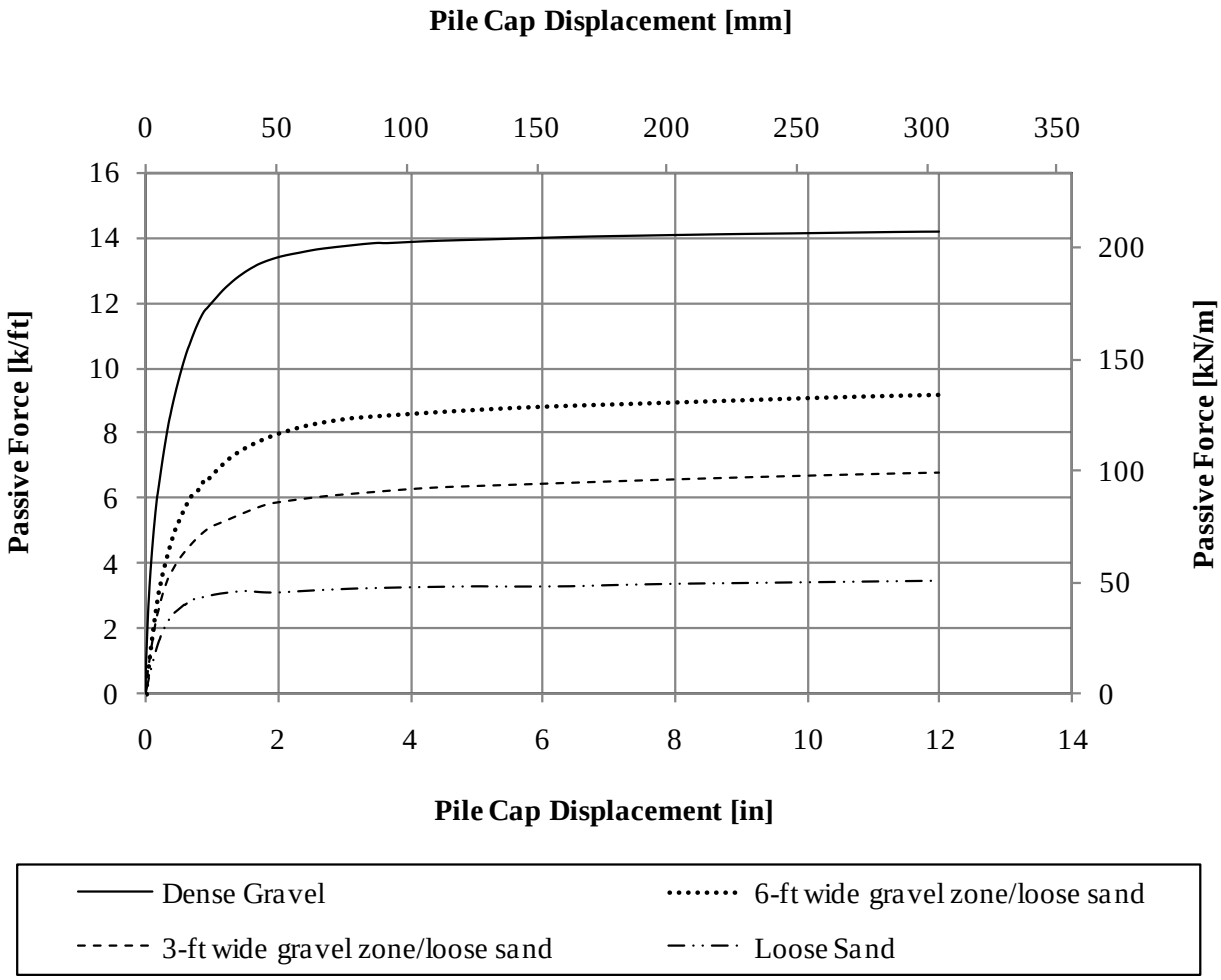

Figure 5-11: Comparison of load-displacement curves computed by PLAXIS for 3.67-ft (1.12-m) deep pile cap with backfills consisting of: (1) full width (homogeneous) dense gravel (2) full width (homogeneous) loose silty sand (3) 3-ft (0.91-m) wide gravel zone and loose silty sand; and (4) 6-ft (1.83-m) wide gravel zone and loose silty sand

5.3.3.2 SLC Airport Testing

Figure 5-12 illustrates the effectiveness of limited width dense gravel backfills in increasing the ultimate plane strain passive resistance of the backfill, associated with the 5.5-ft (1.68-m) deep pile cap tested at the SLC Airport site. Relative to the full width (homogeneous) loose silty sand backfill, placement of the 3-ft (0.91-m) and 6-ft (1.83-m) wide dense gravel

zones between the pile cap and loose silty sand increased the passive resistance of the backfill 60% and 100%, respectively. In addition, the 3-ft (0.91-m) and 6-ft (1.83-m) wide dense gravel zones and loose silty sand backfills mobilized 38% and 48% of the passive resistance associated with the full width (homogeneous) dense gravel backfills, respectively. Similar to the South

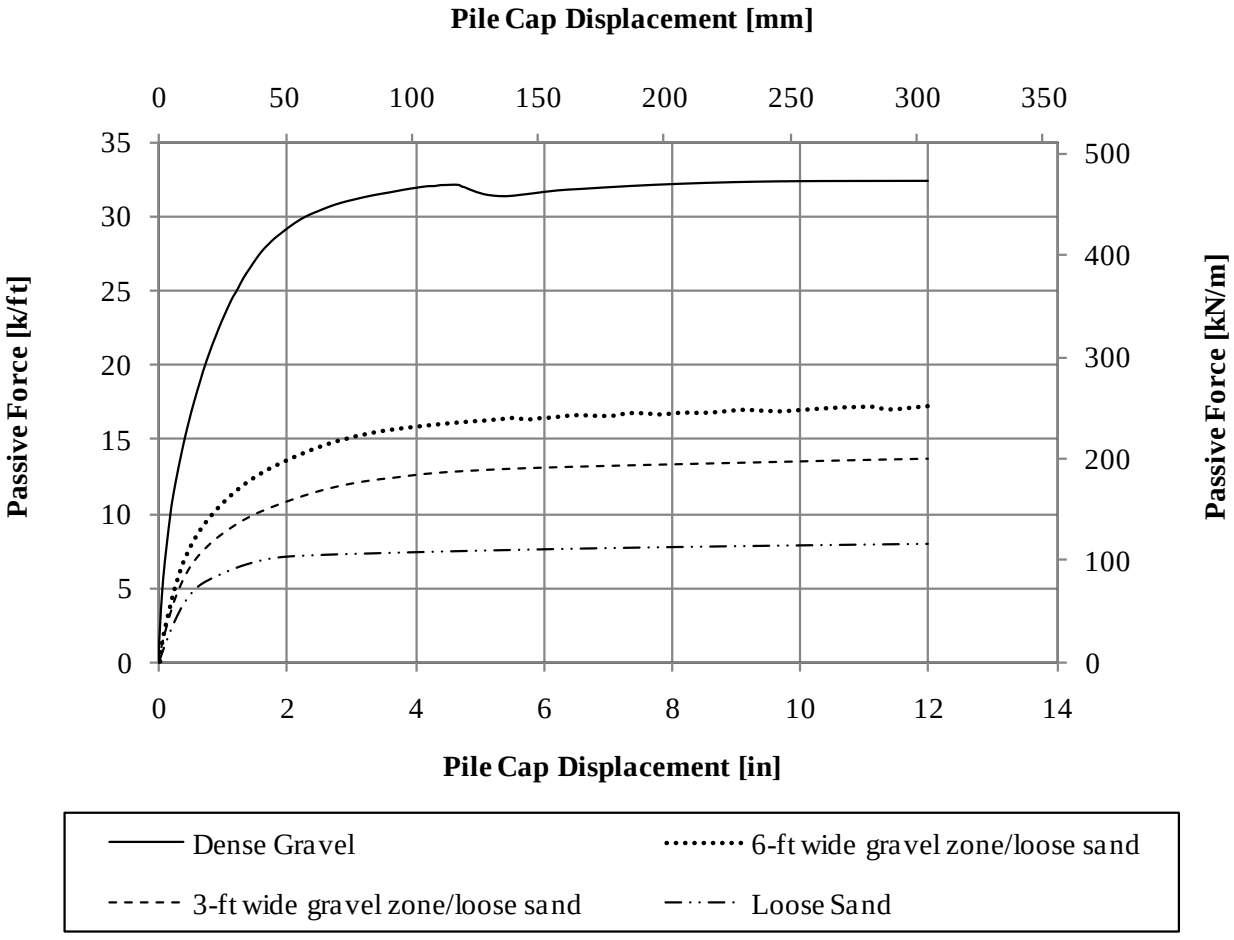

Figure 5-12: Comparison of load-displacement curves computed by PLAXIS for 5.5-ft (1.68-m) deep pile cap with backfills consisting of: (1) full width (homogeneous) dense gravel; (2) full width (homogeneous) loose silty sand; (3) 3-ft (0.91-m) wide gravel zone and loose silty sand; and (4) 6-ft (1.83-m) wide gravel zone and loose silty sand

Temple pile cap geometry, the increases in 2D resistances associated with the SLC Airport pile cap geometry are lower than the increases for the 3D case.

In addition to increasing the lateral passive resistance of the backfill, placement of the 3-ft (0.91-m) wide dense gravel zones between the pile cap and loose silty sand increased the initial loading stiffness by 38% relative to the full width (homogeneous) loose silty sand backfill. For the 6-ft (1.83-m) wide dense gravel zone this increase is 58%.

5.4 Parametric Studies

Following the verification of the numerical models in predicting the analytical passive resistance of various backfill conditions with an acceptable degree of accuracy, a series of parametric studies were executed on the calibrated limited width backfill numerical models. These parametric studies serve as a valuable tool in assessing the passive behavior of various pile cap-limited width backfill systems, as it is economically infeasible to conduct full-scale experimental investigations for all potential soil properties and wall geometries. The main objective of the parametric studies was to assess the impact of a range of selected design parameters, related to the pile cap geometry and backfill soil type, on the passive resistance of limited width backfills. The selected cap geometry and compacted gravel fill soil parameters that were anticipated to have an effect on the passive performance of limited width backfills include: the wall height H, friction angle $\varphi_{(gravel)}$, cohesion c, stiffness parameter E_{50}^{ref}, associated with a reference stress equal to atmospheric pressure p^{ref}, in-situ unit weight γ_m, and the strength reduction parameter R_{inter}. The friction angle of the loose sand portion of the limited width backfill $\varphi_{(sand)}$, was also anticipated to influence the passive resistance of the backfill. The effect of other parameters such as the depth of gravel zone below the base of the pile cap, length of

interface element extensions, and degree of mesh refinement used in PLAXIS was also investigated. A summary of the different parameters and the input values employed in the parametric studies are presented in Table 5-7.

5.4.1 Effect of Pile Cap Height

Numerical simulations were performed to investigate the effect of varying the pile cap height on the mobilized plane strain passive resistance by a limited width dense gravel backfill. The "reference" model for this study is a 3-ft (0.91-m) deep pile cap with a limited width backfill consisting of a 3-ft (0.91-m) wide dense gravel zone and loose silty sand. Hardening Soil model parameters used in this reference model are presented in Table 5-8. Typical pile cap heights analyzed were within the range of 3 to 8 ft (0.9 to 2.4 m).

The results of the parametric study are presented in Figure 5-13, and show the Passive Force Ratio, PFR, versus the pile cap height, H. The passive force ratio is defined as the ratio of the mobilized passive resistance in a limited width dense gravel backfill, P_{LW}, over the mobilized passive resistance of a full width (homogeneous) dense gravel backfill, $P_{FW\text{-}Gravel}$. Specifically in this section, P_{LW} designates the passive resistance of the 3-ft (0.91-m) limited width backfill, corresponding to a deflection-to-wall height ratio of 4%. The passive resistance of the full width (homogeneous) dense gravel backfill, $P_{FW\text{-}Gravel}$, also corresponds to a deflection-to-wall height ratio of 4%.

The trend illustrated in Figure 5-13 highlights the sensitivity of the passive resistance to the variation of pile cap height, for a constant width of gravel zone, (3 ft (0.91m)). The trend shows that the effectiveness of placing a dense gravel layer behind the pile cap decreases with increasing pile cap height.

Table 5-7: Summary of parametric study input values

Parameter	Symbol	Input Value	Unit
Pile cap height	H	3.00 (0.91) 3.67 (1.12) 4.50 (1.37) 5.50 (1.68) 8.00 (2.44)	ft (m)
Friction angle	φ (gravel)	35.0 39.0 42.0	degrees
	φ (sand)	27.7 32.0 36.0	degrees
Gravel cohesion	C	40 (1.9) 100 (4.8) 150 (7.2) 200 (9.6)	psf (kPa)
Gravel stiffness	E_{50}^{ref}	1700 (81.4) 2200 (105.3) 2700 (129.3) 3200 (153.2) 3700 (177.2)	ksf (MPa)
Gravel in-situ unit weight	γ_m	110 (17.3) 130 (20.4) 141 (22.1) 150 (22.1)	pcf (kN/m^3)
Gravel strength reduction factor	R_{inter}	0.3 0.5 0.7	---

Table 5-7: Summary of parametric study input values (continued)

Parameter	Symbol	Input Value	Unit
Depth of gravel treatment	D	1 (0.31) 2 (0.61) 3 (0.91) 4 (1.22)	ft (m)
Deflection-to-wall height ratio	Δ_{max}/H	0.01 0.02 0.03 0.04	---
Interface element extension length	L	0 0.5 (0.15) 1 (0.31) 2 (0.61) 3 (0.91)	ft (m)
Finite element mesh density	---	Very coarse Coarse Medium Fine Very fine	---

A possible explanation for this observation could be that as the pile cap height increases, a lower percentage of the failure surface is embodied within the dense gravel zone, resulting in a relatively smaller percentage of shear strain and displacements occurring within the compacted zone. This effect was illustrated in the shear shading plots shown in Figures 5-9 and 5-10, and is further demonstrated in Figure 5-14, in which total displacement shadings of a 3-ft (0.91-m)

limited width dense gravel backfill is generated from PLAXIS, and plotted for pile cap heights ranging from 3 to 8 ft (0.9 to 2.4-m).

Table 5-8: Summary of Hardening Soil model input parameters used in studying the effect of pile cap height

Parameter	Symbol	Loose Sand	Dense Gravel	Unit
In-situ unit weight	γ_m	110 (17.3)	141 (22.1)	pcf (kN/m^3)
Secant CD triaxial stiffness	E_{50}^{ref}	330 (15.8)	1700 (81.4)	ksf (MPa)
Reference stress	P_{ref}	2 (100)	2 (100)	ksf (kPa)
Cohesion	c_{ref}	10 (0.5)	40 (1.9)	psf (kPa)
Friction angle	φ	27.7	42.0	degrees
Dilation angle	ψ	0	12	degrees
Strength reduction factor	R_{inter}	0.723	0.681	---

To combine the effects of varying the pile cap height and gravel zone width on the reference model, Figure 5-15 plots the PFR against the width of dense gravel zone, normalized by the height of the pile cap, B_F/H. The limited width backfill conditions used in the assessment included the following: (1) full width (homogeneous) loose silty sand; (2) limited width dense gravel backfill consisting of a 3-ft (0.91-m) wide zone of dense gravel between the pile cap and loose silty sand and; (3) limited width dense gravel backfill consisting of a 6-ft (1.83-m) wide zone of dense gravel between the pile cap and loose silty sand. Note that the full width (homogeneous) loose silty sand backfill can be considered a limited width dense gravel backfill, consisting of a 0-ft wide gravel zone placed between the pile cap and loose silty sand.

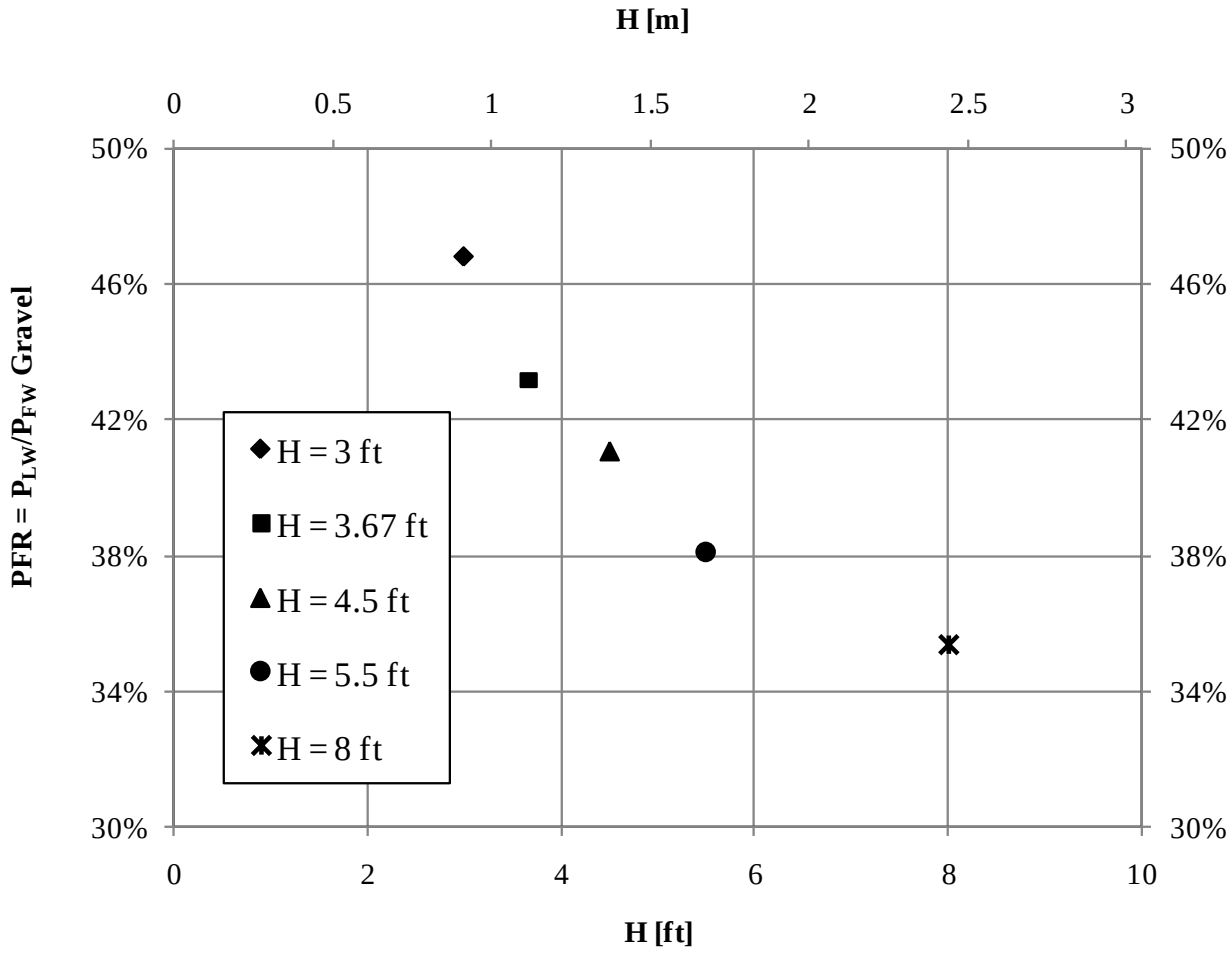

Figure 5-13: Effect of varying pile cap height on the passive resistance of a limited width dense gravel backfill consisting of a 3-ft (0.91-m) wide gravel zone and loose silty sand

Similar to the Figure 5-13, the fairly linear trend observed in Figure 5-15 demonstrates the sensitivity of the passive resistance ratio, PFR, to the B_F/H ratio. It is only when the B_F/ H ratio is greater than about one, that the effect of using a dense gravel backfill of limited width becomes significant. In other words, as the width of gravel zone placed between the pile cap and loose silty sand, becomes approximately greater than the pile cap height, the dense gravel backfill of limited width mobilizes a significant portion (greater than about 50%) of the total

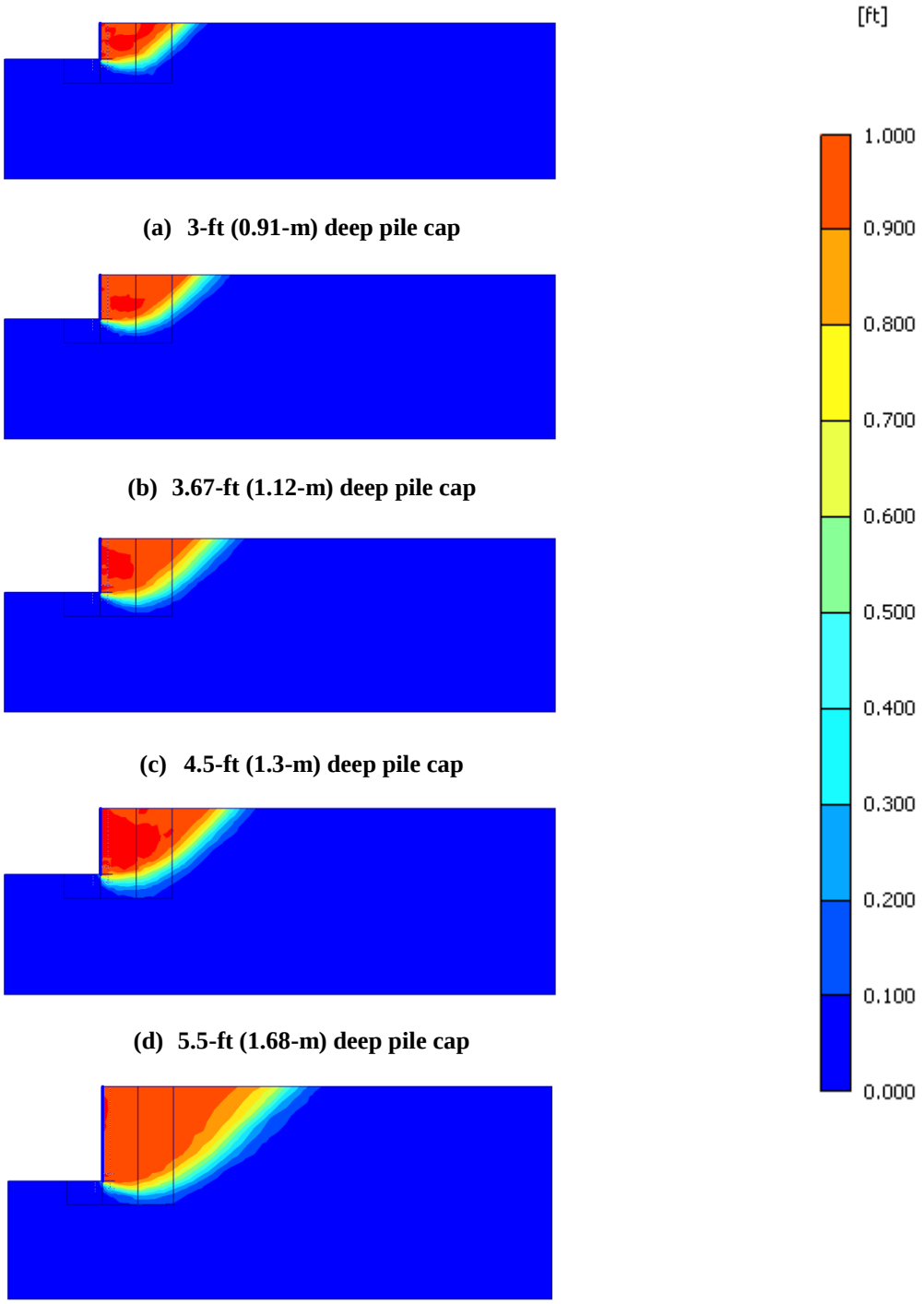

(a) 3-ft (0.91-m) deep pile cap

(b) 3.67-ft (1.12-m) deep pile cap

(c) 4.5-ft (1.3-m) deep pile cap

(d) 5.5-ft (1.68-m) deep pile cap

(e) 8-ft (2.4-m) deep pile cap

Figure 5-14: Total displacement profiles of (a) 3-ft (0.91-m) (b) 3.67-ft (1.12-m) (c) 4.5-ft (1.3-m) (d) 5.5-ft (1.68-m) (e) 8-ft (2.4-m) deep pile caps with limited width backfills consisting of a 3-ft (0.91-m) wide dense gravel zone and loose silty sand

resistance that would have been developed if a full width (homogeneous) dense gravel backfill was used. This observation is consistent with the conclusions made by Hanna and Meyerhof (1980), regarding the enhanced performance of spread footings, in terms of bearing capacity, as the thickness of the compacted gravel fill extends to a depth equal to the width of the footing.

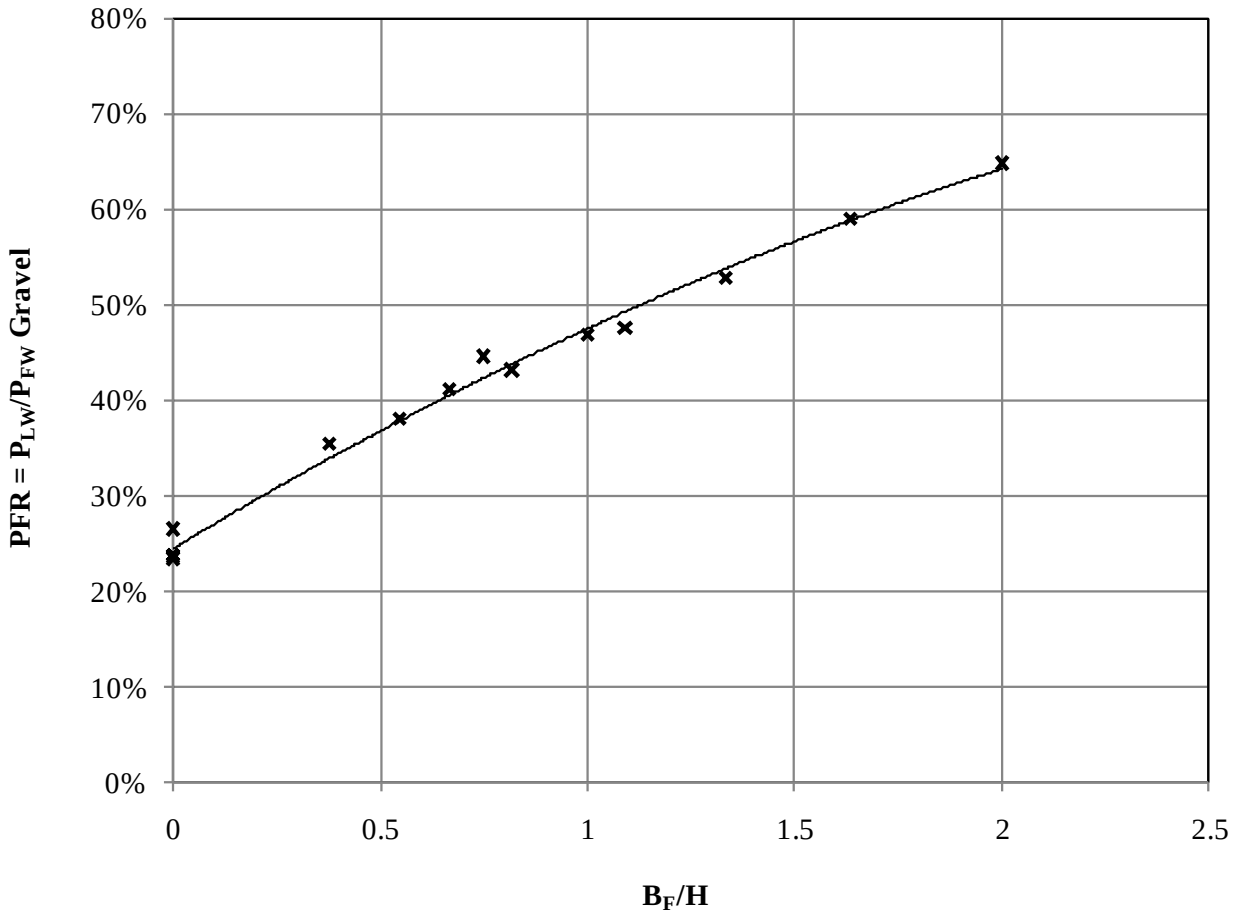

Figure 5-15: Effect of varying pile cap height and gravel zone width on the passive resistance of limited width dense gravel backfills

5.4.2 Effect of Soil Friction Angle

Numerical simulations were also performed to investigate the effect of varying the internal friction angle associated with the gravel compacted fill and loose sand portion of limited width backfills, on the ultimate passive resistance mobilized by the backfill. The results of this parametric study are presented in this section, under six different cases. Each case is designed to illustrate the effect of employing various strength combinations of gravel and sand, on the passive performance of limited width gravel backfills. Unit weight and stiffness characteristics associated with each material combination were based on correlations provided by the U.S. Navy (1982), and API RP2A (1987), respectively. Furthermore, the results of this set of parametric studies were used to develop a simple design method that can serve as an aid in designing limited width dense gravel backfills for plane strain geometries.

5.4.2.1 Effect of Gravel Friction Angle

The effect of varying the internal friction angle associated with the gravel compacted fill, on the ultimate passive resistance of limited width backfills is illustrated by Cases 1, 2 and 3. In each case, the simulations are initially performed on a reference model consisting of a 3.67-ft (1.12-m) deep pile cap with a 3-ft (0.91-m) wide dense gravel zone and loose silty sand limited width backfill. Typical gravel friction angles analyzed were 35°, 39°, and 42.0°. For the looser sand portion of the backfills, friction angles of 27.7°, 32°, and 36.0° were used in the analysis. In addition, the limited width backfill conditions employed in this assessment included the following: (1) full width (homogeneous) loose silty sand (0-ft limited width dense gravel backfill); (2) limited width dense gravel backfill consisting of a 3-ft (0.91-m) wide zone of dense

gravel between the pile cap and loose silty sand and; (3) limited width dense gravel backfill consisting of a 6-ft (1.83-m) wide zone of dense gravel between the pile cap and loose silty sand.

Case 1

Case 1 illustrates the effect of varying the internal friction angle associated with the gravel compacted fill, on the ultimate passive resistance of limited width backfills, consisting of a loose silty sand with a friction angle of 27.7°. Values of other Hardening Soil model parameters used in the reference model associated with Case 1 are presented in Table 5-9.

Table 5-9: Summary of Hardening Soil model input parameters for Case 1

Parameter	Symbol	Loose Sand	Unit
In-situ unit weight	γ_m	110 (17.3)	pcf (kN/m^3)
Secant CD triaxial stiffness	E_{50}^{ref}	330 (15.8)	ksf (MPa)
Reference stress	P_{ref}	2 (100)	ksf (kPa)
Cohesion	c_{ref}	10 (0.5)	psf (kPa)
Friction angle	φ	27.7	degrees
Dilation angle	ψ	0	degrees
Strength reduction factor	R_{inter}	0.723	---

Figure 5-16 shows the effect of varying the internal friction angle of the dense gravel, on the calculated passive resistance. The results show that a higher friction angle in the gravel zone leads to a higher passive force. The plot also indicates that as the width of the gravel zone increases the influence of the gravel friction angle becomes more pronounced.

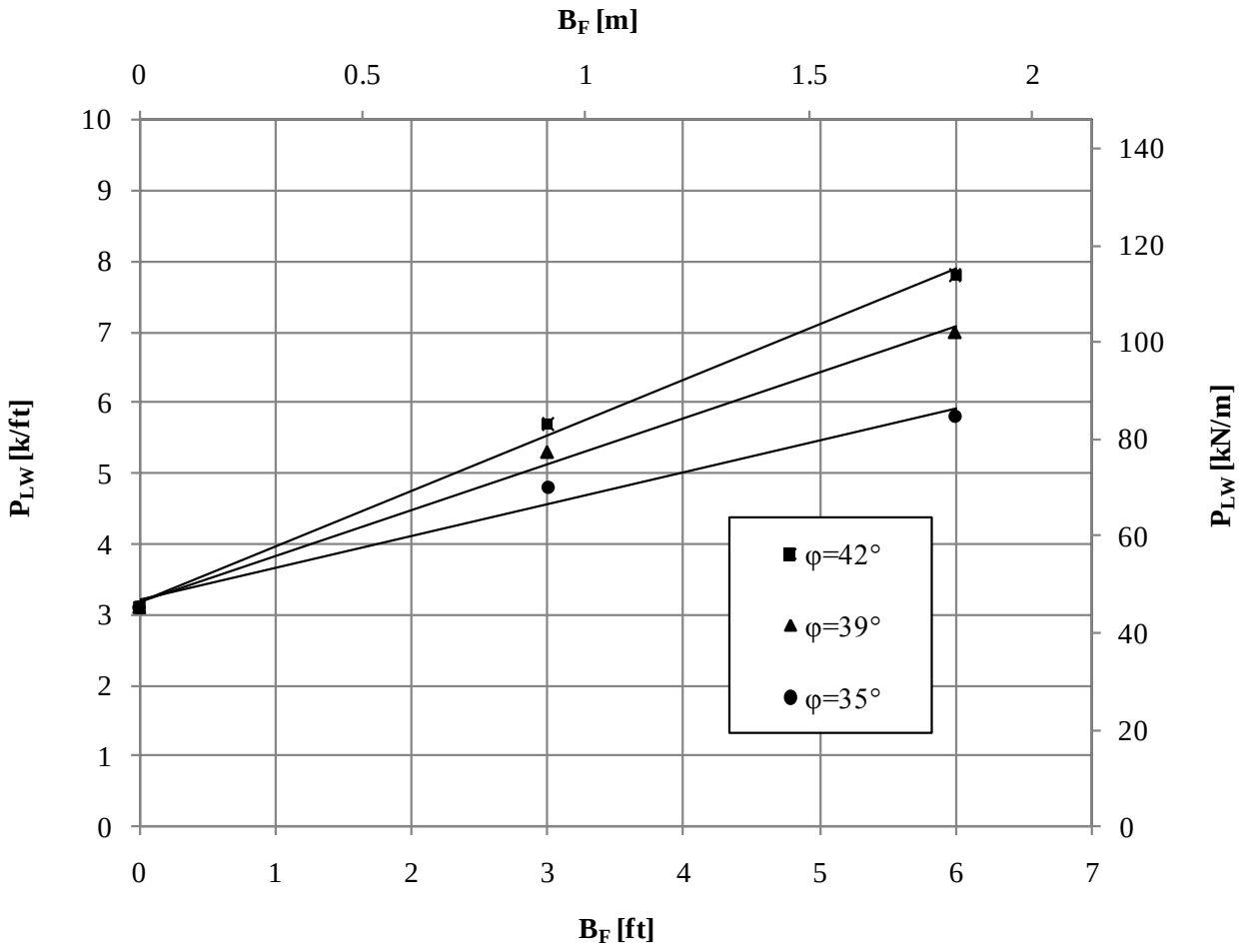

Figure 5-16: Effect of gravel friction angle on the mobilized passive resistance for a 3.67-ft (1.12-m) deep pile cap with a 3-ft (0.91-m) wide dense gravel zone and loose silty sand

The combined effect of varying the pile cap height, compacted gravel fill friction angle, and the gravel zone width, on the mobilized passive resistance, is shown in Figure 5-17. Normalized comparisons are made by plotting the Passive Force Ratio, PFR, versus the width of dense gravel zone, normalized by the height of the pile cap, B_F/H. As mentioned previously, the passive force ratio is defined as the ratio of the mobilized passive resistance in a limited width dense gravel backfill, P_{LW}, over the mobilized passive resistance of a full width (homogeneous)

dense gravel backfill, $P_{FW\text{-}Gravel}$. Specifically in this section, P_{LW} designates the passive resistances of 0-ft, 3-ft (0.91-m) and 6-ft (1.83-m) limited width backfills. P_{LW} corresponds to a deflection-to-wall height ratio of 4% for the limited width backfill conditions involving dense gravel. For full width (homogeneous) loose silty sand backfills, P_{LW} corresponds to a deflection-to-wall height ratio of 6%. $P_{FW\text{-}Gravel}$ is the passive resistance of the full width (homogeneous) dense gravel backfill, corresponding to a deflection to wall height ratio of 4%.

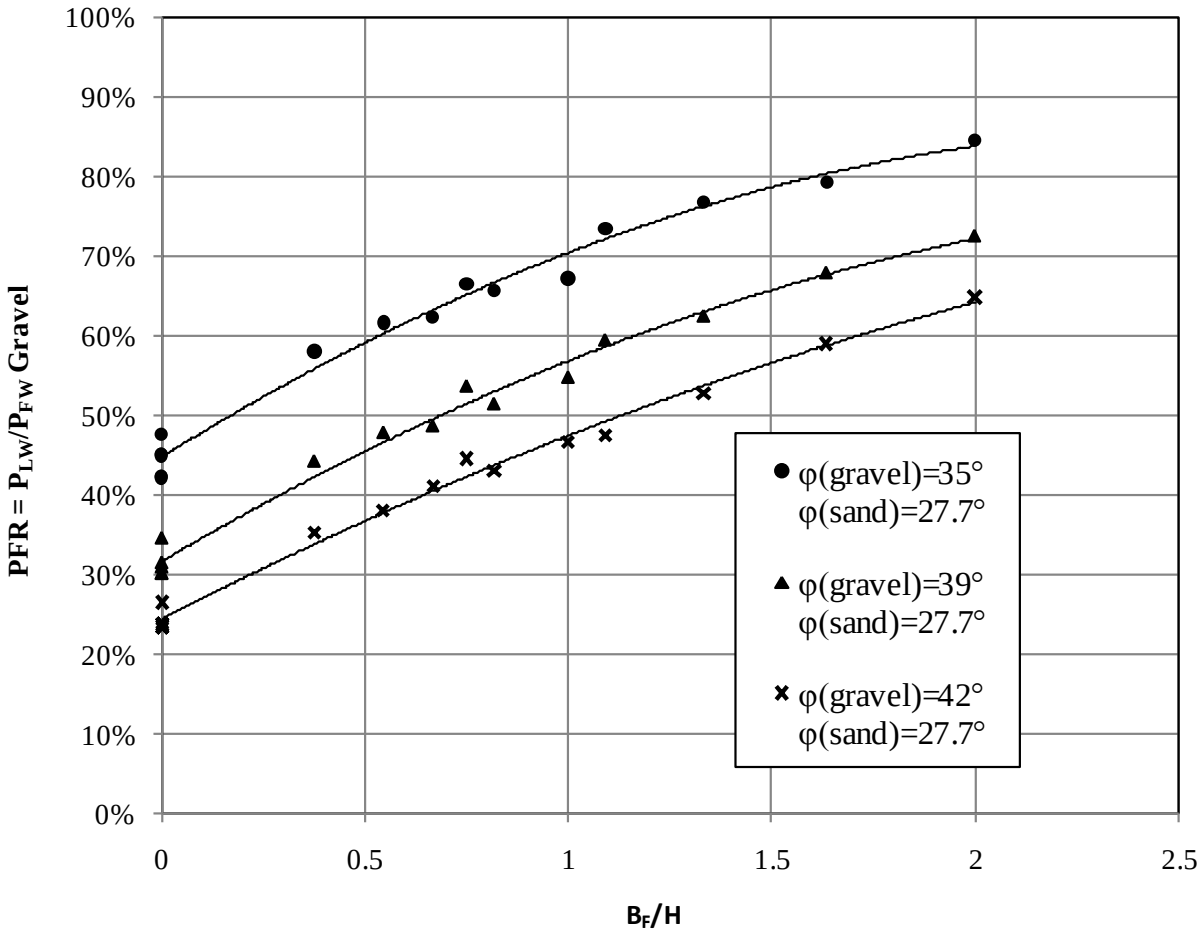

Figure 5-17: Combined effect of dense gravel friction angle, wall height, and gravel zone width on the passive force ratio for $\varphi_{(sand)}$ =27.7°

Despite the fact that a higher friction angle gravel zone yields a higher total passive force (see Figure 5-16), Figure 5-17 indicates that for a given B_F/H value, the PFR is higher for the lower friction angle gravel than for the higher friction angle gravel zone. This is a result of normalizing the limited width passive resistance, P_{LW}, by the passive resistance associated with the full width (homogeneous) dense gravel backfill, $P_{FW\text{-}Gravel}$. Since the passive resistance of a full width (homogeneous) dense gravel backfill would be relatively lower for a looser gravel, and the failure length shorter, placing a 3-ft (0.91-m) dense gravel zone would achieve a greater portion of the full width backfill passive resistance, thus resulting in a relatively higher PFR value for the looser gravel.

For all cases, increasing the width of the gravel zone increased the PFR. However, the trend observed in Figure 5-17 demonstrates the sensitivity of the PFR to the gravel zone width ratio. As this ratio increases, the trend exhibits a fairly linear increase up to about a B_F/H ratio of one. For ratios greater than one, the linear trend gently transitions to a curve with a relatively flatter slope. To quantify the non-linear relationships shown in Figure 5-17, second order polynomial curves were fitted through the values associated with dense gravel friction angles of 35.0°, 39.0°, and 42.0°. The fitted curves led to the development of simple predictive equations that can be used in estimating the plane strain passive resistance of the limited width dense gravel backfills, as a fraction of the passive resistance mobilized in full width (homogeneous) dense gravel backfills ($P_{LW}/P_{FW\text{-}Gravel}$). These equations are presented below:

$$PFR_1 = -0.06\left(\frac{B_F}{H}\right)^2 + 0.32\left(\frac{B_F}{H}\right) + 0.45 \qquad (5\text{-}2)$$

$$PFR_2 = -0.05(\frac{B_F}{H})^2 + 0.30(\frac{B_F}{H}) + 0.32 \quad (5\text{-}3)$$

$$PFR_3 = -0.03(\frac{B_F}{H})^2 + 0.26\left(\frac{B_F}{H}\right) + 0.24 \quad (5\text{-}4)$$

where PFR_1, PFR_2, and PFR_3 are the passive force ratios of limited width dense gravel backfills, associated with dense gravel friction angles of 35.0°, 39.0°, and 42.0°, respectively, and (B_F/H) is the width of dense gravel zone, normalized by the height of the pile cap.

Case 2

Case 2 illustrates the effect of varying the internal friction angle associated with the gravel compacted fill, on the ultimate passive resistance of limited width backfills consisting of loose silty sands with a friction angle of 32.0°. Values of other Hardening Soil model parameters used in the reference model associated with Case 2 are presented Table 5-10.

Figure 5-18 illustrates the combined effect of varying the pile cap height, compacted gravel fill friction angle, and the gravel zone width on the passive force ratio. Trends observed are similar to those presented in the previous case. Equations 5-5, 5-6 and 5-7 are predictive equations associated with the relationships presented in Figure 5-18.

$$PFR_1 = -0.06(\frac{B_F}{H})^2 + 0.27(\frac{B_F}{H}) + 0.55 \quad (5\text{-}5)$$

$$PFR_2 = -0.05(\frac{B_F}{H})^2 + 0.29(\frac{B_F}{H}) + 0.39 \quad (5\text{-}6)$$

$$PFR_3 = -0.03(\frac{B_F}{H})^2 + 0.26\left(\frac{B_F}{H}\right) + 0.30 \quad (5\text{-}7)$$

where PFR_1, PFR_2, and PFR_3 are the passive force ratios of limited width dense gravel backfills, associated with dense gravel friction angles of 35.0°, 39.0°, and 42.0°, respectively, and (B_F/H) is the width of dense gravel zone, normalized by the height of the pile cap.

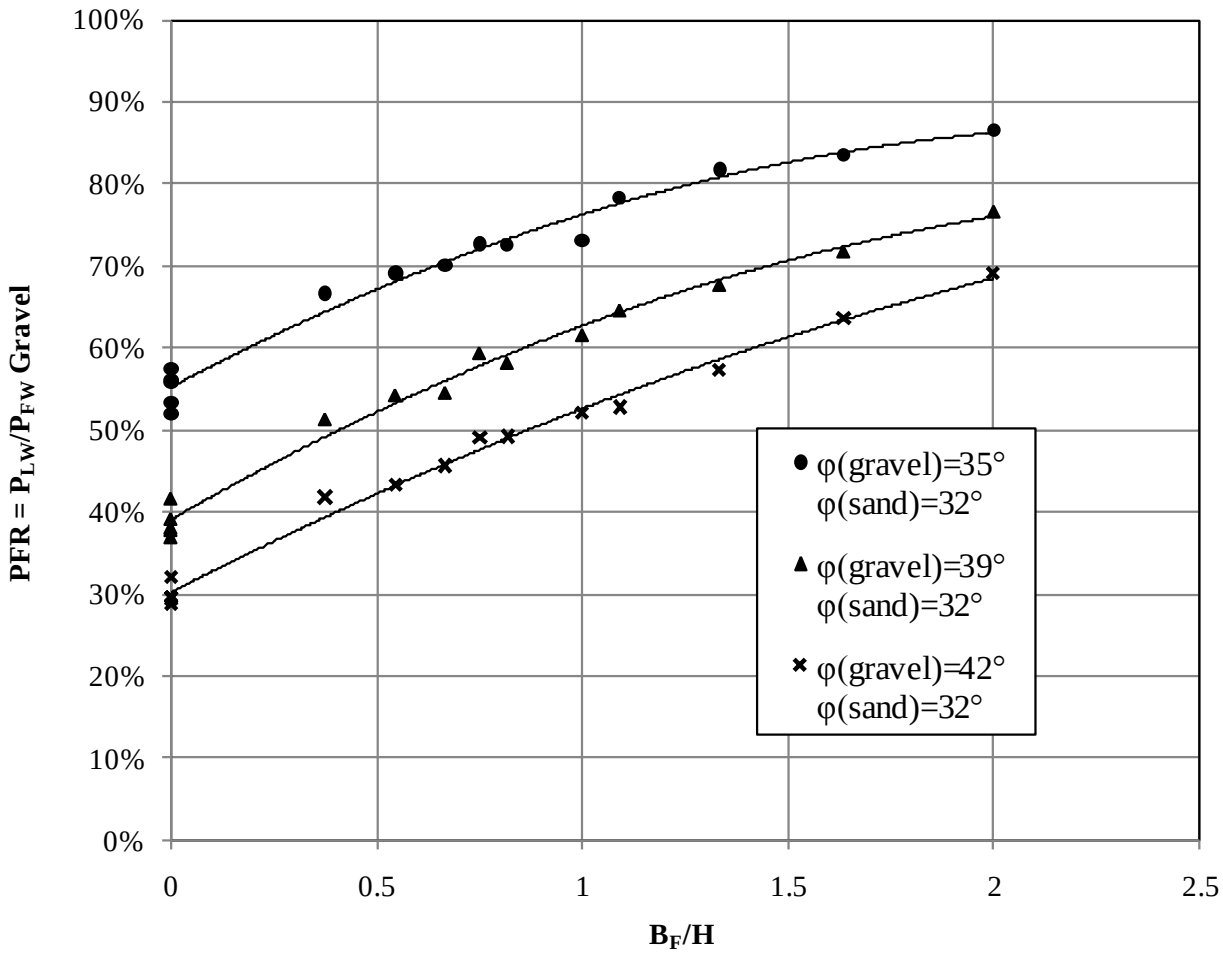

Figure 5-18: Combined effect of dense gravel friction angle, wall height, and gravel zone width on the passive force ratio for $\varphi_{(sand)}$ =32.0°

Table 5-10: Summary of Hardening Soil model input parameters for Case 2

Parameter	Symbol	Loose Sand	Unit
In-situ unit weight	γ_m	119 (16.7)	pcf (kN/m^3)
Secant CD triaxial stiffness	E_{50}^{ref}	387 (18.5)	ksf (MPa)
Reference stress	P_{ref}	2 (100)	ksf (kPa)
Cohesion	c_{ref}	10 (0.5)	psf (kPa)
Friction angle	φ	32.0	degrees
Dilation angle	ψ	0	degrees
Strength reduction factor	R_{inter}	0.713	---

Case 3

Case 3 illustrates the effect of varying the internal friction angle associated with the gravel compacted fill, on the ultimate passive resistance of limited width backfills consisting of loose silty sands with a friction angle of 36.0°. Values of other Hardening Soil model parameters used in the reference model associated with Case 3 are presented in Table 5-11.

Figure 5-19 illustrates the combined effect of varying the pile cap height, compacted gravel fill friction angle, and the gravel zone width on the passive force ratio. Trends observed are similar to those presented in the previous case, with the exception of slightly more scatter observed in the relationship associated with the combination of dense gravel and loose sands of 39° and 36°, respectively. Equations 5-8 and 5-9 are predictive equations associated with the relationships presented in Figure 5-19.

$$PFR_1 = -0.04\left(\frac{B_F}{H}\right)^2 + 0.19\left(\frac{B_F}{H}\right) + 0.60 \qquad (5\text{-}8)$$

$$PFR_2 = -0.03(\frac{B_F}{H})^2 + 0.23(\frac{B_F}{H}) + 0.46 \quad (5\text{-}9)$$

where PFR_1 and PFR_2, are the passive force ratios of limited width dense gravel backfills, associated with dense gravel friction angles of 39.0°, and 42.0°, respectively, and (B_F/H) is the width of dense gravel zone, normalized by the height of the pile cap.

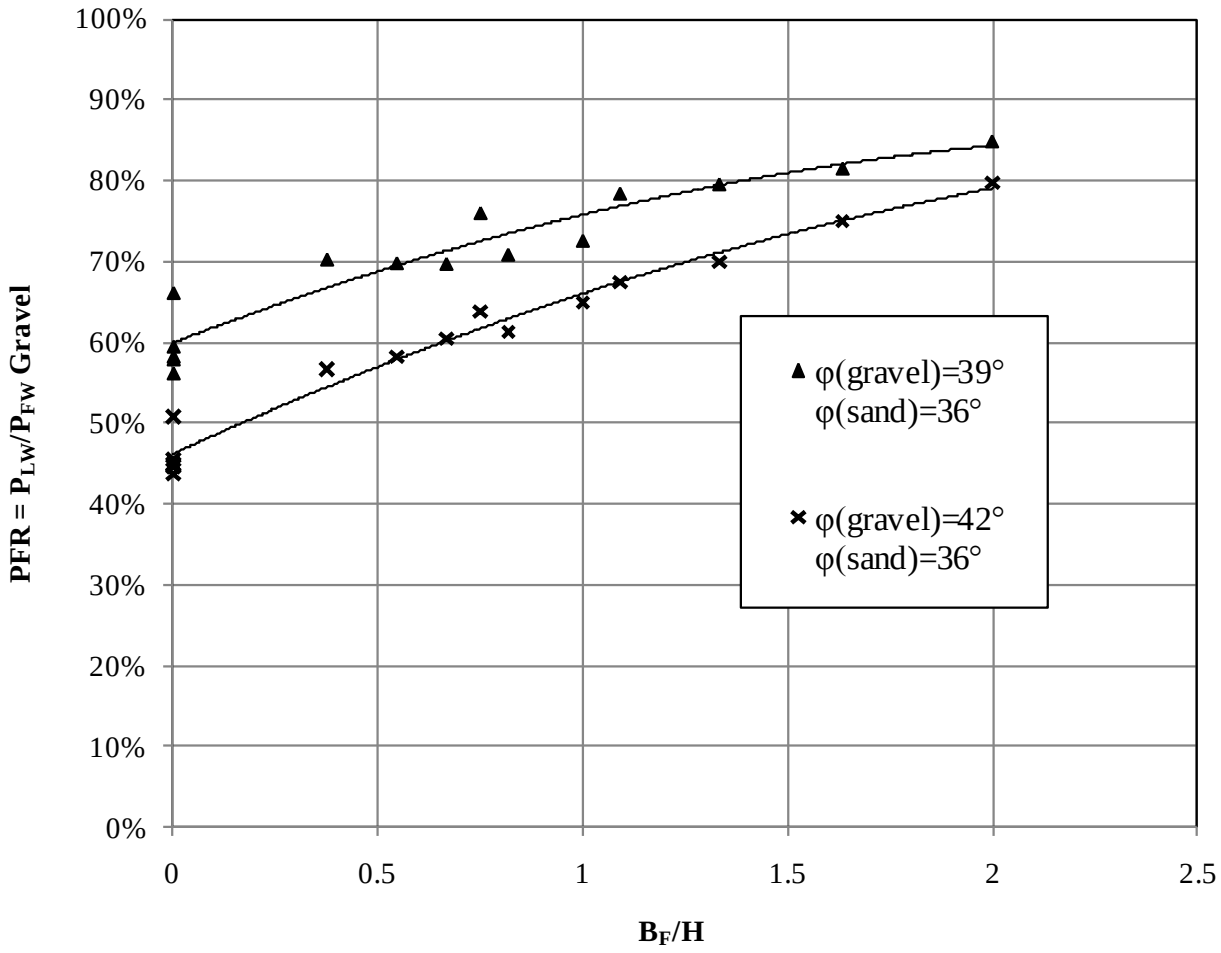

Figure 5-19: Combined effect of dense gravel friction angle, wall height, and gravel zone width on the passive force ratio for φ (sand) =36.0°

Table 5-11: Summary of Hardening Soil model input parameters for Case 3

Parameter	Symbol	Loose Sand	Unit
In-situ unit weight	γ_m	128 (20.1)	pcf (kN/m^3)
Secant CD triaxial stiffness	E_{50}^{ref}	900 (43.1)	ksf (MPa)
Reference stress	P_{ref}	2 (100)	ksf (kPa)
Cohesion	c_{ref}	10 (0.5)	psf (kPa)
Friction angle	φ	36.0	degrees
Dilation angle	ψ	0	degrees
Strength reduction factor	R_{inter}	0.701	---

5.4.2.2 Effect of Sand Fiction Angle

The effect of varying the internal friction angle associated with the gravel compacted fill, on the ultimate passive resistance of limited width backfills is illustrated in Cases 4, 5 and 6. In each case, the simulations are initially performed on a reference model consisting of a 3.67-ft (1.12-m) deep pile cap with a 3-ft (0.91-m) wide dense gravel zone and loose silty sand limited width backfill. Typical gravel friction angles analyzed were 35°, 39°, and 42.0°. For the loose sand portion of the limited width backfill friction angles of 27.7°, 32°, and 36.0° were used in the analysis. In addition, the limited width backfill conditions employed in this assessment included the following: (1) full width (homogeneous) loose silty sand (0-ft limited width dense gravel backfill); (2) limited width dense gravel backfill consisting of a 3-ft (0.91-m) wide zone of dense gravel between the pile cap and loose silty sand and; (3) limited width dense gravel backfill consisting of a 6-ft (1.83-m) wide zone of dense gravel between the pile cap and loose silty sand.

Case 4

Case 4 illustrates the effect of varying the internal friction angle associated with the loose sand portion of the limited width backfill, on the ultimate passive resistance of limited width backfills consisting of compacted gravel fills with a friction angle of 42.0°. Values of other Hardening Soil model parameters used in the reference model associated with Case 4 are presented in Table 5-12.

Table 5-12: Summary of Hardening Soil model input parameters for Case 4

Parameter	Symbol	Dense Gravel	Unit
In-situ unit weight	γ_m	141 (22.1)	pcf (kN/m^3)
Secant CD triaxial stiffness	E_{50}^{ref}	1700 (81.4)	ksf (MPa)
Reference stress	P_{ref}	2 (100)	ksf (kPa)
Cohesion	c_{ref}	40 (1.9)	psf (kPa)
Friction angle	φ	42.0	degrees
Dilation angle	ψ	12	degrees
Strength reduction factor	R_{inter}	0.681	---

Figure 5-20 illustrates the combined effect of varying the pile cap height, compacted gravel fill friction angle, and the gravel zone width on the passive force ratio. The trends observed in Figure 5-20 are similar to those presented in Case 1. As the friction angle of the sand layer increases, the PFR increases. However, the increases are relatively small as friction angle increases from 27.7º to 32º, but are significantly greater as the friction angle increases from 32º to 36º. This observation demonstrates the effect of dilation angle on the passive resistance of

limited width backfills. As the loose sand friction angle increases the effect of the dilation angle on the passive resistance of the backfill becomes more pronounced. Equations 5-10, 5-11, and 5-12 are predictive equations associated with the relationships presented in Figure 5-20:

$$PFR_1 = -0.03(\frac{B_F}{H})^2 + 0.26(\frac{B_F}{H}) + 0.24 \quad (5\text{-}10)$$

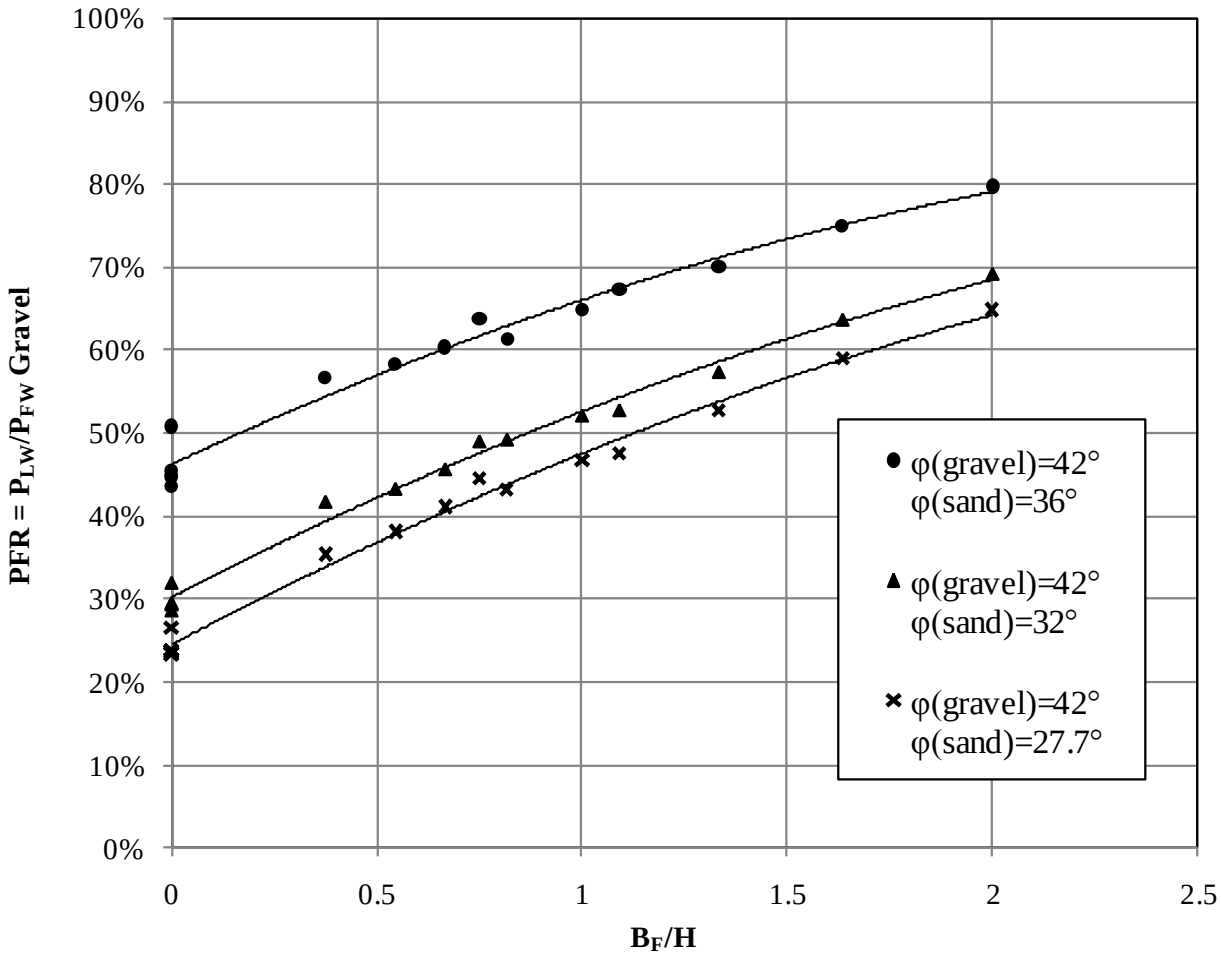

Figure 5-20: Combined effect of dense gravel friction angle, wall height, and gravel zone width on the passive force ratio for $\varphi_{(gravel)}$ =42.0°

$$PFR_2 = -0.03(\frac{B_F}{H})^2 + 0.26(\frac{B_F}{H}) + 0.30 \quad (5\text{-}11)$$

$$PFR_3 = -0.03(\frac{B_F}{H})^2 + 0.23\left(\frac{B_F}{H}\right) + 0.46 \quad (5\text{-}12)$$

where PFR_1, PFR_2, and PFR_3 are the passive force ratios of limited width dense gravel backfills, associated with loose sand friction angles of 27.7°, 32.0°, and 36.0°, respectively, and (B_F/H) is the width of dense gravel zone, normalized by the height of the pile cap.

Case 5

Case 5 illustrates the effect of varying the internal friction angle associated with the loose sand portion of the limited width backfill, on the ultimate passive resistance of limited width backfills consisting of compacted gravel fills with a friction angle of 39.0°. Values of other Hardening Soil model parameters used in the reference model associated with Case 5 are presented in Table 5-13.

Figure 5-21 illustrates the combined effect of varying the pile cap height, compacted gravel fill friction angle, and the gravel zone width on the passive force ratio. Similar to Case 3, slightly more scatter can be observed in the curve associated with the combination of dense gravel and loose sands of 39° and 36°, respectively. Equations 5-13, 5-14, and 5-15 are predictive equations associated with the relationships presented in Figure 5-21:

$$PFR_1 = -0.05(\frac{B_F}{H})^2 + 0.30(\frac{B_F}{H}) + 0.32 \quad (5\text{-}13)$$

$$PFR_2 = -0.05(\frac{B_F}{H})^2 + 0.29(\frac{B_F}{H}) + 0.39 \quad (5\text{-}14)$$

$$PFR_3 = -0.04(\frac{B_F}{H})^2 + 0.19\left(\frac{B_F}{H}\right) + 0.60 \quad (5\text{-}15)$$

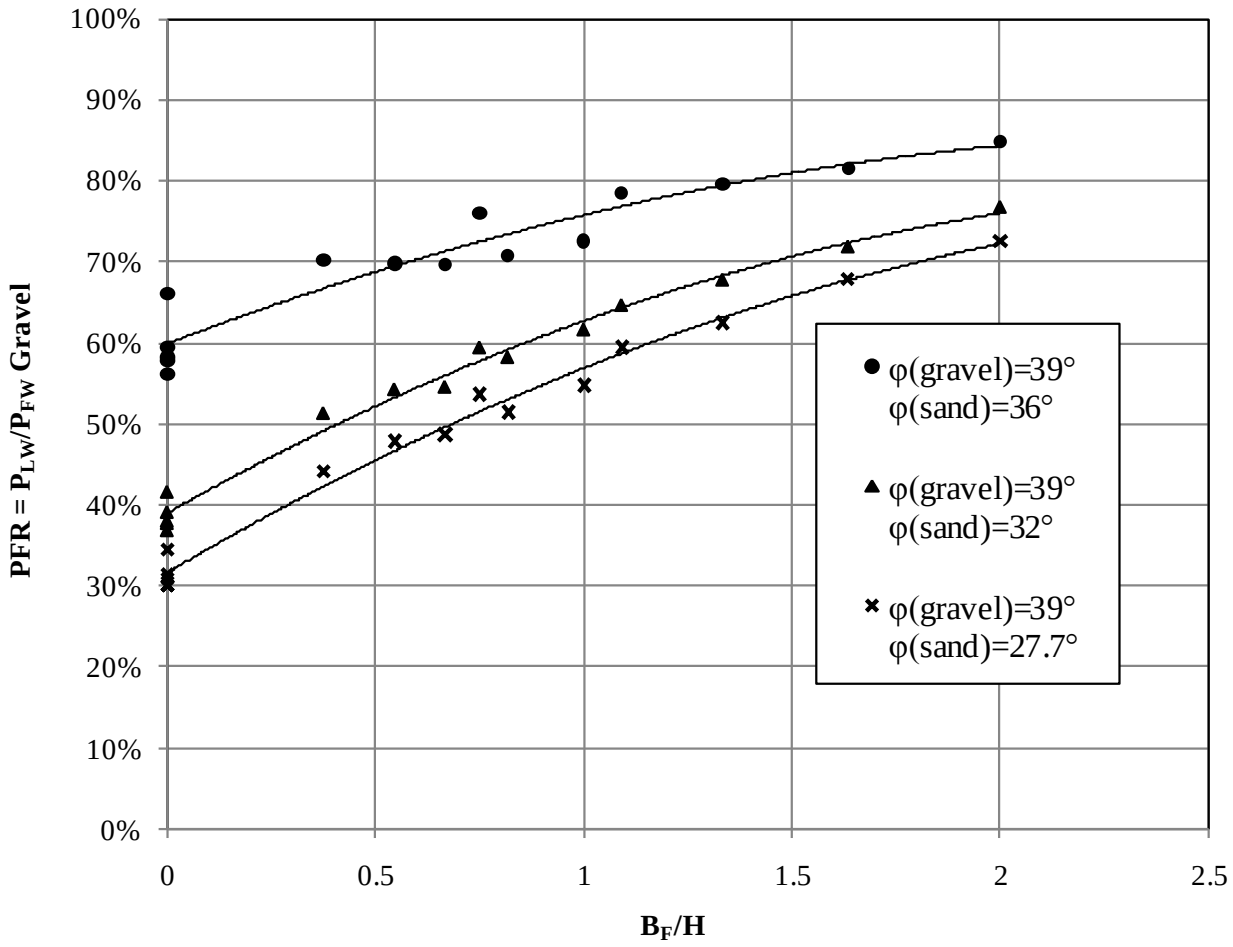

Figure 5-21: Combined effect of dense gravel friction angle, wall height, and gravel zone width on the passive force ratio for $\varphi_{(gravel)}$ =39.0°

where PFR_1, PFR_2, and PFR_3 are the passive force ratios of limited width dense gravel backfills, associated with loose sand friction angles of 27.7°, 32.0°, and 36.0°, respectively, and (B_F/H) is the width of dense gravel zone, normalized by the height of the pile cap.

Table 5-13: Summary of Hardening Soil model input parameters for Case 5

Parameter	Symbol	Dense Gravel	Unit
In-situ unit weight	γ_m	129 (19.0)	pcf (kN/m^3)
Secant CD triaxial stiffness	E_{50}^{ref}	1386 (66.4)	ksf (MPa)
Reference stress	P_{ref}	2 (100)	ksf (kPa)
Cohesion	c_{ref}	40 (1.9)	psf (kPa)
Friction angle	φ	39.0	degrees
Dilation angle	ψ	9	degrees
Strength reduction factor	R_{inter}	0.692	---

Case 6

Case 6 illustrates the effect of varying the internal friction angle associated with the loose sand portion of the limited width backfill, on the ultimate passive resistance of limited width backfills consisting of compacted gravel fills with a friction angle of 35.0°. Values of other Hardening Soil model parameters used in the reference model associated with Case 6 are presented in Table 5-14.

Figure 5-22 illustrates the combined effect of varying the pile cap height, compacted gravel fill friction angle, and the gravel zone width on the passive force ratio. Trends observed

are similar to those presented in the Case 4. Equations 5-16, and 5-17 are predictive equations associated with the relationships presented in Figure 5-22.

$$PFR_1 = -0.06(\frac{B_F}{H})^2 + 0.32(\frac{B_F}{H}) + 0.45 \quad (5\text{-}16)$$

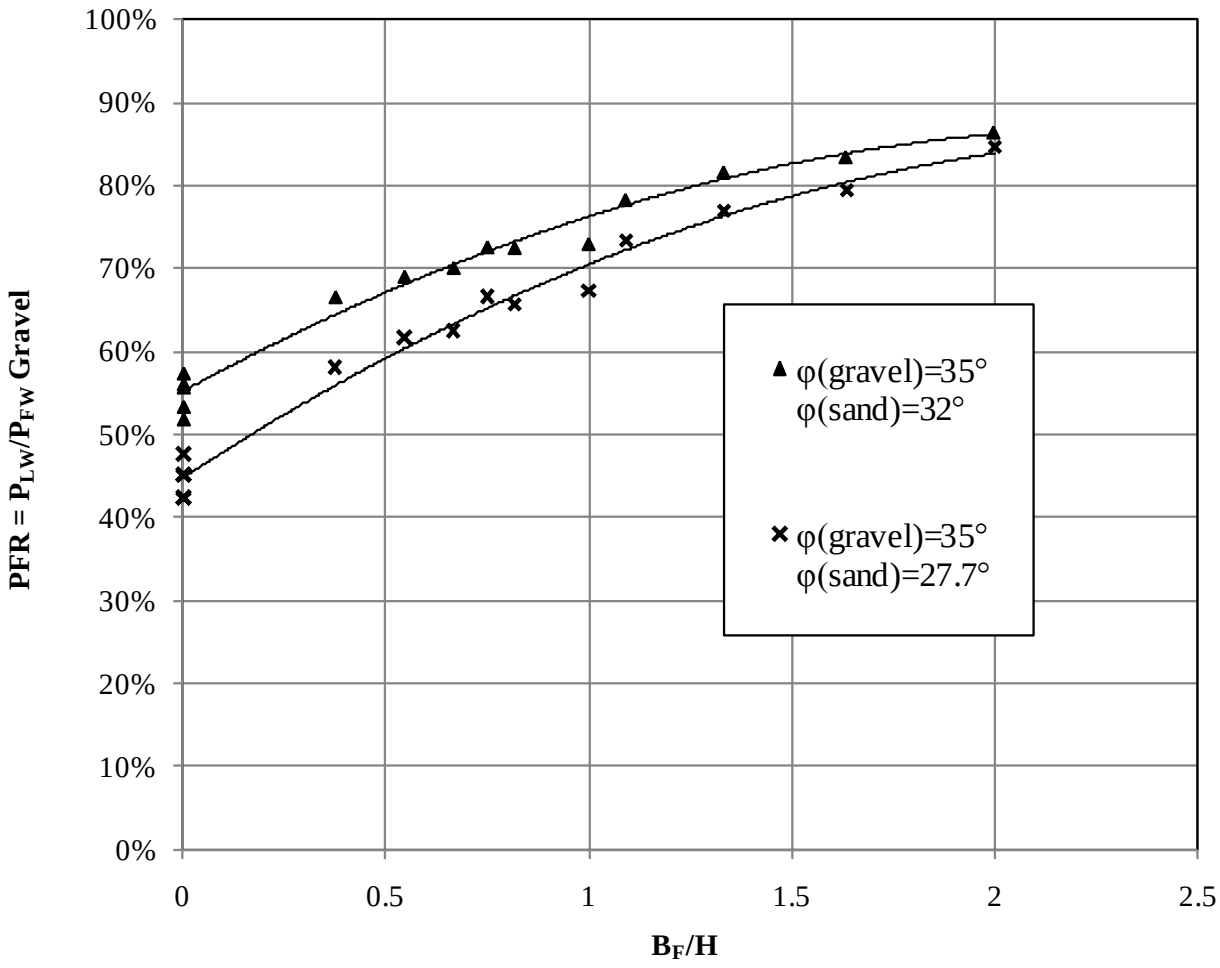

Figure 5-22: Combined effect of dense gravel friction angle, wall height, and gravel zone width on the passive force ratio for $\varphi_{(gravel)}$ =35.0°

$$PFR_2 = -0.06(\frac{B_F}{H})^2 + 0.27(\frac{B_F}{H}) + 0.55 \quad (5\text{-}17)$$

where PFR_1 and PFR_2, are the passive force ratios of limited width dense gravel backfills, associated with loose sand friction angles of 27.7° and 32.0°, respectively, and (B_F/H) is the width of dense gravel zone, normalized by the height of the pile cap.

Table 5-14: Summary of Hardening Soil model input parameters for Case 6

Parameter	Symbol	Dense Gravel	Unit
In-situ unit weight	γ_m	121 (20.3)	pcf (kN/m^3)
Secant CD triaxial stiffness	E_{50}^{ref}	758 (36.3)	ksf (MPa)
Reference stress	P_{ref}	2 (100)	ksf (kPa)
Cohesion	c_{ref}	40 (1.9)	psf (kPa)
Friction angle	φ	35.0	degrees
Dilation angle	ψ	5	degrees
Strength reduction factor	R_{inter}	0.704	---

To develop a single unifying design equation that can be used to predict the passive force ratio of limited width backfills for any given material strength combination, a second order polynomial model was fitted through the data points shown in Figures 5-17 through 5-22. This model, defined in Equation 5-18, is used to express the coefficients determined in Equations 5-2 through 5-17 as a function of the gravel and sand friction angles, by combining the effect of the sand friction angle, φ_s, gravel friction angle, φ_g, and the gravel zone width normalized by the pile cap height, B_F/H. Relative to the passive force ratio determined from Equations 5-2 through 5-

17, the absolute percentage error associated with Equation 5-18 is +8% of under-prediction in an extreme case. The model over-predicts the passive force ratio by a maximum absolute error of -4%. However, predicted passive force ratio values within the 25th and 75th percentile fall in an error range of -2 to +1%.

$$PFR = 3.418 - 0.139\,\varphi_s - 0.033\,\varphi_g + 0.484\,\frac{B_F}{H} - 0.043\,(\frac{B_F}{H})^2 + 0.003\,{\varphi_s}^2 - 0.007\,\varphi_s\frac{B_F}{H} \quad (5\text{-}18)$$

5.4.2.3 Summary

Parametric studies were performed on limited width dense gravel backfills to investigate the effect of varying backfill soil friction angles on the passive resistance. Typical dense gravel and loose sand friction angles analyzed were withiin the range of 27.7° to 42.0°. Results indicate that the friction angles associated with the gravel and sand have a significant effect on the mobilized passive resistance of limited width backfills, for the range of values that would be typical of a dense compacted zone and looser sands. Furthermore, conclusions drawn from these studies were used to develop a simple design approach that can be used as an aid in designing limited width backfills for plane strain geometries. This design method was presented in Figures 5-17 through 5-22, along with Equations 5-2 through 5-18.

It is important to emphasize that the results presented in this section have been developed based on plane strain numerical simulations of limited width gravel backfill conditions, tested experimentally. Under this assumption, the contribution of 3D edge effects on the passive

resistance of the analyzed backfills is ignored, and the simulations carried out do not simulate the actual 3D passive response of the full-scale tests. As such, the results presented in this section serve as a guide for the plane strain approximation of the mobilized passive resistance in limited width backfills, and are only applicable to situations in which applying plane strain conditions is a reasonable assumption. An example of this condition would be a relatively long abutment wall where the edge effects have negligible impact on the passive resistance mobilized in the adjacent backfill. In addition results presented in this section are valid under the assumption that the depth of gravel zone treatment extends 2 ft (0.61 m) below the base of the pile cap, and that the pile cap would be capable of tolerating movements equal to 4% for limited width backfills. At the end of this chapter, a design example illustrating the application of the developed model is presented for a relatively long abutment wall.

5.4.3 Effect of Gravel Zone Depth

Numerical analyses were performed on limited width backfills to investigate the effect of varying the depth of the dense gravel compacted between the pile cap and looser sand, on the passive force ratio. Dense gravel depths analyzed ranged from 1 to 4 ft (0.31 to 1.22 m). The reference model used initially for this parametric study is a 3.67-ft (1.12-m) deep pile cap with a limited width backfill consisting of a 3-ft (0.91-m) wide dense gravel zone and loose silty sand. Hardening Soil model parameters used in this reference model are presented in Table 5-8.

The combined effect of varying the depth of gravel zone, pile cap height, and the gravel zone width, on the mobilized passive resistance is shown in Figure 5-23. Comparisons are made by plotting the Passive Force Ratio, PFR, versus the width of dense gravel zone width, normalized by the height of the pile cap, B_F/H. The trends observed in Figure 5-23 indicate that

for B_F/H ratios less than one, increasing the gravel zone depth from 1 to 2 ft (0.30 to 0.61 m) does not have a very significant effect on increasing the passive force ratio (less than 5% increase in passive force ratio). However, for ratios greater than one, the deviation between the 1 ft and 2 ft (0.30 to 0.61 m) trend lines becomes greater, providing a more significant gain in passive resistance with increasing depth of treatment. In addition, it appears that for all combinations of pile cap height and gravel zone width, increasing the depth of gravel treatment

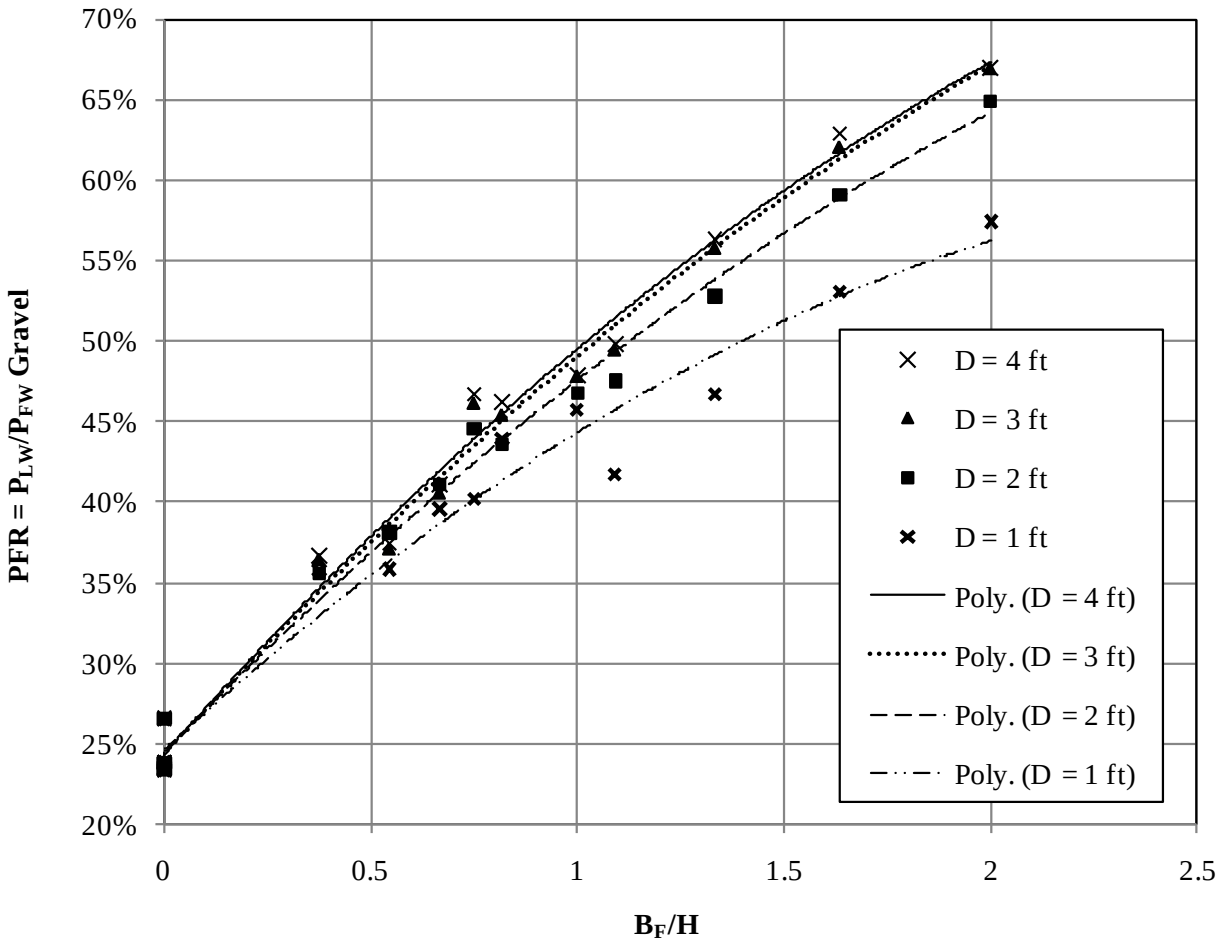

Figure 5-23: Combined effect of gravel zone depth, wall height, and gravel zone width on the passive force ratio

greater than 2 ft (0.61 m) is relatively ineffective (less than 3% increase in passive force ratio) in providing additional passive resistance.

5.4.4 Effect of Other Gravel Parameters

Figures 5-24, 5-25, and 5-26 illustrate the effect of varying gravel fill soil parameters including the cohesion c, soil stiffness parameter E_{50}^{ref}, and the in-situ unit weight γ_m, respectively, on the calculated passive resistance of a limited width dense gravel backfill. The reference model for this study is a 3.67-ft (1.12-m) deep pile cap with a limited width backfill consisting of a 3-ft (0.91-m) wide dense gravel zone and loose silty sand. Hardening Soil model parameters used in this reference model are presented in Table 5-15.

Table 5-15: Summary of Hardening Soil model input parameters used in studying the effect of the following gravel fill soil parameters: cohesion, c, soil stiffness parameter, $E_{ref,50}$, in-situ unit weight, γ_m, and the strength reduction parameter, R_{inter}

Parameter	Symbol	Loose Sand	Dense Gravel	Unit
In-situ unit weight	γ_m	110 (17.3)	141 (22.1)	pcf (kN/m^3)
Secant CD triaxial stiffness	E_{50}^{ref}	330 (15.8)	1700 (81.4)	ksf (MPa)
Reference stress	P_{ref}	2 (100)	2 (100)	ksf (kPa)
Cohesion	c_{ref}	10 (0.5)	40 (1.9)	psf (kPa)
Friction angle	φ	27.7	42.0	degrees
Dilation angle	ψ	0	12	degrees
Strength reduction factor	R_{inter}	0.723	0.681≅0.7	---

Results from this study indicate that the soil cohesion, soil stiffness parameter, and soil unit weight associated with the gravel compacted fill have minimal effects on the passive resistance of the limited width backfill. This result suggests that the dense gravel could be replaced by a dense sand with lower cohesion, unit weight or stiffness as long as the friction angle remained high.

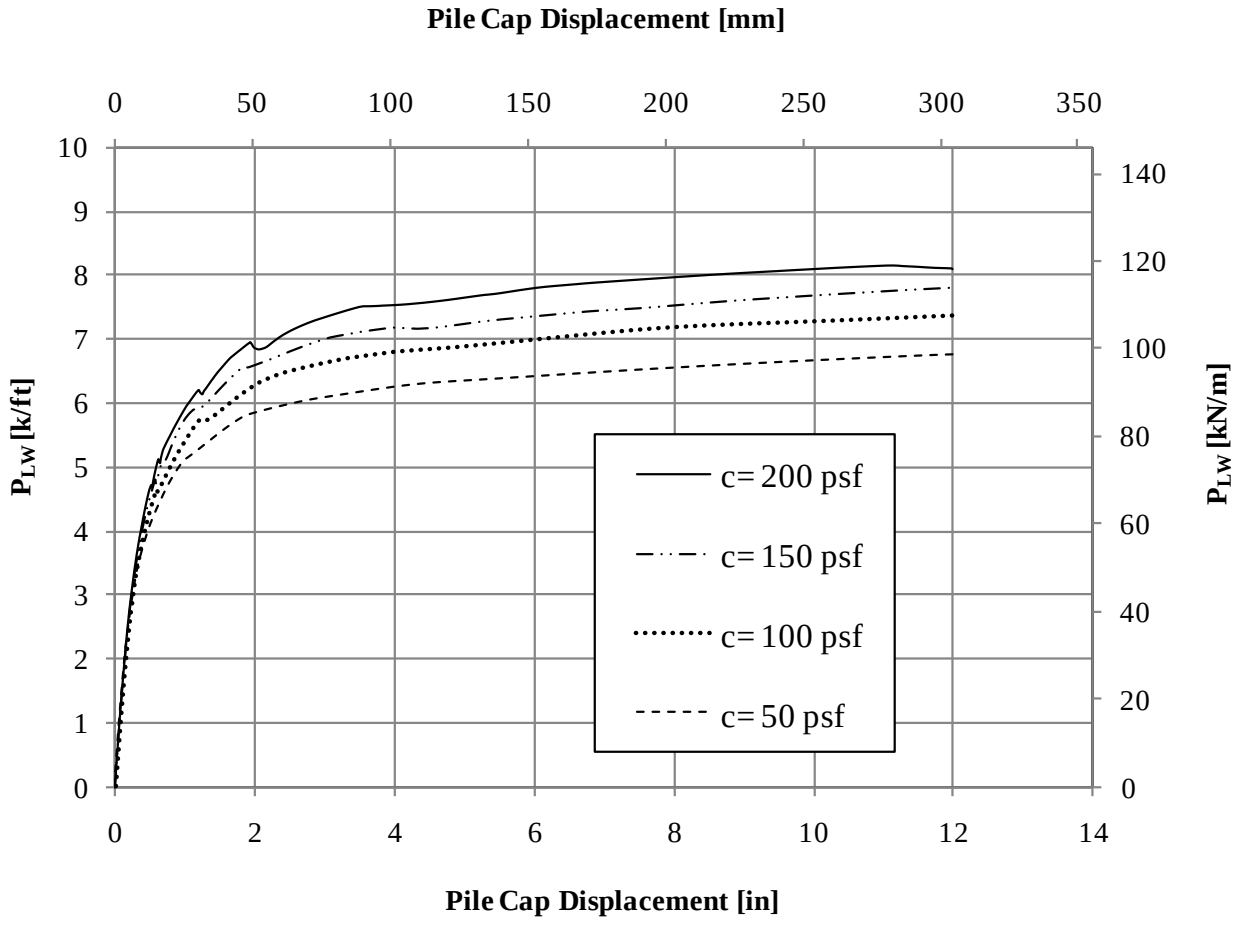

Figure 5-24: Effect of soil cohesion intercept, c, on the mobilized passive resistance of a limited width dense gravel backfill consisting of a 3-ft (0.91-m) wide gravel zone and loose silty sand

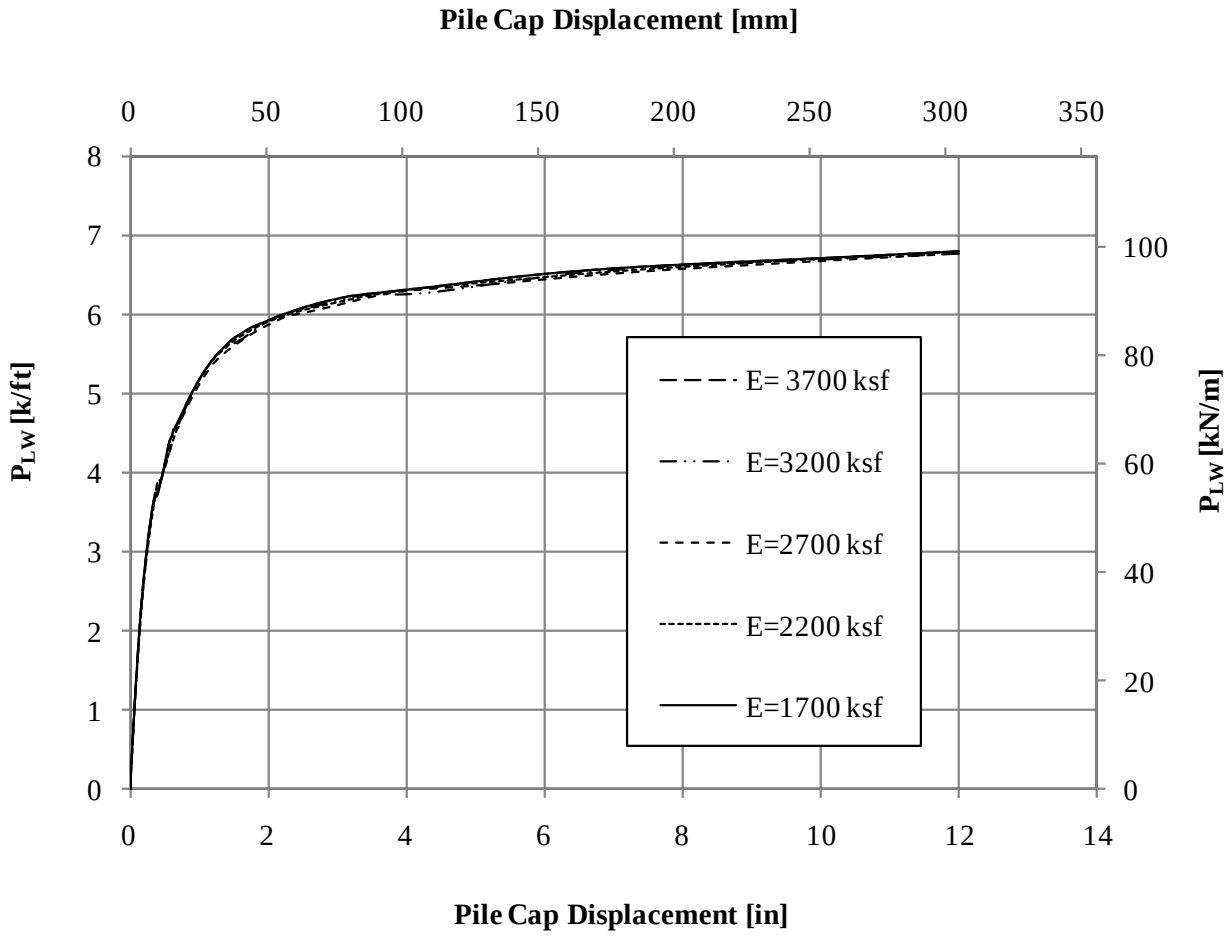

Figure 5-25: Effect of soil stiffness parameter, $E_{ref,50}$, on the mobilized passive resistance of a limited width dense gravel backfill consisting of a 3-ft (0.91-m) wide gravel zone and loose silty sand

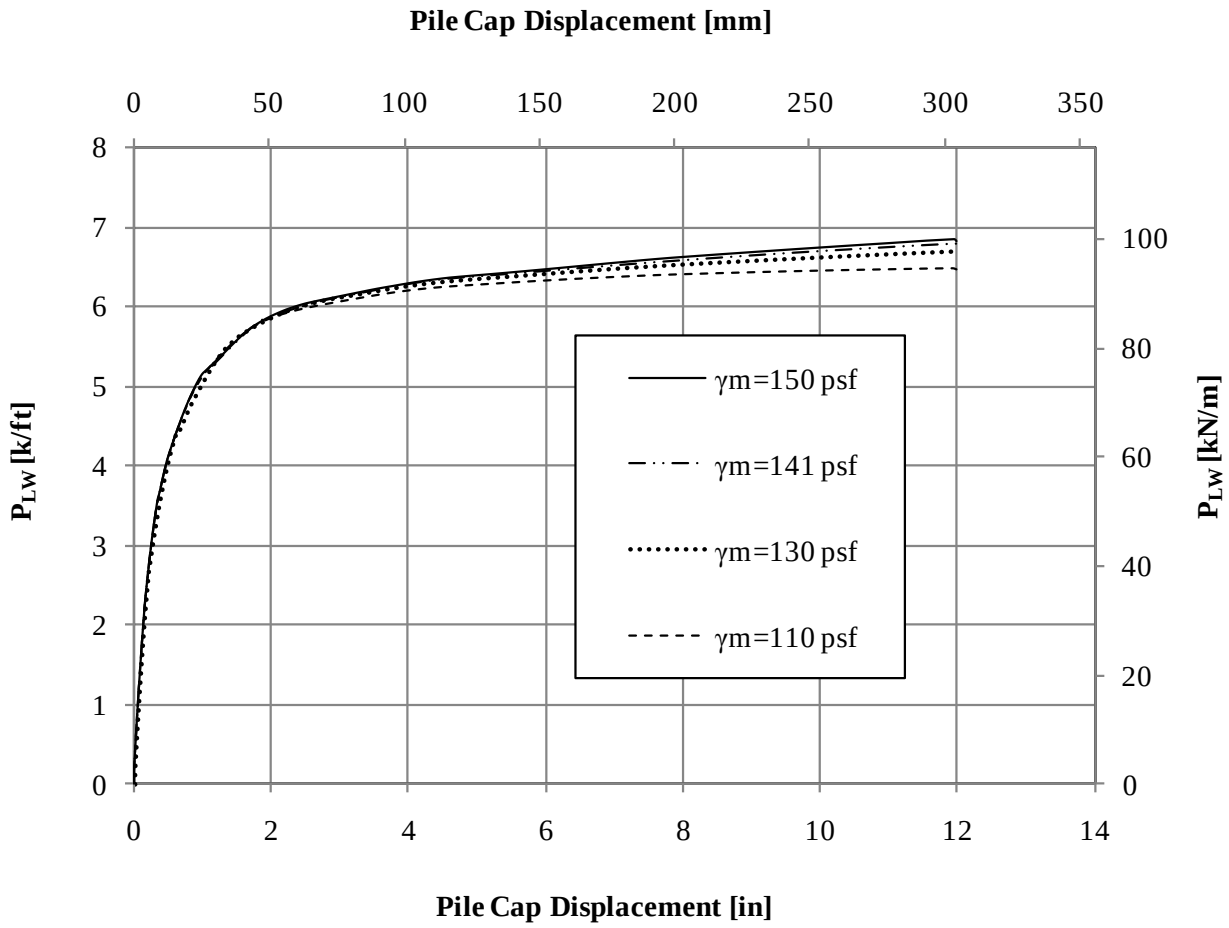

Figure 5-26: Effect of soil unit weight, γ_m, on the mobilized passive resistance of a limited width dense gravel backfill consisting of a 3-ft (0.91-m) wide gravel zone and loose silty sand

5.4.5 Effect of Deflection-to-Wall Height Ratio

The combined effect of varying the deflection-to-wall height ratio, pile cap height, and the gravel zone width, on the mobilized passive resistance is shown in Figure 5-27. Comparisons are made by plotting the Passive Force Ratio, PFR, versus the width of dense gravel zone width, normalized by the height of the pile cap, B_F/H. The trends observed in Figure 5-27 indicate that for B_F/H ratios less than one, varying the deflection-to-wall height ratio does

not have a very significant effect on the passive force ratio. However, for ratios greater than about one, the deviation between the 0.04 and 0.01 trend lines becomes greater, and consequently the sensitivity of the passive force ratio to the deflection-to-wall height ratio becomes more pronounced.

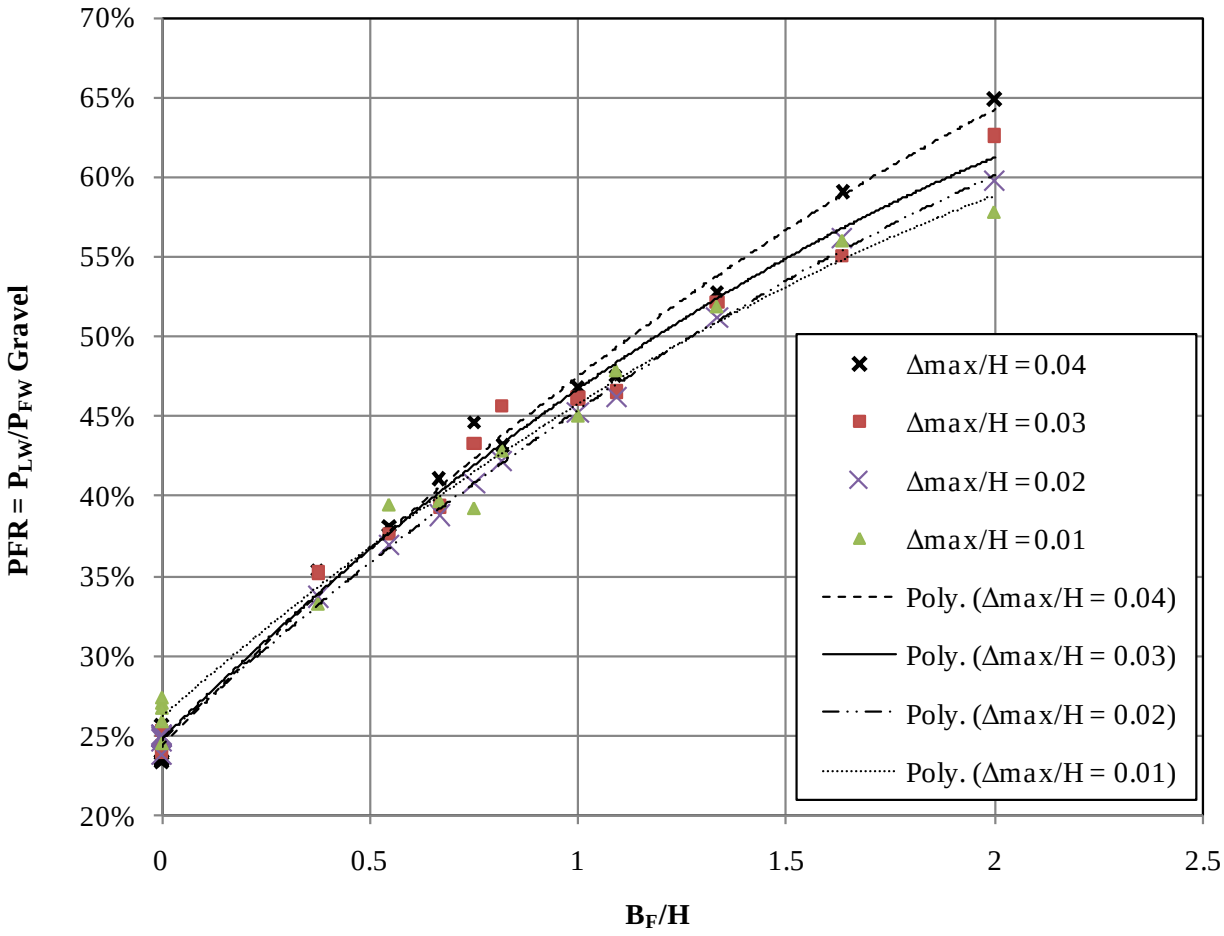

Figure 5-27: Combined effect of deflection-to-wall height ratio, Δ_{max}/H, wall height, and gravel zone width on the passive force ratio

5.4.6 Effect of Strength Reduction Factor

Figures 5-28 illustrates the effect of varying the strength reduction parameter, R_{inter}, on the calculated passive resistance of a limited width dense gravel backfill. The reference model for this study is a 3.67-ft (1.12-m) deep pile cap with a limited width backfill consisting of a 3-ft (0.91-m) wide dense gravel zone and loose silty sand. Hardening Soil model parameters used in this reference model are presented in Table 5-15.

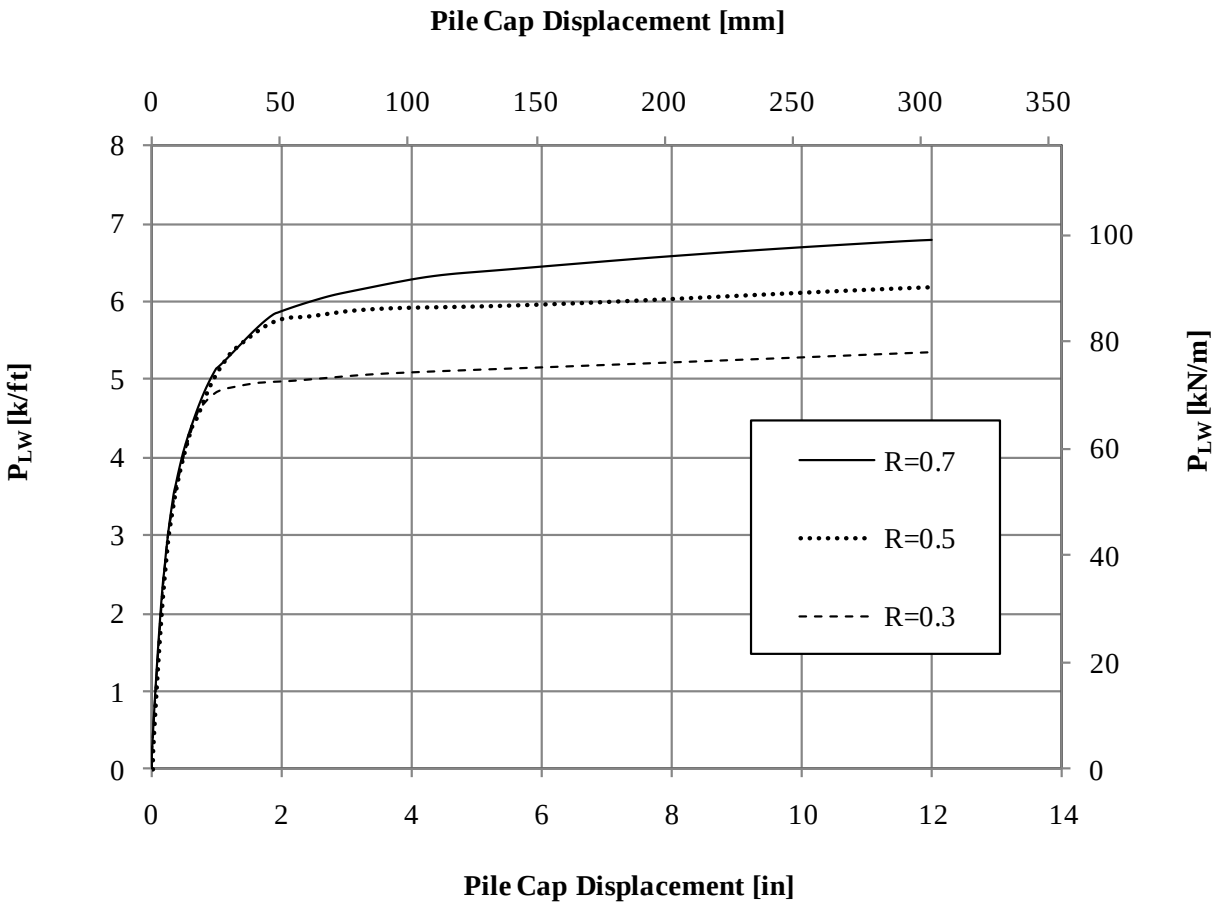

Figure 5-28: Effect of strength reduction parameter, R_{inter}, on the mobilized passive resistance of a limited width dense gravel backfill consisting of a 3-ft (0.91-m) wide gravel zone and loose silty sand

As explained previously, the strength reduction factor is used as the basic interface element property in PLAXIS, to relate the wall friction and adhesion to the soil cohesion and internal friction angle. In contrast to gravel parameters including the cohesion, stiffness, and the in-situ unit weight, the strength reduction parameter appears to have a relatively significant effect on the passive resistance mobilized by the limited width dense gravel backfill. Therefore, an appropriate selection of this parameter is important in providing an accurate assessment of the expected passive resistance. This result would be expected based on the sensitivity of the passive earth pressure coefficient, K_P, to the interface friction angle for homogeneous backfills.

The combined effect of varying the strength reduction factor, pile cap height, and gravel zone width was also investigated on the passive force ratio. Figure 5-29 illustrates this effect by plotting the Passive Force Ratio, PFR, versus the width of dense gravel zone, normalized by the height of the pile cap, B_F/H. Despite the fact that a higher strength reduction factor yields a higher total passive force (see Figure 5-28), the trends observed in Figure 5-29 show that for a given B_F/H value, the PFR is higher for a lower strength reduction factor. As mentioned previously, this is a result of normalizing the limited width passive resistance, P_{LW}, by the passive resistance associated with the full width (homogeneous) dense gravel backfill, $P_{FW\text{-}Gravel}$. However, the increases in PFR are relatively small as the strength reduction factor decreases from 0.85 to 0.75º, but become significantly greater as the strength reduction factor decreases from 0.75 to 0.5.

5.4.7 Effect of Finite Element Mesh Density

The degree of finite element mesh refinement dependency was investigated by analyzing five different mesh densities, very coarse, coarse, medium, fine, and very fine, for a 3.67-ft

(1.12-m) deep pile cap with a limited width backfill consisting of a 3-ft (0.91-m) wide dense gravel zone and loose silty sand. Hardening Soil model parameters used for this backfill condition are presented in Table 5-8.

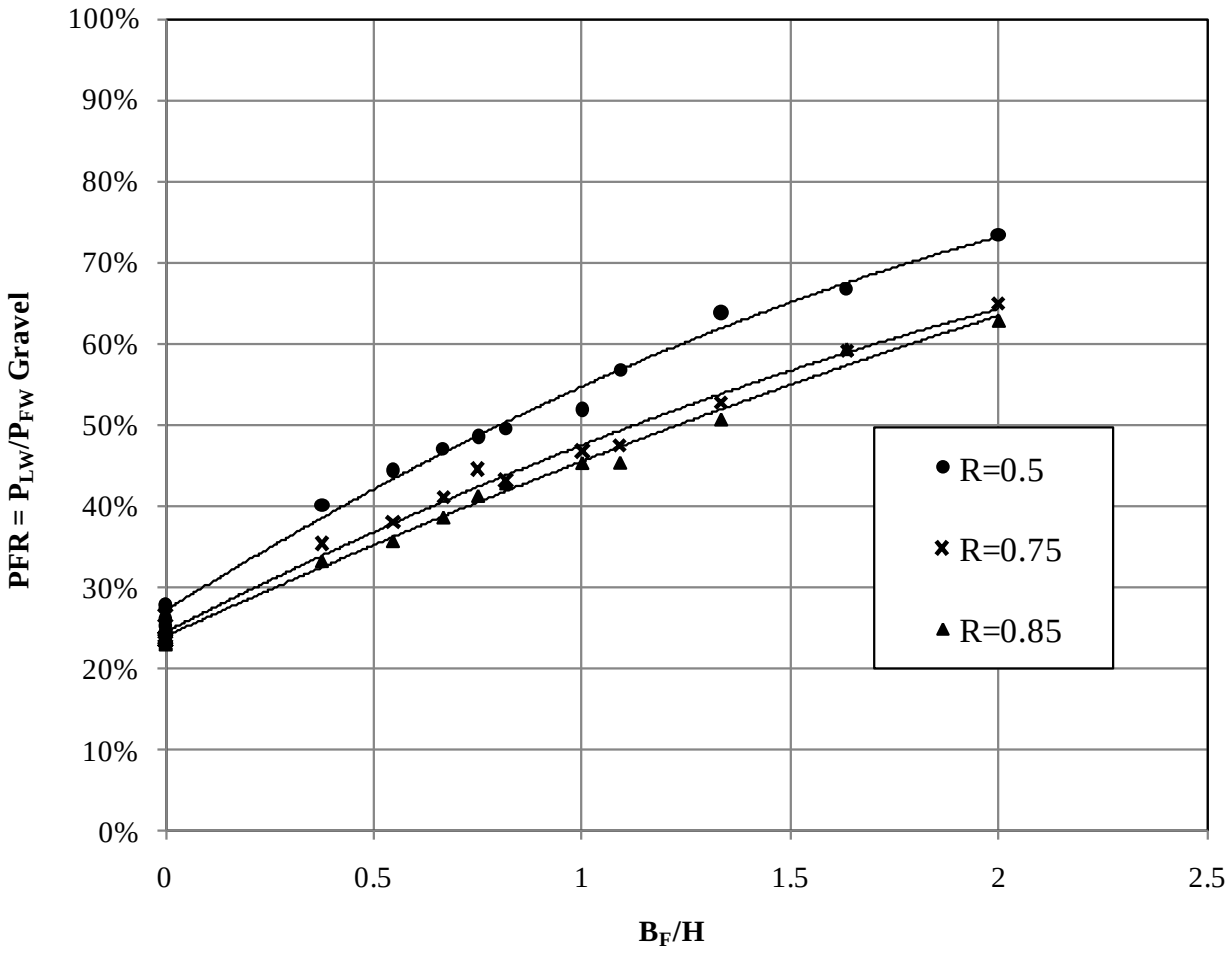

Figure 5-29: Combined effect of strength reduction parameter, R_{inter}, wall height, and gravel zone width on the passive force ratio

A comparison of load-displacement curves associated with each mesh density is presented in Figure 5-30. As is shown, the five curves perform identically up to a pile cap displacement of about 0.5 in (12.7 mm). After this displacement level, deviations from the curve associated with the very fine mesh coarseness start to occur. The very coarse and coarse curves over-predict the ultimate passive resistance of the backfill by about 15 and 9%, respectively.

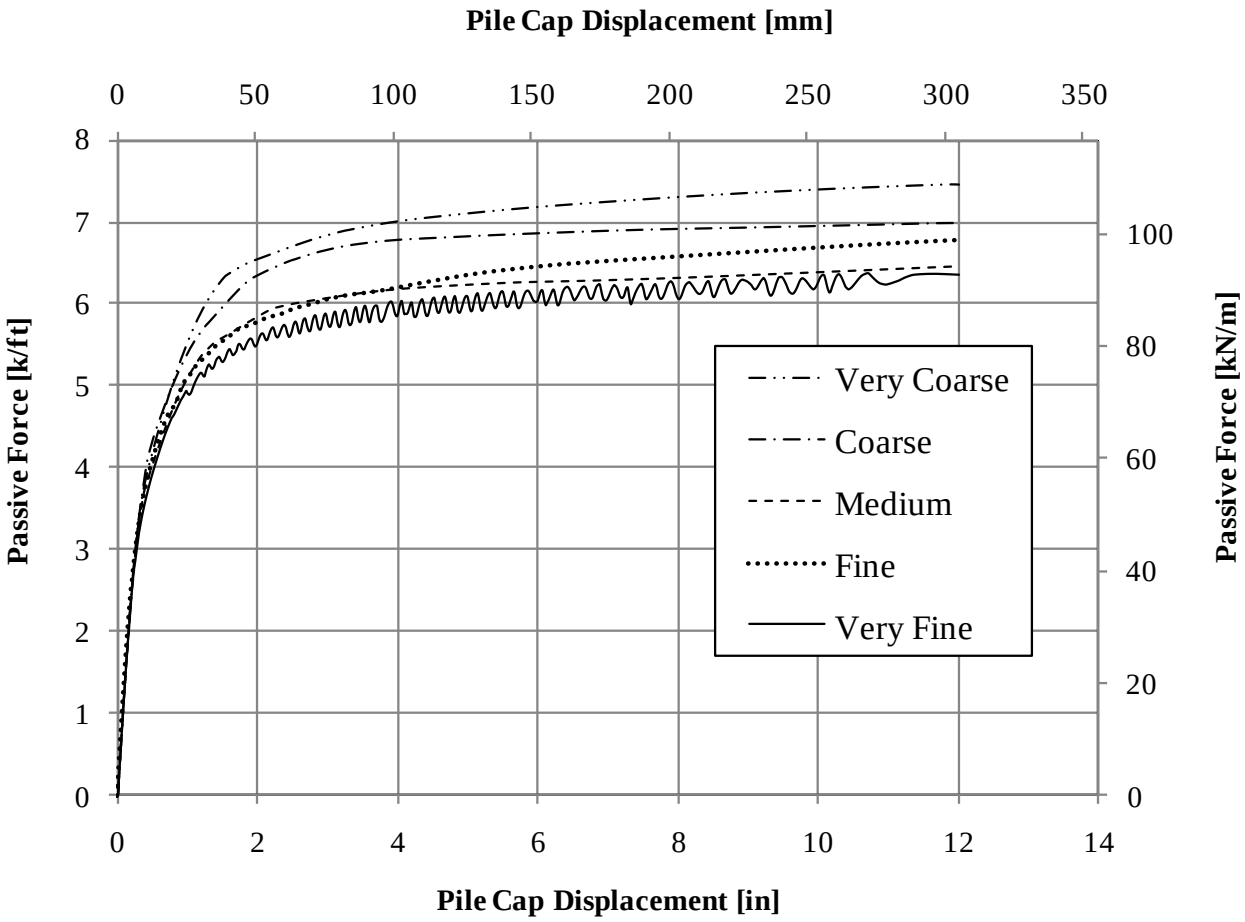

Figure 5-30: Load-displacement curves associated with 3.67-ft (1.12-m) deep pile cap with a 3-ft (0.91-m) limited width gravel backfill, illustrating mesh dependency of numerical results

On the other hand, the medium curve predicts slightly above the very fine curve, with an almost identical prediction of the ultimate resistance, associated with the very fine curve (6.45 k/ft (94.13 kN/m)).

Results from this parametric study indicate that the degree of finite element mesh refinement does not have a significant effect on the ultimate passive resistance mobilized by the backfill (investigated effects are less than 15% of deviation). In addition, based on the trends presented in Figure 5-30, it can be concluded that using a medium density finite element mesh in this study provides results which are a reasonable balance between computational time and accuracy. This result is also consistent with the recommendation provided by Shamsabadi (2006) related to the degree of mesh coarseness used in PLAXIS for geotechnical applications.

5.4.8 Effect Interface Element Extension Length

To investigate the effect of varying the length of interface element extensions around the base of the beam element on the passive resistance, five different extension lengths were analyzed for a 3.67-ft (1.12-m) deep pile cap with a limited width backfill consisting of a 3-ft (0.91-m) wide dense gravel zone and loose silty sand. Hardening Soil model parameters used for this backfill condition are presented in Table 5-8. Load-displacement curves associated with each extension length are presented in Figure 5-31. As is shown, the five curves perform identically up to a pile cap displacement of about 1 in (25.4 mm). After this displacement level, deviations start to occur from the curve associated with the 1 ft (0.3 m) extension length, which provides the lowest prediction of passive resistance after a displacement level of 1 in (25.4 mm). Based on this observation, it can be concluded that using 1 ft (0.3 m) for the numerical analyses

performed in this study provides conservative results compared to other extension lengths analyzed.

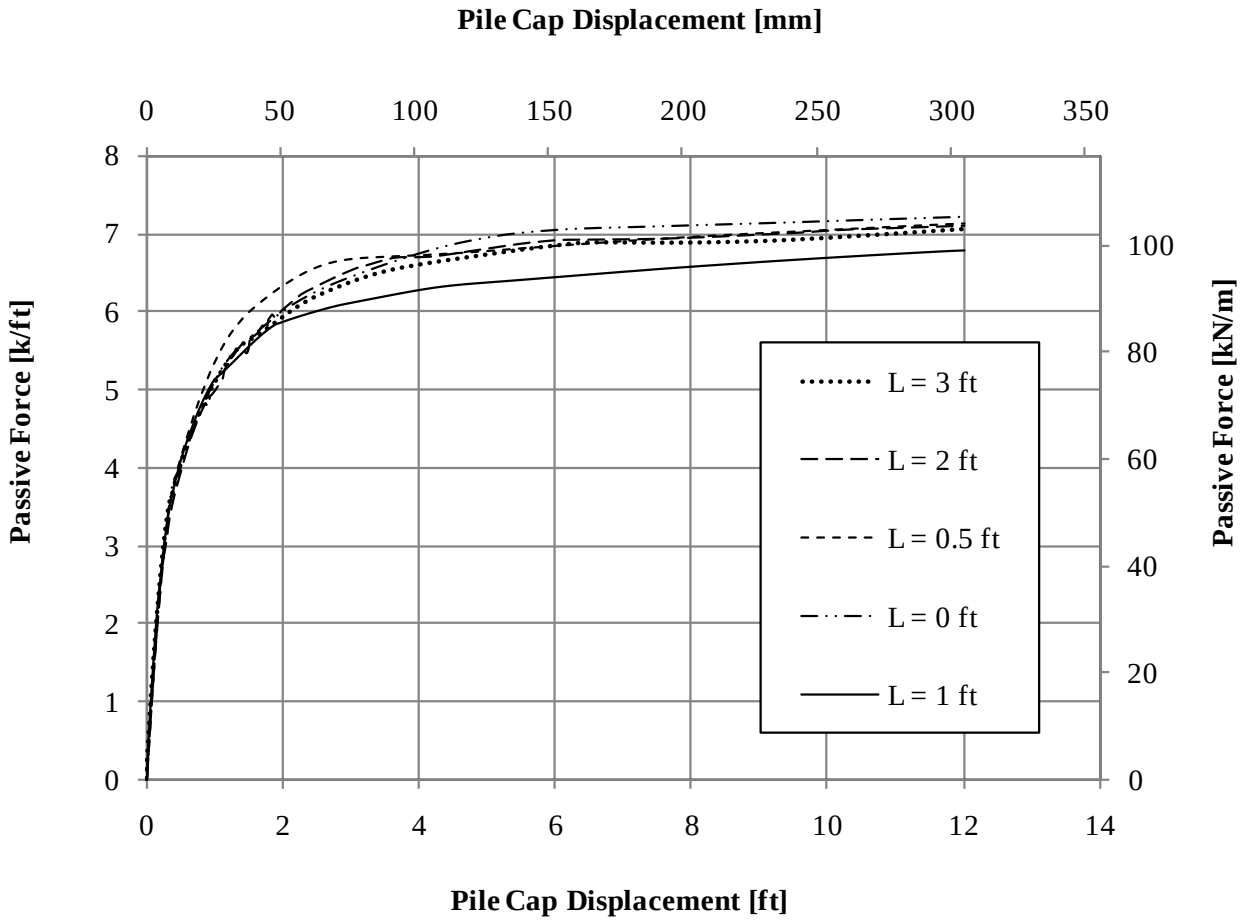

Figure 5-31: Load-displacement curves associated with 3.67-ft (1.12-m) deep pile cap with a 3-ft (0.91-m) limited width gravel backfill, illustrating the effect of varying the length of interface element extensions

5.5 Comparison of Numerical and Experimental Results

The experimental results of BYU lateral pile cap tests, conducted at the South Temple site in 2005, and at the SLC Airport site in 2007 provide a set of valuable data for evaluating the static passive behavior of limited width dense gravel backfills in three dimensions. To quantify the contribution of 3D pile cap end effects on the mobilized passive resistance of limited width backfills, plane strain numerical simulations were performed on limited width backfill conditions tested experimentally. The results obtained from these simulations were presented and thoroughly discussed in section 5.3, in terms of total displacements, total shear strains, and load-displacement curves. In this section, the measured 3D peak passive resistances of limited width backfills are compared with the plane strain results, to better understand the contributing effects of the edges of the pile cap to the total passive resistance mobilized by the backfills.

5.5.1 South Temple Testing

Figure 5-32 plots the passive resistance P_{LW}, of the 3.67-ft (1.12-m) deep pile cap, with limited width dense gravel backfills, against the width of the dense gravel compacted between the pile cap and loose silty sand, B_F, for the computed plane strain case and the measured 3D field case. As mentioned previously, P_{LW} designates the passive resistances of the 0-ft, 3-ft (0.91-m) and 6-ft (1.83-m) limited width backfills. P_{LW} corresponds to a deflection-to-wall height ratio of 4% for the limited width backfill conditions involving dense gravel. For full width (homogeneous) loose silty sand backfills, P_{LW} corresponds to a deflection-to-wall height ratio of 6%. Specifically, the comparison is provided for the following backfill conditions, for which experimental data was available: (1) full width (homogeneous) loose silty sand backfill (0-ft limited width dense gravel backfill); (2) limited width dense gravel backfill consisting of a 3-ft

(0.91-m) wide zone of dense gravel between the cap and loose silty sand; and (3) limited width dense gravel backfill consisting of 6-ft (1.83-m) wide zone of dense gravel between the cap and loose silty sand.

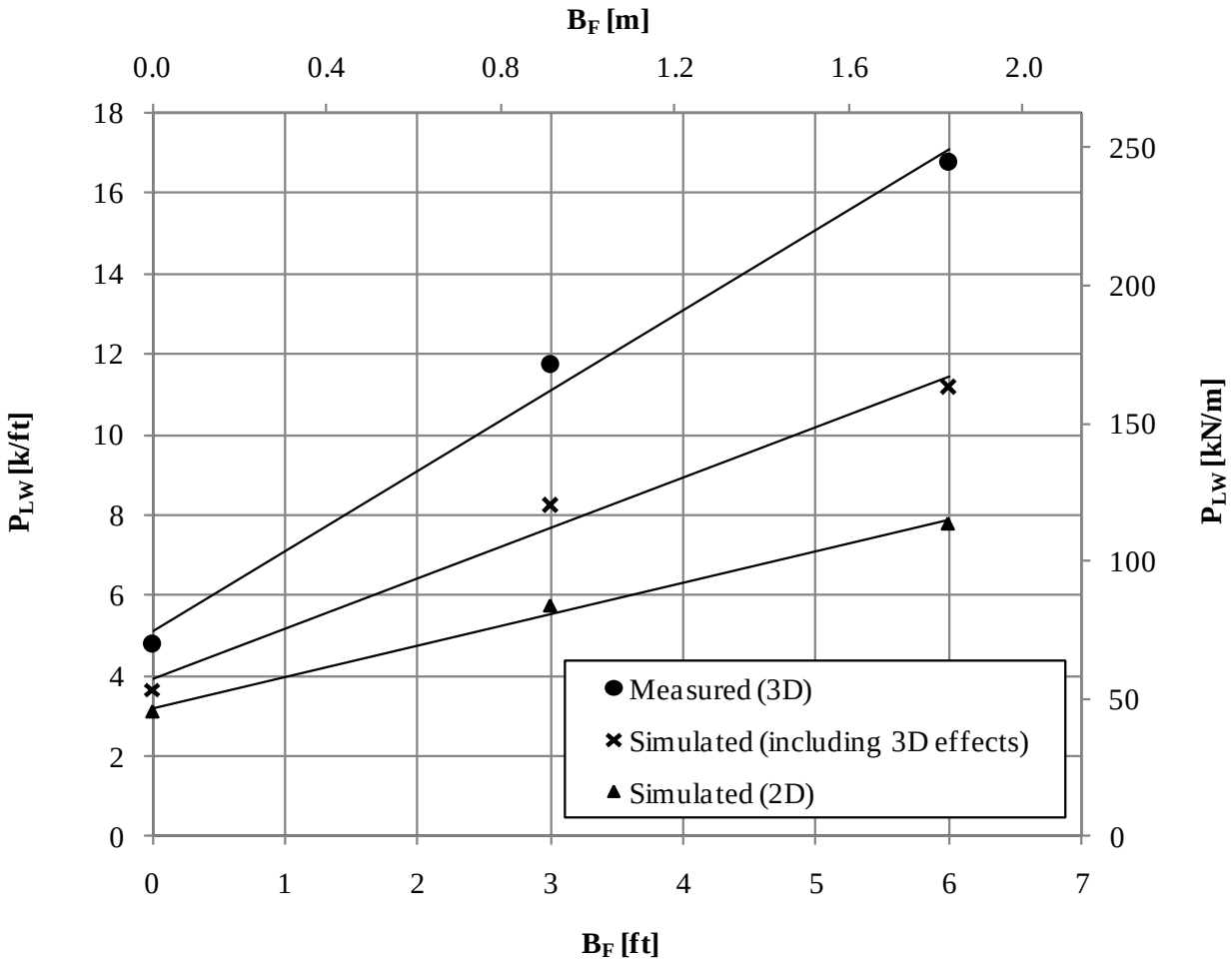

Figure 5-32: Comparison of 3D and 2D maximum passive resistance of 3.67-ft (1.12-m) deep pile cap with backfills consisting of: (1) full width (homogeneous) loose silty sand; (2) 3-ft (0.91-m) wide gravel zone and loose silty sand; and (3) 6-ft (1.83-m) wide gravel zone and loose silty sand

Based on the curves in Figure 5-32, the passive force computed for plane strain or 2D conditions is typically only about one-half of that measured for 3D conditions. In an effort to account for 3D end effects, the computed 2D passive force was then multiplied by the Brinch-Hansen factor, R_{3D}, and the results are also plotted in Figure 5-32 for comparison. Even after multiplying by the 3D correction factor, the computed passive force is still only about two-thirds of the measured 3D passive force. These comparisons indicate that in the case of limited width backfills tested at the South Temple site, a larger portion of the passive resistance can be attributed to 3D edge effects than would be the case for homogeneous backfills. This also suggests that the 3D edge effects are a major contributor to the increased passive force that was observed in the field tests, for the pile cap geometry at South Temple.

5.5.2 SLC Airport Testing

Figure 5-33 plots the passive resistance P_{LW}, of the 5.5-ft (1.68-m) deep pile cap with limited width dense gravel backfills, against the width of the dense gravel compacted between the pile cap and loose silty sand, B_F, for the computed plane strain case and the measured 3D field cases. Specifically, the comparison is provided for the following backfill conditions, for which experimental data was available: (1) full width (homogeneous) loose silty sand backfill (0-ft limited width dense gravel backfill); (2) limited width dense gravel backfill consisting of a 3-ft (0.91-m) wide zone of dense gravel between the cap and loose silty sand; and (3) limited width dense gravel backfill consisting of 6-ft (1.83-m) wide zone of dense gravel between the cap and loose silty sand.

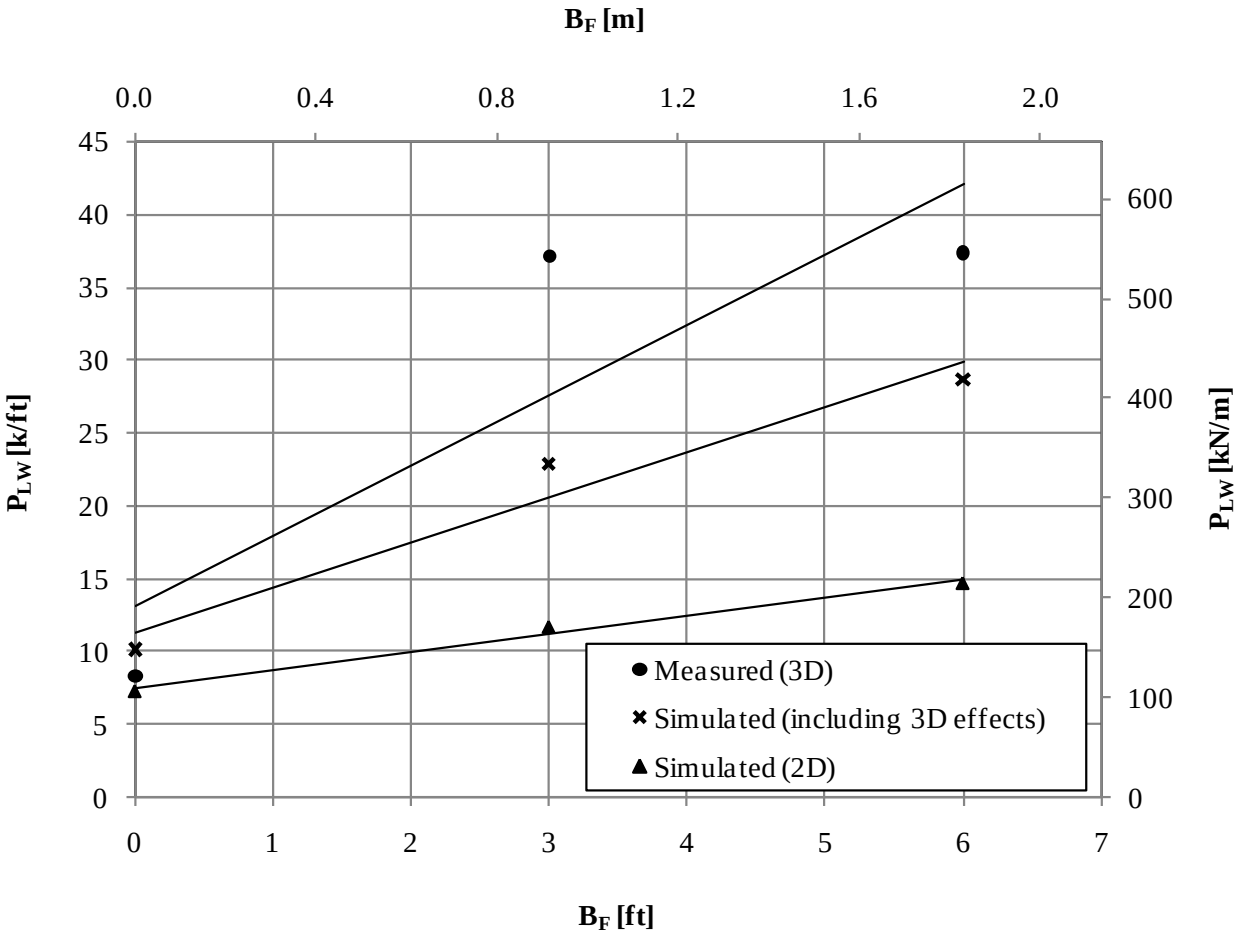

Figure 5-33: Comparison of 3D and 2D maximum passive resistances of 5.5-ft (1.68-m) deep pile cap with backfills consisting of: (1) full width (homogeneous) loose clean sand; (2) 3-ft (0.91-m) wide gravel zone and loose clean sand; and (3) 6-ft (1.83-m) wide gravel zone and loose clean sand

In this case, the computed 2D passive force is only about 35 to 40% of the measured passive for the 3D field case. Once again, multiplication of the computed 2D passive force by the Brinch Hansen 3D factor brings the computed passive force to about two-thirds of the measured 3D passive force. Similar to the 3.67-ft (1.12-m) deep pile cap, a larger portion of the resistance of limited width backfills tested at the SLC Airport site, can be attributed to 3D edge effects than would be the case of homogeneous backfills. As the width of the dense gravel zones

increase from 0-ft to 3-ft (0.91-m), the effect of the resistance provided by the edges of the pile cap becomes more pronounced. However, this trend is not followed when a 6-ft (1.83-m) wide dense gravel zone is used. This is due to the fact that the 3-ft (0.91-m) and 6-ft (1.83-m) limited width backfills tested at the SLC Airport site, exhibit passive behaviors that are quite similar at the displacement levels tested. As discussed previously in Chapter 3, this similar response is unexpected, considering the fact that the 3-ft (0.91-m) and 6-ft (1.83-m) limited width backfills tested at the South Temple site, showed a notable increase in resistance with increasing width of dense gravel zone. The reason behind this occurrence is not fully understood. However, as discussed in chapter 3, differences in pile cap face aspect ratios, and dense gravel width to pile cap height ratios are possible contributing factors.

To assess the 3D effect present in the experimental 3D limited width backfill tests, two additional resistance factors are computed and presented for comparison in Table 5-16, using the data presented in Figures 5-32 and 5-33. These factors, designated as $R_{BC-(2D)}$, and $R_{BC-(3D)}$ are computed by comparing the measured 3D peak passive resistances, with resistances obtained from plane strain numerical simulations, and plane strain numerical simulations adjusted for pile cap 3D edge effects. $R_{BC-(2D)}$, referred to as the 2D back-calculated factor, is determined by computing the ratio of measured 3D passive resistances, over 2D simulated resistances obtained from PLAXIS. The ratio of measured 3D passive resistances over 2D simulated resistances, including 3D edge effects is calculated and referred to as the 3D back-calculated factor, $R_{BC-(3D)}$. 3D edge effects are accounted for in plane strain simulations by multiplying 2D simulated resistances obtained from PLAXIS, with Brinch-Hansen 3D correction factors, computed using PYCAP. Including the 3D effects in the computed plane strain resistances, provides a means for assessing the amount of actual 3D effect that is captured by the Brinch-Hansen 3D correction

factor for limited width dense gravel backfills tested experimentally. Lastly, the Brinch-Hansen 3D correction factor, designated as R_{3D}, is calculated using Equation 2-8 in PYCAP for full width (homogeneous) loose silty sand, and full width (homogeneous) dense gravel backfills, tested at the South Temple and SLC Airport sites.

By comparing the data presented in Table 5-16, it can be shown that for the limited width backfills, the difference between Brinch-Hansen correction factors and computed 2D back-calculated factors, is relatively greater than would be the case for homogeneous backfills. This comparison implies that 3D edge effects contributing to the increase in passive resistance in limited width are not fully captured by the Brinch-Hansen 3D correction factor.

Table 5-16: Computed resistance factors for 3.67-ft (1.12-m) and 5.5-ft (1.68-m) deep pile caps with limited width dense gravel backfills

Pile Cap Height, ft (m)	Backfill Type	R_{3D}	$R_{BC-(2D)}$	$R_{BC-(3D)}$
3.67 (1.12)	Loose silty sand	1.176	1.547	1.316
	3-ft (0.91-m) gravel zone	1.434	2.044	1.425
	6-ft (1.83-m) gravel zone	1.434	2.151	1.500
5.5 (1.68)	Loose silty sand	1.387	1.135	0.819
	3-ft (0.91-m) gravel zone	1.954	3.176	1.626
	6-ft (1.83-m) gravel zone	1.954	2.545	1.302

Also, comparison of 2D back-calculated values, $R_{BC-(2D)}$, computed from the South Temple and SLC Airport tests provide information regarding the contribution of 2D stress effects

and 3D geometric end effects on the total passive resistance mobilized by the limited width backfills analyzed. For the 3-ft (0.91-m) and 6-ft (1.83-m) limited width backfills SLC Airport $R_{BC-(2D)}$ factors, are higher than those computed for the South Temple tests, by a factor of 1.5 and 1.2, respectively. This comparison implies that for limited backfill conditions tested at the South Temple site, a larger portion of the total passive resistance is due to 2D stress distribution effects in the backfill, relative to 3D edge effects. In contrast, for limited backfill conditions tested at the SLC Airport site, 3D edge effects have a more significant impact on the total passive resistance mobilized by the backfills.

In addition, the Brinch Hansen 3D correction factors are generally less than the 2D back-calculated values. This suggests that using the Brinch-Hansen 3D correction factors as a multiplier to the plane strain resistances, will be a conservative estimate of the actual 3D effect present in the passive response of the full-scale limited width backfill conditions tested experimentally. An exception is present in this case for the 5.5-ft (1.68-m) deep pile cap with the loose clean sand backfill, for which the Brinch-Hansen factor is greater than the 2D back-calculated value, $R_{BC-(2D)}$. As stated previously in chapter 3, the malfunctioning of equipment during the 5.5-ft (1.68-m) deep pile cap with the loose clean sand backfill test affected the extent to which data was recorded for this test. Therefore, the ultimate resistance recorded at the end of the test may not be the actual peak passive resistance associated with the loose clean sand backfill. It is likely that the maximum measured resistance of the backfill may have increased if the pile cap was able to displace further into the backfill, resulting in a higher computed 2D back-calculated value for this test.

Finally, the $R_{BC-(3D)}$ factor is typically greater than 1.3 suggesting that the 3D edge effect has at least a 30% greater effect in increasing the passive force for the limited width gravel

backfills than would be the case for a homogenous backfill. This would suggest that the ultimate passive force in these cases could potentially be increased by an additional 30%. However, the unexpected similar passive behavior of the 3-ft (0.91-m) and 6-ft (1.83-m) limited width backfills tested at the SLC Airport site, has led to uncertainties regarding the passive behavior of limited width backfills tested at the site. Nevertheless, what appears certain based on the tests conducted at both sites is that using the Brinch-Hansen 3D correction factors as a multiplier to the plane strain resistances, will still provide a conservative estimate of the 3D effect present in the experimental tests. Hence, due to the limited availability of test data, it is recommended to use a more conservative estimate of the 3D passive resistance in limited width backfills, using the data presented in this study. For pile caps in which 3D edge effects have a significant effect on the passive resistance mobilized in limited width dense gravel backfills, a conservative estimate of the 3D passive resistance can be calculated by multiplying the Brinch-Hansen 3D correction factor by the plane strain resistances obtained from Equation 5-2 through 5-18 or Figures 5-17 through 5-22. A design example illustrating the application of this approach for a typical pile cap is presented in the following section.

5.6 Design Examples

Two design examples are presented in this section to demonstrate the application of the developed model in predicting the passive resistance of limited width gravel backfills for both plane strain conditions and 3D geometries. The first example is related to the design of a limited width dense gravel backfill for a relatively long abutment wall supporting the superstructure of a bridge. In the second example a limited width dense gravel backfill is designed adjacent to a typical pile foundation system.

5.6.1 Example 1: Relatively Long Abutment Wall

Presentation

A reinforced concrete abutment wall is to be constructed at a site for the purpose of supporting a highway bridge deck. The abutment wall is approximately 51-ft (15.5-m) wide, 3-ft (0.91-m) long, and 8-ft (2.4-m) deep, and is expected to be able to tolerate 6 in (152 mm) of lateral movement under passive conditions. The general soil profile at the site consists of silty sands and clays. The first 10 ft (3.0 m) of the soil profile consists of alternating layers of relatively loose silty sand and sand, while deeper soils in the subsurface profile consist of highly plastic clays. The ground water table is predicted to be located well below the base of the abutment wall during and after construction. The engineering characteristics of the loose silty sand material were determined from a series of in-situ and laboratory-based tests. These parameters along with the abutment wall friction angle are presented in Table 5-17.

Table 5-17: Engineering properties for loose silty sand backfill material-example 1

Soil Type	γ_m pcf (kN/m^3)	Dr (%)	Φ (°)	c psf (kPa)	δ (°)
Loose silty sand	110 (17.3)	40	28	10 (0.5)	21

Due to the accessibility of loose sandy soil at the location of the project and the financial implications of using a backfill consisting of entirely dense gravel, the engineer has decided to take advantage of using a limited width dense gravel backfill to support the approach slab and

achieve a necessary horizontal passive resistance of 28 k/ft (409 kN/m). The engineering characteristics of the dense gravel material intended to be used for the backfill are presented in Table 5-18. It is desired to determine the width of the gravel zone required to mobilize the required passive resistance, assuming that the abutment will displace to its maximum tolerable deflection.

Table 5-18: Engineering properties for dense gravel backfill material-example 1

Soil Type	γ_m pcf (kN/m^3)	Dr (%)	Φ (°)	c psf (kPa)	δ (°)
Dense gravel	150 (23.6)	85	39	50 (2.4)	29.2

Solution

Due to the fact that the length of the abutment wall is relatively long with respect to its width, it is reasonable to assume plane strain conditions in this case, as 3D edge effects are not anticipated to contribute significantly to the mobilized passive resistance. The following steps are taken to determine the required width of gravel zone:

1) The 2D horizontal passive resistance mobilized in a full width (homogeneous) dense gravel backfill, per unit length of the abutment wall, $P_{FW\text{-}Gravel}$, is determined. This is accomplished by using the modified PYCAP spreadsheet program. Figure 5-34 shows the summary worksheet generated using PYCAP for the full width

(homogeneous) dense gravel backfill adjacent to the abutment wall. PYCAP predicts a 2D ultimate passive force of 55.2 k/ft (805.5 kN/m) of the wall.

2) Based on the required horizontal passive resistance of 28 k/ft (409 kN/m), the Passive Force Ratio, PFR is calculated as below:

$$PFR = \frac{P_{LW}}{P_{FW-Gravel}} = \frac{28\ (k/ft)}{55.2\ (k/ft)} \cong 0.5 \qquad (5\text{-}19)$$

3) Figure 5-35 is used to determine the width of gravel zone required to place between the abutment wall and loose silty sand to mobilize the desired passive resistance.

$$\frac{B_F}{H} \cong 0.7 \Longrightarrow B_F = 5.6\ ft\ say\ 6\ ft\ (1.68\ m) \qquad (5\text{-}20)$$

A 6-ft (1.68-m) wide zone of dense gravel must be compacted between the abutment wall and the loose silty sand backfill to achieve a horizontal passive resistance of 28 k/ft (409 kN/m).

5.6.2 Example 2: Relatively Narrow Pile Cap

Presentation

A reinforced concrete pile cap is to be constructed at a similar site presented in the previous example, as part of the pile foundation system supporting a bridge. The pile cap is approximately 15-ft (4.6-m) wide, 10 ft (3.05-m) long, and 4-ft (1.2-m) deep, and is expected to be able to tolerate 3 in (76.2 mm) of lateral movement under passive conditions.

Ultimate Capacity Calculation Sheet

Created by R.L. Mokwa and J.M. Duncan - August 1999

Date:	4/28/2010
Description:	Dense Gravel
Engineer:	MN

Input Values (red)

cap width,	b (ft) =	51.00
cap height,	H (ft) =	8.00
embedment depth,	z (ft) =	0.00
surcharge,	qs (psf) =	0.0
cohesion,	c (psf) =	50.0
soil friction angle,	f (deg.) =	39.0
wall friction,	d (deg.) =	29.25
initial soil modulus,	Ei (kip/ft2) =	1040
poisson's ratio,	n =	0.25
soil unit weight,	gm (pcf) =	150.0
adhesion factor,	a =	1.00
Dmax/H, (0.04 suggested, see notes) =		0.04

Calculated Values (blue)

Ka (Rankine) =	0.23
Kp (Rankine) =	4.40
Kp (Coulomb) =	21.01
Kpf (Log Spiral, soil weight) =	12.36
Kpq (Log Spiral, surcharge) =	0.00
Kpc (Log Spiral, cohesion) =	4.97
Ep (kip/ft) =	63.29
Ovesen's 3-D factor, R =	1.257
kmax, elastic stiffness (kip/in) =	5070.8
Pult (horz+vert) (kips) =	4056.8
Pult (horz) (kips/ft) =	55.2

Figure 5-34: Summary worksheet from PYCAP for dense gravel-example 1

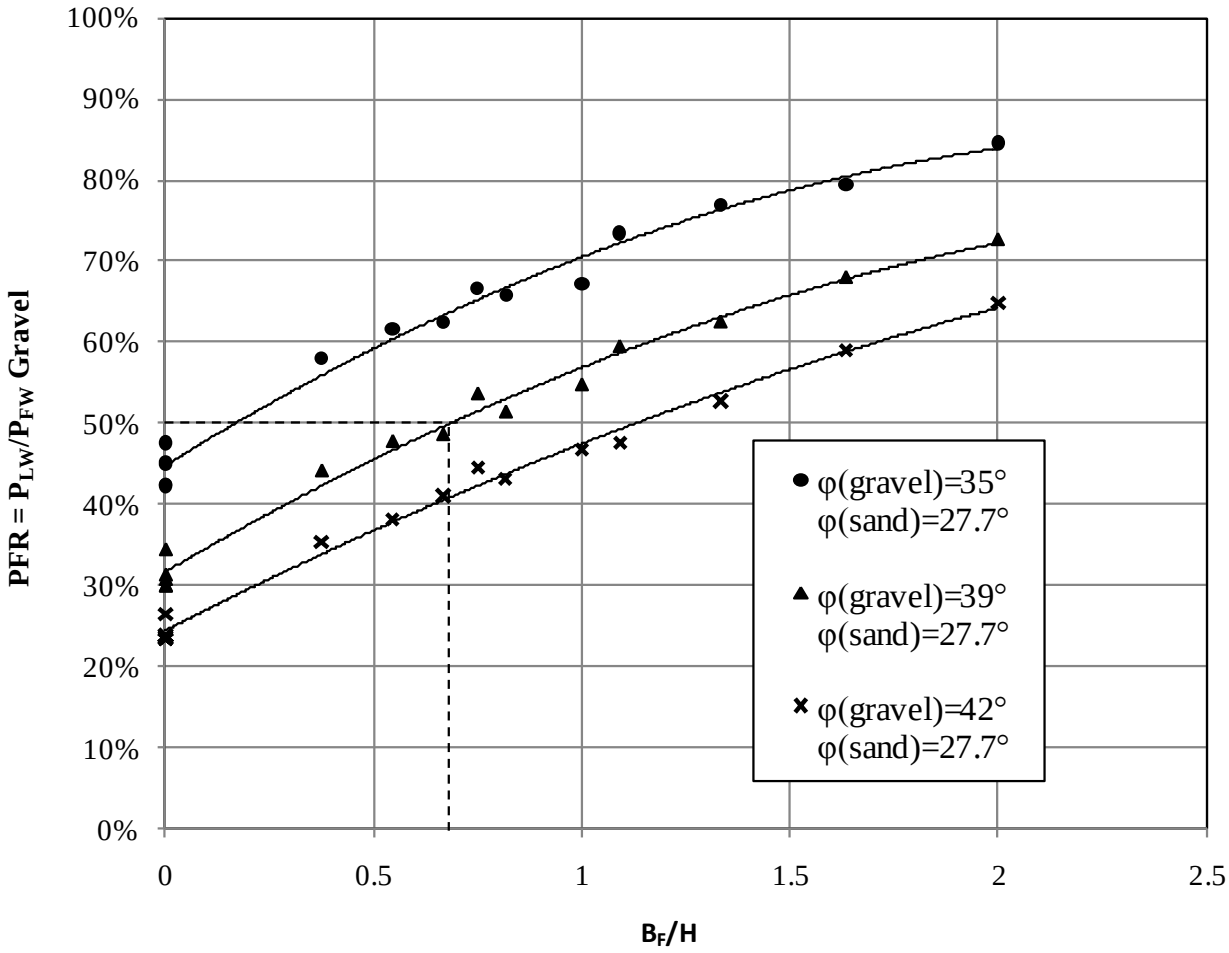

Figure 5-35: Determining the B_F/H ratio from the developed 2D model-example 1

To increase the passive resistance of loose native soil existing around the pile cap, a 3-ft (0.91-m) wide zone of gravel is to be compacted around the pile cap, between the cap and loose native soil. Assuming that the dense gravel used in the limited width backfill has similar properties to the gravel used in the previous problem, it is desired to determine the expected passive force for the limited width backfill, assuming that the pile cap will displace to its maximum tolerable deflection.

Solution

In the case of a pile cap, 3D edge effects are expected to play a significant role in increasing the mobilized plane strain passive resistance in the limited width backfill. To provide a conservative estimate of the anticipated 3D effects, the Brinch-Hansen 3D correction factor, R_{3D}, can be used to adjust plane strain resistances for 3D effects. The following steps are taken to determine the anticipated passive force for the limited width backfill:

1) The gravel zone width ratio, (B_F/H), is calculated as follows:

$$\frac{B_F}{H} = \frac{3\ ft}{4\ ft} = 0.75 \qquad (5\text{-}21)$$

2) Using Figure 5-35, the Passive Force Ratio, PFR, is determined to be about 53%.
3) Similar to the previous problem, PYCAP is used to determine the 2D horizontal passive resistance mobilized by a full width (homogeneous) dense gravel backfill, per unit length of the abutment wall, $P_{FW\text{-}Gravel}$. Figure 5-36 shows the summary worksheet generated using PYCAP for the full width (homogeneous) dense gravel backfill adjacent to the pile cap. PYCAP predicts a 2D ultimate passive force of 14.7 k/ft (214.5 kN/m) of the wall.

4) The 2D horizontal passive resistance, $P_{LW}(2D)$, mobilized by the limited width backfill is determined as follows:

$$PFR = \frac{P_{LW}(2D)}{P_{FW-Gravel}} = \frac{P_{LW}(2D)}{14.7\ (k/ft)} \cong 0.53$$

$$\Longrightarrow P_{LW}(2D) = 7.8\ k/ft \qquad (5\text{-}22)$$

5) The 3D horizontal passive resistance, $P_{LW}(3D)$, mobilized by the limited width backfill is determined as follows:

$$P_{LW}(2D) = \frac{P_{LW}(3D)}{R_{3D}} = \frac{P_{LW}(3D)}{1.428\ (k/ft)} \cong 7.8$$

$$\Longrightarrow P_{LW}(3D) = 11.1\ k/ft \qquad (5\text{-}23)$$

6) The 3-ft (0.91-m) limited width gravel backfill can be expected to mobilize a horizontal passive resistance of 11.1 k/ft (162.0 kN/m).

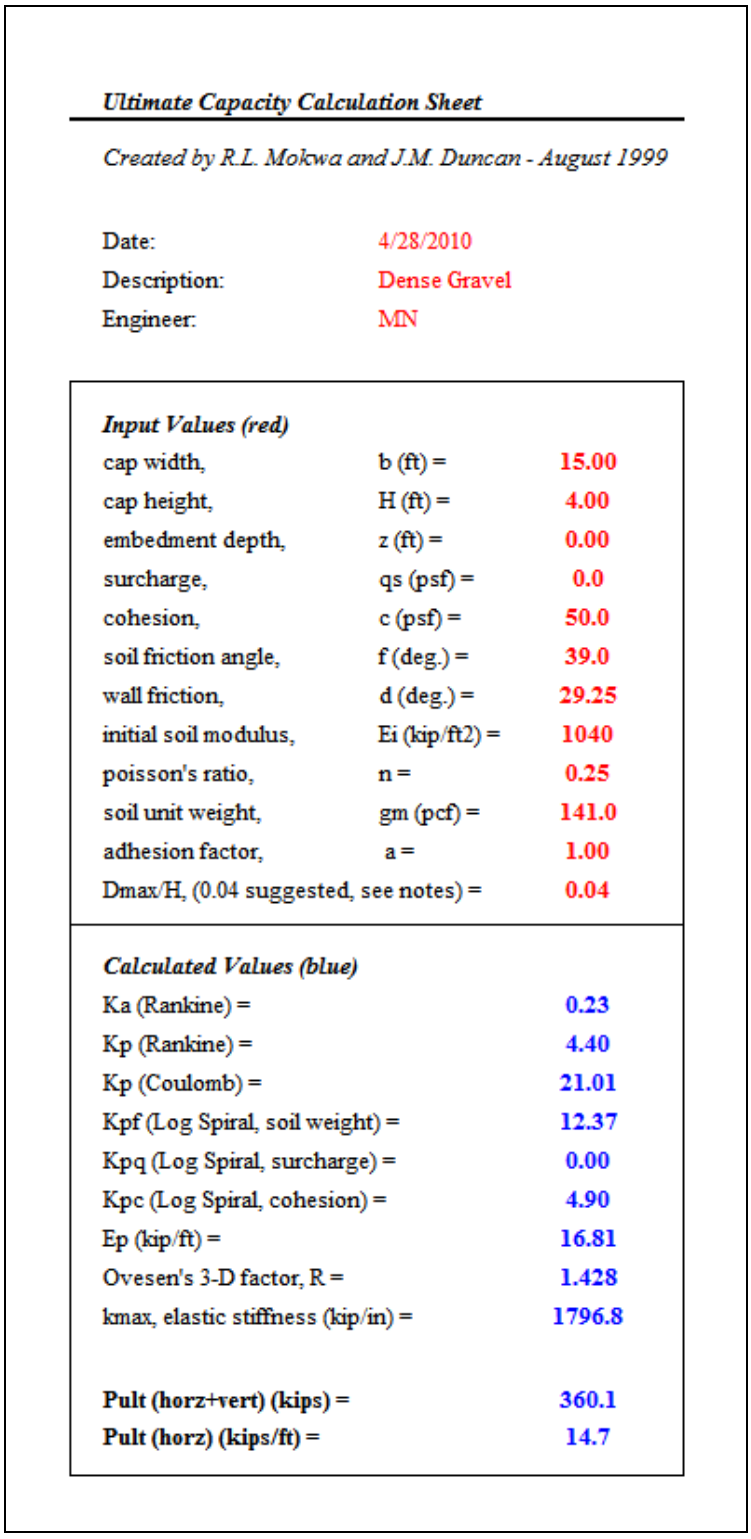

Ultimate Capacity Calculation Sheet

Created by R.L. Mokwa and J.M. Duncan - August 1999

Date:	4/28/2010
Description:	Dense Gravel
Engineer:	MN

Input Values (red)

cap width,	b (ft) =	15.00
cap height,	H (ft) =	4.00
embedment depth,	z (ft) =	0.00
surcharge,	qs (psf) =	0.0
cohesion,	c (psf) =	50.0
soil friction angle,	f (deg.) =	39.0
wall friction,	d (deg.) =	29.25
initial soil modulus,	Ei (kip/ft2) =	1040
poisson's ratio,	n =	0.25
soil unit weight,	gm (pcf) =	141.0
adhesion factor,	a =	1.00
Dmax/H, (0.04 suggested, see notes) =		0.04

Calculated Values (blue)

Ka (Rankine) =	0.23
Kp (Rankine) =	4.40
Kp (Coulomb) =	21.01
Kpf (Log Spiral, soil weight) =	12.37
Kpq (Log Spiral, surcharge) =	0.00
Kpc (Log Spiral, cohesion) =	4.90
Ep (kip/ft) =	16.81
Ovesen's 3-D factor, R =	1.428
kmax, elastic stiffness (kip/in) =	1796.8
Pult (horz+vert) (kips) =	360.1
Pult (horz) (kips/ft) =	14.7

Figure 5-36: Summary worksheet from PYCAP for dense gravel-example 2

6 CONCLUSIONS

6.1 Introduction

This research study simulates the plane strain passive behavior of 3.67-ft (1.12-m) and 5.5-ft (1.68-m) deep pile caps with the following backfill conditions: (1) full width (homogeneous) loose silty sand; (2) full width (homogeneous) dense gravel; (3) limited width dense gravel backfill consisting of a 3-ft (0.91-m) wide zone of dense gravel between the pile cap and loose silty sand and; (4) limited width dense gravel backfill consisting of a 6-ft (1.83-m) wide zone of dense gravel between the pile cap and loose silty sand. The results presented in this study were derived from performing the following tasks: (1) calibration of numerical models against analytical models for dense gravel and loose silty sand homogeneous backfills; (2) plane strain numerical simulation of limited width backfills; (3) implementation of parametric studies for limited width dense gravel backfills; and (4) comparison of measured passive resistance data with simulated plane strain results obtained for limited width dense gravel backfills.

The calibration procedure involved comparing load-displacement curves generated by the numerical models with those obtained from analytical models. The calibrated numerical models were also verified by comparing measured load-displacement curves with 3D curves computed using the analytical models, for the homogeneous backfills. Results obtained from the plane strain numerical simulation of limited width dense gravel backfills were presented in terms of

predicted total displacements, total shear strains, and load-displacement curves. The load displacement results were used to assess the effectiveness of limited width backfills, on the mobilized plane strain passive resistance. Parametric studies were executed to assess the effect of various design parameters on the plan strain passive resistance of limited width dense gravel backfills. Comparisons between measured and simulated plane strain results, helped quantify the contribution of 2D stress effects and 3D geometric end effects to the total passive resistance mobilized in dense gravel backfills of limited width. Based on the results obtained from these tasks, a simple design approach was developed for designing limited width dense gravel backfills for both plane strain and 3D conditions. The developed design approach was also accompanied by design examples to demonstrate its application.

In general, the calibrated models provided reasonable predictions of the plane strain load-displacement relationships of the analyzed backfills, relative to those generated by analytical methods with similar soil property assumptions. On the basis of this satisfactory agreement the following conclusions can be drawn for each completed task:

6.2 Calibration of Numerical Models against Analytical Models

1) The analytical models used in the calibration process (PYCAP and ABUTMENT) predict within 5 and 30% of measured ultimate passive resistances, for the full width (homogeneous) dense gravel and full width (homogeneous) loose sand backfills respectively, that were tested experimentally.
2) For the 3.67-ft (1.12-m) and 5.5-ft (1.83-m) deep pile caps with full width (homogeneous) loose silty sand backfills, reasonable agreement (within 9%) is

achieved between numerical and analytical plane strain passive resistances, at a deflection-to-wall height ratio (Δ_{max}/H) of 6 %.

3) For the 3.67-ft (1.12-m) and 5.5-ft (1.83-m) deep pile caps with full width (homogeneous) dense gravel backfills, reasonable agreement (within 5%) is achieved between numerical and analytical plane strain passive resistances, at a deflection-to-wall height ratio (Δ_{max}/H) of 4 %.

6.3 Numerical Simulation of Limited Width Dense Gravel Backfills

1) The plane strain numerical simulations were able to capture the passive response of full width (homogeneous) and limited width backfills reasonably well, in terms of horizontal and vertical movements and failure mechanisms. In general, numerical model predictions were also fairly consistent with field observations.
2) Predicted heaving profiles and shear shading plots show that major horizontal movements and strains are concentrated at the base of the pile cap, where the shear zone displaces the soil. This observation emphasizes the importance of ensuring that the compacted dense gravel fill extends beneath the pile cap to intercept the shear zone particularly for gravel zones of limited width.
3) For full width (homogeneous) loose silty sand backfills, the failure surface resembles a typical planar failure surface assumed in the Rankine theory of passive earth pressure. This may be the results of possible punching shear behavior of the pile cap. Full width (homogeneous) dense gravel backfills and the limited width backfills, show a more curvilinear failure mechanism, which is similar to the log spiral failure surface assumed in the log spiral theory of passive earth pressure.

4) Comparison of heaving profiles and shear strain shadings for the full width (homogeneous) and limited width backfills, indicate that the failure surface intersects the ground surface beyond the zone of significant heaving, at a distance where the deformed mesh profile starts to approach the initial elevation of the backfill surface.

5) For the 3.67-ft (1.12-m) deep pile cap, with increasing width of the gravel zone, the failure zone appears to remain well within the gravel zone, providing greater passive resistance with increasing width of the gravel zone. In contrast, for the 5.5-ft (1.68-m) deep pile cap, the failure surface appears to extend below the bottom of the gravel zone, with increasing width of the zone. In this case, a smaller percentage of the failure surface would be contained in the gravel zone, relative to the 3.67-ft (1.12-m) deep pile cap, reducing the effectiveness of the compacted fill in increasing the passive resistance of the backfill.

6) Limited width dense gravel backfills increased the plane strain ultimate passive resistance of the backfills, considerably, compared to the full width (homogeneous) loose silty sand backfill. Furthermore, the plane strain ultimate resistance mobilized in the limited width dense gravel backfills constituted a significant portion of the passive resistance that would have been provided, if a full width (homogeneous) dense gravel backfill had been used. This result indicates the effectiveness of using limited width dense gravel backfills, despite the relatively narrow width of the dense gravel zones placed between the pile cap and loose silty sand in comparison to the length of the log spiral failure surface.

7) In the case of the 3.67-ft (1.12-m) deep pile cap analyzed, placement of the 3-ft (0.91-m) and 6-ft (1.83-m) wide dense gravel zones between the pile cap and loose silty

sand increased the passive resistance of the backfill 84% and 152%, respectively, relative to a full width loose silty sand backfill. For the 5.5-ft (1.68-m) deep pile cap, placement of the 3-ft (0.91-m) and 6-ft (1.83-m) wide dense gravel zones between the pile cap and loose silty sand increased the passive resistance of the backfill 60% and 100%, respectively, relative to a full width loose silty sand backfill. These comparisons were made at deflection-to-wall height ratios of 4 % and 6 %, for limited width dense gravel and full width (homogeneous) loose silty sand backfills, respectively.

8) In the case of the 3.67-ft (1.12-m) deep pile cap, the 3-ft (0.91-m) and 6-ft (1.83-m) wide dense gravel zones and loose silty sand backfills mobilized 43% and 59%, respectively, of the passive resistance associated with the full width dense gravel backfills. For the 5.5-ft (1.68-m) deep pile cap analyzed, the 3-ft (0.91-m) and 6-ft (1.83-m) wide dense gravel zones and loose silty sand backfills mobilized 38% and 48%, respectively, of the passive resistance associated with the full width dense gravel backfills. These comparisons were made at a deflection-to-wall height ratio of 4 %.

9) In addition to providing increased lateral passive resistance, placement of the 3-ft (0.91-m) and 6-ft (1.83-m) wide dense gravel zones, for the 3.67-ft (1.12-m) deep pile cap, increased the initial loading stiffness by 53 and 77%, respectively, relative to the full width (homogeneous) loose silty sand backfill. In the case of the 5.5-ft (1.68-m) deep pile cap analyzed, the 3-ft (0.91-m) and 6-ft (1.83-m) wide dense gravel zones increased the initial loading stiffness by 34 and 58%, respectively.

6.4 Parametric Studies

1) The effectiveness of using a limited width backfill decreases with increasing pile cap height, for a constant width of gravel zone placed between the pile cap and loose silty sand.
2) In a limited width dense gravel backfill, for the range of friction angle values that would be typical of the gravel compacted fill and weaker native sands, the value of friction angles associated with these materials has a significant effect on the mobilized passive resistance in the backfill. Based on these results, an appropriate selection of the compacted fill friction angle is important in providing an accurate assessment of the expected passive resistance. In addition, the strength of the weaker sand must also be accounted for in the assessment of passive resistance.
3) Increasing the gravel zone depth from 1 to 2 ft (0.30 to 0.61 m) does not appear to have a significant effect on the mobilized passive resistance for B_F/H ratios less than one. For ratios greater than one, increasing the gravel zone depth from 1 to 2 ft (0.30 to 0.61 m) provides a more significant gain in passive resistance. In addition, for all combinations of pile cap height and gravel zone width, increasing the depth of gravel treatment greater than 2 ft (0.61 m) is relatively ineffective in providing additional passive resistance.
4) Similar to the friction angle of the compacted fill, the strength reduction parameter, R_{inter}, appears to have a relatively significant effect on the passive resistance mobilized by limited width dense gravel backfills. Based on these results, an appropriate selection of this parameter is important in providing an accurate assessment of the expected passive resistance.

5) Dense gravel soil parameters such as the cohesion, in-situ unit weight, and stiffness are not important influential parameters in increasing the passive resistance of limited width dense gravel backfills. Varying these parameters does not substantially influence the passive resistance of the limited width backfill. This result suggests that the dense gravel could be replaced by a dense sand with lower cohesion, unit weight or stiffness as long as the friction angle remained high.

6) Design charts shown in Figures 5-17 through 5-22 provide a simple design method for estimating the plane strain passive resistance of limited width dense gravel backfills. These charts were developed based on plane strain numerical simulations of full-scale limited width backfill conditions, tested experimentally, and thereby account for important geotechnical design parameters. Equations 5-2 through 5-18 represent the relationships provided in the abovementioned design charts.

6.5 Comparison of Numerical and Experimental Results

1) For the limited width backfills tested at the South Temple and SLC Airport sites, a larger portion of the increased resistance can be attributed to 3D edge effects than would be the case of homogeneous backfills tested at the site. This result suggests the 3D edge effects were a major contributor to the increased resistance observed in full-scale limited width gravel passive force tests.

2) Brinch Hansen 3D correction factors, R_{3D}, appeared to be generally less than the 2D back-calculated values, $R_{BC\text{-}(2D)}$, based on a range of full-scale tests results. This suggests that using the Brinch-Hansen 3D correction factors, as a multiplier to the

plane strain resistances, will provide a conservative estimate of the actual 3D passive response of a pile cap with a limited width backfill.

3) Typically, the measured 3D passive force was at least 30% higher than would be predicted by the 2D Plaxis analysis passive force multiplied by the Brinch Hansen 3D correction factor, R_{3D}.

7 RECCOMENDATION FOR FUTURE WORKS

Comparisons presented in this study, indicate that the influence of 3D edge effects on the mobilized passive resistance in limited width dense gravel backfills, becomes more pronounced with increasing width of gravel zone. In addition, it was found that the extent of the influence of 3D edge effects is related to the aspect ratio of the pile cap. These findings highlight the significance of performing 3D numerical simulations to better understand the development of 3D passive resistance for pile caps with different aspect ratios. 3D simulations would also shed light on the differences observed in the measured passive resistances of the South Temple and SLC Airport tests involving limited width backfills, and help in better quantifying the actual failure mechanisms involved in these tests.

REFERENCES

American Petroleum Institute, *Recommended Practice for Planning, Designing and Constructing Fixed Offshore Platforms, API Recommended Practice 2A (RP 2A)*, Seventeenth Edition, April 1, 1987.

Ashour, M., Norris, G., and Pilling, P. (1998). "Lateral loading of a pile in layered soil using the strain wedge model." *Journal of Geotechnical and Geoenvironmental Engineering*, 124(4), 303–315.

Aysen, A., (2002). *Soil Mechanics: Basic Concepts and Engineering Applications. 1st edition*, Taylor and Francis Group plc, London, UK.

Brinch-Hansen, J. (1966). "Resistance of a rectangular anchor slab." *Bulletin No. 21*, Danish Geotechnical Institute, Copenhagen, 12–13.

Caquot, A., and Kerisel, F. (1948). Tables for the calculation of passive pressure, active pressure and bearing capacity of foundations, Gauthier-Villars, Paris.

Christensen, D.S. (2006). "Full scale static lateral load test of a 9 pile group in sand," *MS Thesis*, Dept. of Civil and Environmental Engineering, Brigham Young University, Provo, Utah.

Clough, G.W. and Duncan, J.M. (1991). Earth retaining structures, *In Foundation engineering handbook*. 2nd Ed. H.Y. Fang, Ed. Van Nostrand Reinholdt, New York.

Clough, G.W. and Duncan, J.M. (1971). "Finite Element Analyses of Retaining Wall Behavior," *ASCE Journal of Soil Mechanics*, Vol. 97, No. SM12, 1657-1673.

Cole, R. T., and Rollins, K. M. (2006). "Passive earth pressure mobilization during cyclic loading." *Journal of Geotechnical and Geoenvironmental Engineering*, ASCE Vol. 132(9), 1154-1164.

Cole, R. T. (2003). "Full-scale effects of passive earth pressure on the lateral resistance of pile caps," *Ph.D. Dissertation*, Department of Civil and Environmental Engineering, Brigham Young University, Provo, Utah.

Coulomb, C.A. (1776). "Essai sur une application des regles des maximis et minimis a quelques problemes de statique relatifs a l'architecture," *Memoires de l'Academie Royale pres Divers Savants*, Vol. 7.

Duncan, J. M., and Mokwa, R. L. (2001). "Passive earth pressures: theories and tests." *Journal of Geotechnical and Geoenvironmental Engineering*, ASCE Vol. 127(3), 248-257.

Duncan, J. M., and Chang, C. Y. (1970). "Nonlinear analysis of stress and strain in soil." *Journal of Soil Mechanics and Foundations Division*, ASCE 96, 1629-1653.

Fang, Y. S., Chen, T. J., Wu, B. F. (1994). "Passive earth pressures with various wall movements." *Journal of Geotechnical and Geoenvironmental Engineering*, ASCE Vol. 120(8), 1307-1323.

Gadre, A. (1997). "Lateral response of pile-cap foundation system and seat-type bridge abutments in dry sand." PhD Thesis, Rensselaer Polytechnic Institute, Troy, New York.

Gerber, T M., Rollins, K M., Cummins, C. R., and Pruett, J.M. (2010). *Dynamic passive earth pressure on abutments and pile caps. Final report prepared for Utah Dept of Transportation Research Division Lead Agency for Pooled-Fund Study*. Unpublished raw data.

Hanna, A. M., and Meyerhof, G. G. (1980). "Design charts for ultimate bearing capacity of foundations on sand overlying soft clay." *Canadian Geotechnical Journal*, 17(2), 300–303.

Hueckel, S. M. (1957). Model tests on anchoring capacity of vertical and inclined plates." *Proceedings of the 4th International Conference on Soil Mechanics and Foundation Engineering*, Vol. 2, London, England.

Janbu, J., (1963). Soil Compressibility as Determined by Oedometer and Triaxial Tests. Proceedings ECSMFE Wiesbaden, Vol. 1, 19-25.

Kwon, K.H. (2007). "Thin gravel zones for increasing passive resistance on pile caps under cyclic and dynamic loading." *MS Thesis*, Dept. of Civil and Environmental Engineering, Brigham Young University, Provo, Utah.

Lambe, T. W. and Whitman, R. V. (1969). *Soil Mechanics*. John Wiley & Sons, Inc., New York, NY.

Lee, K.L. and Singh, A. (1971). "Relative density and relative compaction." *Journal of the Soil Mechanics and Foundations Division*, ASCE, 97(7), 1049-1052.

Material Models Manual: *PLAXIS 2D-Version8; Edited by R.B.J. Brinkgreve; Delft University of Technology & PLAXIS b.v.; The Netherlands*

Mokwa, R. L., and Duncan, J. M. (2001). "Experimental evaluation of lateral-load resistance of pile caps." *Journal of Geotechnical and Geoenvironmental Engineering*, ASCE Vol. 127(2), 185-192.

Norris, G. M. (1977). "The drained shear strength of uniform quartz sand as related to particle size and natural variation in particle shape and surface roughness." Ph.D. thesis, University of California, Berkeley, California.

Ovesen, N. K., and Stromann, H. (1972). "Design method for vertical anchor slabs in sand." ASCE *Proceedings, Specialty Conference on Performance of Earth and Earth-Supported Structures*, Vol. 1(2), New York, 1481-1500.

Ovesen NK (1966). "Anchor slabs, calculation methods, and model tests". *Bulletin No. 16*, Danish Geotechnical Institute, Copenhagen, 5–39.

Peterson, K.T. (1996). "Static and dynamic lateral load testing a full-scale pile group in clay." *MS Thesis*, Dept. of Civil and Environmental Engineering, Brigham Young University, Provo, Utah.

Potyondy, J. G. (1961). "Skin friction between various soils and construction materials." *Geotechnique*, Vol. 11(1), 339-353.

Rankine, W. (1857). "On the stability of loose earth," *Philosophical Transactions of the Royal Society of London*, Vol. 147.

Reference Manual: *PLAXIS 2D-Version8; Edited by R.B.J. Brinkgreve; Delft University of Technology & PLAXIS b.v.; The Netherlands*

Rollins, K M., Gerber, T M., and Ku Hyun Kwon. (2010). "Increased Lateral Abutment Resistance from Gravel Backfills of Limited Width." *Journal of Geotechnical and Geoenvironmental Engineering*, ASCE Vol. 136(1), 230-238.

Rollins, K. M. and Cole, R. T. (2006). "Cyclic lateral load behavior of a pile cap and backfill." *Journal of Geotechnical and Geoenvironmental Engineering*, 132(9), 1143-1153.

Rollins, K.M., King, R., Snyder, J.E., and Johnson, S.R. (2005b). "Full-scale lateral load tests of pile groups and drilled shafts in clay." *Procs. Intl. Conf. on Soil-Structure Interaction, Calculation Methods and Engineering Practice*, Vol. 1, Ulitsky, V.M., Ed., ASV Publishers, Moscow: 287-292.

Rollins, K.M., Snyder, J.L., and Broderick, R.D. (2005a). "Static and dynamic lateral response of a 15 pile group." *Procs. 16th Intl. Conf. on Soil Mechanics and Geotechnical Engineering*, Vol. 4, Millpress, Rotterdam, Netherlands: 2035-2040.

Rollins, K. M., Olsen, R. J., Egbert, J. J., Olsen, K. G., Jensen, D. H., and Garrett, B. H. (2003). "Response, analysis, and design of pile groups subjected to static and dynamic lateral loads." *Rep. No. UT-03.03*, Utah Department of Transportation Research Div., Salt Lake City, Utah.

Rollins, K. M. and Sparks, A. E. (2002). "Lateral load capacity of a full-scale fixed-head pile group." *Journal of Geotechnical and Geoenvironmental Engineering*, 128(9), 711–723.

Shamsabadi, A., Rollins, K. M., and Kapuskar, M. (2007). "Nonlinear soil-abutment-bridge structure interaction for seismic performance-based design." *Journal of Geotechnical and Geoenvironmental Engineering*, ASCE Vol. 133(6), 707-720.

Shamsabadi, A., (2006). Modeling passive earth pressures on bridge abutments for nonlinear seismic soil-structure interaction using PLAXIS. *Plaxis Bulletin* Issue 20, October 2006.

Schanz, T., Vermeer, P.A., Bonnier, P.G., (1999). The Hardening-Soil Model: Formulation and verification. In: R.B.J. Brinkgreve Beyond 2000 in Computational Geotechnics. Balkema, Rotterdam: 281-290.

Soubra, A.-H. and Regenass, P. (2000). "Three-dimensional passive earth pressures by kinematical approach." *Journal of Geotechnical and Geoenvironmental Engineering*, ASCE Vol. 126(11), 969-978.

Martin, G. R., Lam, I. P., Yan, L.-P., Kapuskar, M., and Law, H. (1996). "Bridge abutments-Modeling for seismic response analysis." *Proc.,4th CALTRANS Seismic Research Workshop*, California Department of Transportation, Sacramento, Calif., 15.

Scientific Manual: *PLAXIS 2D-Version8; Edited by R.B.J. Brinkgreve; Delft University of Technology & PLAXIS b.v.; The Netherlands*

Taylor, A.J. (2006). "Full-scale-lateral-load test of a 1.2 m diameter drilled shaft in sand." *MS Thesis*, Dept. of Civil and Environmental Engineering, Brigham Young University, Provo, Utah.

Terzaghi, K., (1943). *Theoretical Soil Mechanics*. Wiley, New York.

Terzaghi, K., Peck, R., and Mesri, G. (1996). *Soil mechanics in engineering practice, 3rd edition*, John Wiley and Sons, Inc. New York, NY.

Tutorial Manual: *PLAXIS 2D-Version8; Edited by R.B.J. Brinkgreve; Delft University of Technology & PLAXIS b.v.; The Netherlands*

U.S. Naval Civil Engineering Laboratory (1966). "Deadman anchorages in sand." Report number Y-F015-15-001, Alexandria, VA.

U.S. Navy, (1982). *Foundations and earth structures design manual 7.2*, Department of the Navy, Naval Facilities Engineering Command, Alexandria, Va.